Cost Effective Joint Energy & Production Operations Decision Making for Sustainable Manufacturing System

BY

FADWA DABABNEH
B.S., University of Illinois at Chicago, 2014
M.S., University of Illinois at Chicago, 2016

THESIS

Submitted as partial fulfillment of the requirements for the degree of Doctor of Philosophy in Industrial Engineering and Operations Research in the Graduate College of the University of Illinois at Chicago, 2018

Chicago, Illinois

Defense Committee:

Dr. Lin Li, Chair and Advisor
Dr. David He
Dr. Houshang Darabi
Dr. W.J. Minkowycz
Dr. Jianhui Wang, Southern Methodist University

DEDICATION

To my loving parents, Mr. Fares Naji Dababneh and Ms. Hala Issa Gammoh.

ACKNOWLEDGMENTS

First, I would like to thank my family, especially my parents, (Mr. Fares Dababneh and Ms. Hala Gammoh) and my siblings (Mr. Naji Dababneh, Ms. Hiba Dababneh, and Mr. Issa Dababneh) for all of their unwavering support. They have motivated me and pushed me to be the best version of myself. They are certainly the reason that I strive to be successful. Their trust in both my academic capabilities and personal stature has reinforced me personally and professionally throughout this journey.

Furthermore, I would like to thank my advisor, Dr. Lin Li, Associate Professor in the Department of Mechanical and Industrial Engineering at the University of Illinois at Chicago, for allowing me to join the Sustainable Manufacturing Systems Research Laboratory and for helping me realize my dream of pursuing higher education. He has provided me with all the necessary tools to make this research and my future career plans successful.

Additionally, I would like to thank Dr. David He, Dr. Houshang Darabi, Dr. W.J. Minkowycz, and Dr. Jianhui Wang for serving as my graduate committee. Their guidance has been an indispensable and integral part of my doctoral dissertation.

Meanwhile, I would to thank all the present and former lab members from the Sustainable Manufacturing Systems Research Laboratory, Dr. Zeyi Sun, Dr. Yong Wang, Ms. Yiran Yang, Mr. Yuntian Ge, Ms. Azadeh Haghighi, Ms. Jing Zhao, and Mr. Rahul Shah for all of the help they have provided in this research.

Last but not least, I would like to acknowledge the financial support from the National Science Foundation (CMMI 1131537) and U.S. Department of Energy (DE-EE0007722).

Fadwa Dababneh

CONTRIBUTION OF AUTHORS

Chapter 1 represents an introduction with the background, challenges, objectives, and literature review.

Chapter 2 represents three published papers (Sun, Z., Dababneh, F. and Li, L., 2018. Joint Energy, Maintenance, and Throughput Modeling for Sustainable Manufacturing Systems. *IEEE Transactions on Systems, Man, and Cybernetics: Systems*. DOI:10.1109/TSMC.2018.2799740; Dababneh, F., Li, L., Shah, R. and Haefke, C., 2018. Demand Response-Driven Production and Maintenance Decision-Making for Cost-Effective Manufacturing. *Journal of Manufacturing Science and Engineering*, *140*(6), p.061008.; and Dababneh, Fadwa, Rahul Shah, Zeyi Sun, and Lin Li. "Framework and sensitivity analysis of joint energy and maintenance planning considering production throughput requirements." In *ASME 2017 12th International Manufacturing Science and Engineering Conference collocated with the JSME/ASME 2017 6th International Conference on Materials and Processing*, pp. V003T04A062-V003T04A062. American Society of Mechanical Engineers, 2017.). I was the major driver of the research. Dr. Zeyi Sun contributed to research idea generation. Mr. Rahul Shah contributed to the simulation execution and analysis. Dr. Lin Li and Mr. Cliff Haefke contributed to guiding the research quality, providing data, and paper revision.

Chapter 3 represents two published papers (Dababneh, F., Li, L. and Sun, Z., 2016. Peak power demand reduction for combined manufacturing and HVAC system considering heat transfer characteristics. *International Journal of Production Economics*, *177*, pp.44-52.; and Dababneh, F., Atanasov, M., Sun, Z. and Li, L., 2015, June. Simulation-based electricity demand response for

combined manufacturing and HVAC system towards sustainability. In *ASME 2015 International Manufacturing Science and Engineering Conference* (pp. V002T05A009-V002T05A009). American Society of Mechanical Engineers.). I was the major driver of the research and contributed to research idea generation. Dr. Zeyi Sun and Dr. Lin Li contributed to improving the research quality, providing data, and paper revision.

Chapter 4 represents one of my published papers (Dababneh, F. and Li, L., 2018. Integrated Electricity and Natural Gas Demand Response for Manufacturers in the Smart Grid. *IEEE Transactions on Smart Grid*. DOI: 10.1109/TSG.2018.2850841). I was the main driver of this research and contributed to the idea generation. Dr. Lin Li contributed to guiding the research quality and to the paper revision.

Chapter 5 represents the conclusions of the research presented in this thesis.

SUMMARY

Industry leaders must find ways to fulfill consumer demand and meet societal needs while reducing cost and environmental burdens. Incorporating Demand Response practices and programs into manufacturing production decision-making opens up many opportunities for manufacturers address economic, environmental, and societal concerns from the industrial sector, simultaneously. Much research on the implementation of electricity demand response for residential and commercial sectors has been reported in literature, however, research on demand response for manufacturers is less developed and impeded by complex production system dynamics. This leads to lost opportunities for economic and environmental sustainability by manufacturers. In this dissertation, demand response driven cost-effective joint energy and production operations decision making methodology for sustainable manufacturing systems is presented. More specifically, frameworks aiming to integrate sustainable manufacturing, production scheduling, and electricity demand response for manufacturers are presented from three lenses, i.e., the manufacturing production system-level, the plant-level, and the utility-level. In all, the frameworks presented provide manufacturers with analytical tools for implementing cost-effective joint energy and production management towards sustainability and support the industrial sector's immersion in the Smart Grid.

TABLE OF CONTENTS

LIST OF TABLES

LIST OF FIGURES

LIST OF ABBREVIATIONS

DR	Demand Response
EE	Energy Efficiency
FERC	Federal Energy Regulatory Commission
GHG	Greenhouse Gas
HD	Hamming Distance
HVAC	Heating, Ventilation, and Air Conditioning
MSA	Modified Simulated Annealing
PSO	Particle Swarm Optimization
SA	Simulated Annealing
SG	Smart Grid
TOU	Time-of-Use

1 Introduction

1.1 Motivation, Challenges, and Objectives

As the reliance on manufactured products grows, the industrial sector's role in the country's security, the economy, and consumers' everyday life increases. Meanwhile, to maintain a competitive advantage and satisfy the growing demand for manufactured products, matters of economic and environmental viability must be considered. Through sustainable manufacturing industry leaders can fulfill consumer demand and societal needs while reducing cost and environmental burdens. According to the U.S. Department of Commerce, Sustainable manufacturing is defined as "the creation of manufactured products that use processes that minimize negative environmental impacts; conserve energy and natural resources; are safe for employees and communities; and are economically sound" (Moldavska and Welo, 2017).

Within manufacturing, energy costs account for a large portion of the overall production costs; which in some industries is the largest share following that of raw materials (Ernst & Young-EY, 2018). The U.S. manufacturing sector's onsite energy use and emissions are 14,064 TBtu and 580 MMT of CO_2, respectively (U.S. Department of Energy, 2010). Manufacturers can integrate sustainability considerations in production and maintenance planning with energy management and emission reduction activities to help reduce the manufacturers' energy and carbon footprint.

Among the major energy sources that manufacturers must consider, when seeking to promote sustainable manufacturing and implement energy aware production strategies, is electricity. The industrial sector alone consumes 27% of the total electricity in the U.S. and has a significant influence on the country's growing electricity demand (U.S. Energy Information Administration, 2017). It is projected that by 2030 about $1.5-$2 trillion will be needed for new electricity generation capacities and transmission and distribution infrastructure to meet the

growing electricity demand (Chupka et al., 2008); this in turn will impact electricity end-users, energy providers, and manufacturers. Moreover, manufacturers not only have a significant impact on the need for excess generation capacities and transmission and distribution infrastructure, but also on the rising environmental concerns from the electricity generation sector. One kW of power demand during peak demand hours is expected to lead to 65 kWh of electricity consumption (Siddiqui et al., 2008). Meanwhile, one kWh of electricity generation may incur 1.52 pounds carbon dioxide (CO_2) emissions (Environmental Protection Agency, 2014).

Luckily, demand-side energy management programs, such as Demand Response (DR) and Energy Efficiency (EE) programs, have been introduced and provide valuable opportunities to address energy, environmental, and economic concerns for energy end-users and energy providers simultaneously. EE programs aim to reduce the overall electricity consumption over the entire planning horizon. Unfortunately, EE programs may not always be able to address peak demand concerns. In particular, DR programs bring benefits to both electricity suppliers and electricity consumers by promoting environmental and economic sustainability through peak load management. More specifically, DR is defined by the Federal Energy Regulatory Commission (FERC) as "the changes in electricity usage by end-use customers from their normal consumption patterns in response to the changes in the price of electricity over time or the incentive payments designed to induce lower electricity use at times of high wholesale market prices or when system reliability is jeopardized" (Federal Energy Regulatory Commission, 2013). DR can help reduce the need for peak power plants which are built to satisfy the increasing electricity demand yet are only utilized a few hundred hours a year and require large financial investments (Kintner-Meyer et al., 2007).

Figure 1 summarizes the different DR programs. The two main types of programs are price-based programs and incentive programs. Price-based DR programs are such that the cost of electricity varies over time. These programs consist of Time-of-Use (TOU) rates, day-ahead hourly pricing, and real-time hourly pricing. Meanwhile, incentive-based DR programs are typically event driven. These programs consist of ancillary service programs, demand bidding/buyback, emergency programs, interruptible programs, and direct load control.

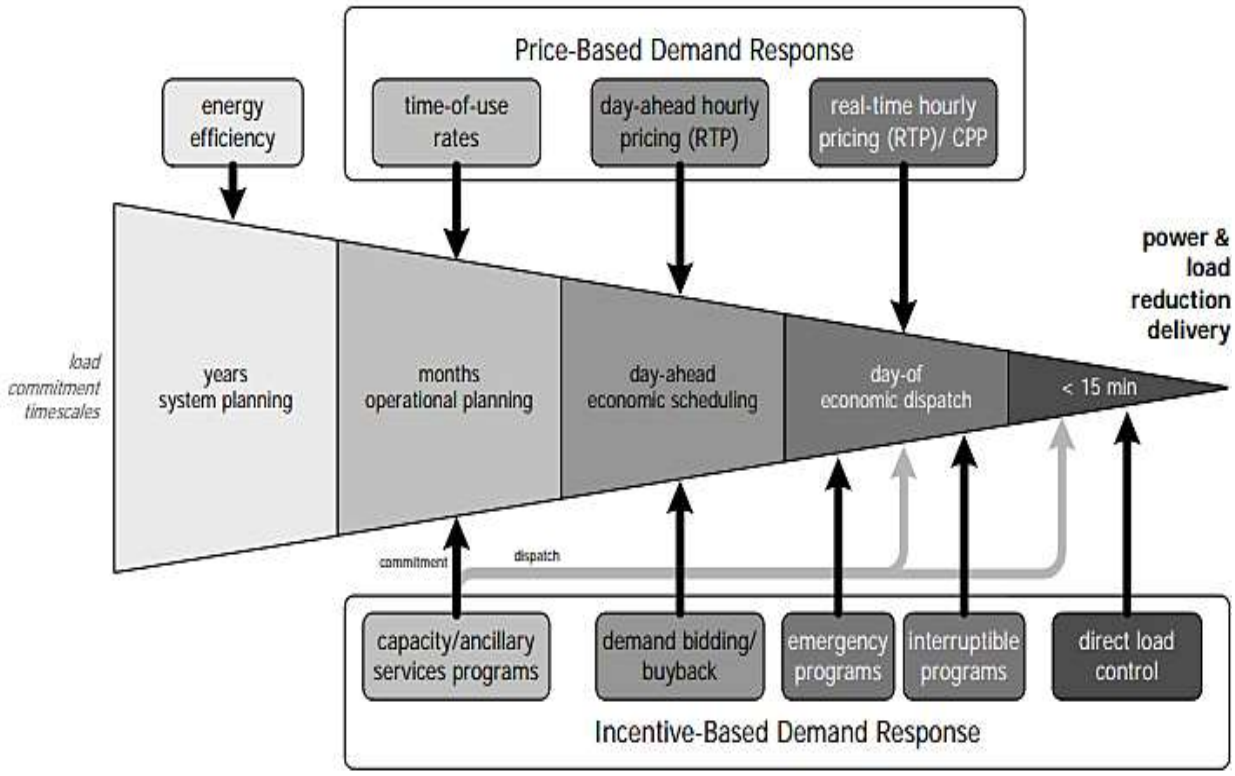

Figure 1 Demand Response Programs (U.S. Department of Energy, 2006)

To avoid the need to build excess power plants that are only used for a few hours a year, energy end-users can use DR programs to guide their energy management practices and policies. Accordingly, DR has been gaining more attention in industry and academia. However, the available research and technology is mainly geared toward building type loads (i.e. HVAC, lighting, and driers). Although such loads may be primary loads for commercial and residential electricity consumers, building type loads are minor for manufacturers where 87.8% of manufacturers total energy use is due to production related energy consumption (U.S. Department of Energy, 2010). Moreover, the majority of manufacturers' total energy consumption is wasted due to inefficient production system scheduling and idle time (Chang et al., 2013). This translates into excess operational costs for manufacturing, higher costs for consumer products, avoidable emissions, and supply and demand balancing burdens on energy providers.

Manufacturer adoption of DR programs alongside production scheduling decision making frameworks can address energy, environmental, and economic objectives from energy providers and end-users and stimulate sustainable manufacturing. Unfortunately, cost effective joint energy and production operations decision making and end-user DR for manufacturers' faces many challenges. To address the challenges and aid the technological readiness of manufacturers in implementing cost effective production and energy decision making and scheduling methodology for manufacturers is needed.

Nevertheless, even for a single product serial production line (the simplest and most fundamental production line), modeling complexity and solvability challenges are present since most production scheduling problems are nonlinear combinatorics and recognized to be NP-Hard (Hemmecke et al., 2010 and Yuan & Ghanem, 2016). Meanwhile, although maintenance and machine degradation dynamics have a significant impact on manufacturers' ability to participate

in DR, further adding energy and maintenance costs and constraint functions will lead to more complexity in the model formulation, solvability, and solution robustness. Hence, a system level decision making model for serial and/or dependent manufacturing processes within manufacturing production lines that can represent DR frameworks, energy demand, production dynamics, and maintenance requirements is needed.

Additionally, electricity metering and billing are typical done at the plant level. Depending on the manufacturing industry, a system-level production and energy management approach may not be sufficient if there are other interrelated systems within the manufacturing plant that are energy intensive. In such cases, it is valuable to establish methodology that links system-level and plant-level energy consumption and demand. Typical electric loads in manufacturing facilities come from production equipment, lighting, HVAC (Heating, Ventilation, and Air Conditioning), material handling, etc. In particular, HVAC energy consumption is one of the largest electricity consumers following the production system. Moreover, it can be controlled and is directly impacted by the production line's operational states. Integrating manufacturing production and HVAC scheduling can lead to added savings at the plant-level when implementing DR. To do this the manufacturing production line heat load considering convective and radiant heat from the production line must be modeled analytically. Meanwhile, the HVAC power demand must be represented as a function of the internal heat load from the production line.

Finally, manufacturers have a large impact on the cost and environmental sustainability of power utilities due to their large electricity demand (contributing to peak power) and large natural gas usage (due to the increasing dependency of the electricity sector on gas-fired generation). To support the adoption of end-user DR by manufacturers and facilitate manufactures' immersion in the SG, agile and utility aware manufacturing decision making methodology is needed in case of

DR program changes and to ensure that DR programs are in fact reaping economic and environmental sustainability benefits. Moreover, reactive manufacturing decision making is also necessary to help manufacturers overcome production disruptions hindering DR participation and aid manufacturers in leveraging event-based DR. Hence, integrated electricity and natural gas DR for manufacturers in the SG is needed. Moreover, real-time decision-making methodology for production scheduling problems must be established.

1.2 Literature Review

A literature review summarizing the research efforts related to cost effective joint energy and production operations decision making and end-user DR is presented. More specifically, the literature on joint maintenance and energy planning, plant level energy management, and SG oriented electricity and natural gas DR for manufacturers is discussed.

1.2.1 System Level Production, Energy, and Maintenance Management

Several research studies focusing on optimizing energy and environmental performance at the manufacturing processes have been conducted. For example, Winter et al. (2014) presents an approach to identify the process parameters that lead to Pareto-optimal solutions for advancing the eco-efficiency of grinding operations. Frigerio and Matta (2015) propose a framework for energy-efficient control of machine tools with stochastic arrivals. Bhushan (2013) proposes a model for selecting optimum cutting conditions for machining, based on minimum energy requirements and maximum tool life. Moreover, Mouzon and Yildirim (2008) present a framework to minimize the total energy consumption and total tardiness on a single machine using a greedy randomized adaptive search meta-heuristic.

Meanwhile, studies optimizing manufacturing energy consumption performance and peak power demand reduction, at the system level, considering multiple manufacturing processes have also been conducted. For example in Sun and Li (2013), the authors propose a dynamic energy control model for energy efficiency improvement of manufacturing systems using Markov decision process. Meanwhile, in Fernandez et al. (2013) the authors present a "Just-For-Peak" buffer for power demand reduction of manufacturing systems. Sun et al. (2014) propose inventory control methodology for peak power demand reduction and study the tradeoff between production loss and energy savings were studied. Additionally, Chang et al. (2013) studies the energy saving opportunity for serial automotive production lines and uses a quantitative analysis for identifying the energy saving opportunity. More detailed review on the research on energy and resource efficiency for discrete manufacturing can be found in Duflou et al., 2012.

While ample and promising, the aforementioned studies either focus on (1) the single process level and aim to identify the optimal process parameters within a manufacturing system so that the process energy consumption and/or carbon footprints can be minimized; or (2) solely on minimizing the energy related factors, such as energy consumption, energy cost, or power demand of the manufacturing system, while neglecting maintenance planning and machine degradation.

Maintenance is a critical component to consider when assessing the energy consumption and cost efficiency of a production system. Moreover, maintenance is essential to maintain and improve equipment reliability and production capability. Maintenance accounts for a substantial portion of the total operational cost and efficiency of the production system. Literature has illustrated that the maintenance cost for domestic plants had reached more than $600 billion in 1981; meanwhile, this figure has doubled in the past decades (Mobley, 2011). Not surprisingly,

research on effective maintenance decision making has drawn wide attention from both industry and academia. Several research studies on maintenance policies (Frenk et al., 1997; and Wang and Pham, 1999), diagnostics and prognostics (Dong and He, 2007; Wang et al., 2016; and He et al., 2011), and reliability modeling for degrading manufacturing equipment (Coit, 1997; Wang et al., 2012; and Ramírez-Márquez and Wei Jiang, 2006) can be found in literature. A more detailed review of the current research challenges and opportunities for these topics is summarized in (Jardine et. al, 2006; Wang, 2002; and Heng et al., 2009).

While the above-mentioned studies consider maintenance costs and constraints, energy considerations alongside to maintenance decision making are rarely considered. Nonetheless, two papers focusing on the opportunity window for maintenance and energy management, reveal the feasibility of jointly modeling decision making regarding both maintenance and energy. The first paper (Chang et al., 2007) analyzes a deterministic opportunity window for maintenance implementation in manufacturing systems without influencing production throughput. Next, Sun and Li (2013) investigate the energy saving opportunity window in manufacturing systems considering stochastic production factors without influencing system throughput. These papers study the time duration quantification for the opportunity windows of the machines in the manufacturing production line, which can be shut down for the purpose of maintenance and energy saving, respectively. More recently, Yao et al. (2015 and 2016) presents a simulation-based method to investigate the feasibility of joint energy and maintenance decision making in manufacturing systems and explores the potential benefits of such joint decision making using heuristic methods. Accordingly, maintenance activities were rescheduled while considering energy cost. Various rescheduling policies were simulated and maintenance cost, energy consumption cost, and throughput were investigated and compared. The results illustrate that with the appropriate policy,

joint energy and maintenance decision making in manufacturing can lead energy cost reduction and productivity improvement. Nevertheless, simulation-based methods have several drawbacks such as lack of flexibility, time-consuming model construction, and intractability for real-time application (Chang and Ni, 2009).

In all, the stated literature fails to consider research opportunities from an integrated planning and decision making perspective that comprehensively investigates system level energy profiles, production throughput, and machine degradation tradeoffs and constraints. This impedes joint energy, maintenance, and production management. Hence, an analytical method that can dually consider maintenance and energy costs and constraints as a function of production system dynamics is needed.

1.2.2 Plant Level Energy Management

Alongside to the production system, there may be other systems within the manufacturing plant that are influenced by the production system and are energy intensive. Plant-level manufacturing energy management is necessary since there may be other systems in the manufacturing plant that are influenced by the manufacturing system and will have an impact on the manufacturer's power demand profile. Solely controlling the production line's energy profile may not translate to direct changes in the manufacturing plant's energy profile.

Among the most common non-production related energy consumers within a manufacturing plant are building type loads. Detail on the different types of energy consumers and management practices for manufacturing plants can be found in Boyd et. al (2008). In this paper, the authors present a study on the ENERGY STAR® energy performance and benchmarking system for industrial manufacturing plants' energy use. Furthermore, they discuss examples from specific industry sectors and energy management conditions. Meanwhile, in Feng et al. (2016a),

the authors study energy, economy, and environmental characteristics of manufacturing plants and propose a method for optimizing the manufacturing plants energy supply system. Correspondingly, Feng et al (2016b) analyze and identify the factors influencing the energy consumption breakdown of automotive manufacturing plants. Nguyen and Aiello (2013) present a survey on intelligent energy control for building HVAC, lighting, and plug loads based on user activities. Braun (1990) develop a thermal storage utilization method to reduce the power demand of buildings during peak periods. Lastly, Ghislain and Mckane (2006) investigate the impact turning off unnecessary lights, fans, and motors, when production is off, or during peak periods alongside to HVAC system management in manufacturing plants.

In particular, HVAC energy consumption is among the most significant building-type electricity end-use activities. A great number of studies on HVAC system energy management, towards sustainability, have been conducted to reduce the electricity consumption and power demand for buildings. For example, Wang et al. (2012) propose a hierarchical multiagent control system with an intelligent optimizer to minimize the power consumption while considering customer comfort. Similarly, Corno and Razzak (2012) develop an approach that can intelligently find the balance between user requirements and energy saving opportunities for smart buildings. They consider user intentions and automatic control of device states. Liang et al. (2012) propose an optimal thermostat control policy that considers the tradeoff between customer comfort and energy cost for DR in residential buildings (Liang et al., 2012). Li et al. (2017) study effective power management modeling of aggregated HVAC loads with lazy state switching. Moreover, methodology for thermal storage utilization (Henze et al., 2004) and HVAC load prediction (Braun and Chaturvedi, 2002) can also be found in literature. In all, the aforementioned literature addresses HVAC energy, cost, and comfort objectives simultaneously. Unfortunately, while

valuable, these methods are not sufficient for manufacturing plants since HVAC heating and cooling loads may be influenced by manufacturing production dynamics and production equipment's operating states.

Recently, some initial investigations that integrate manufacturing production and HVAC system costs and energy management have been reported. For example, Liu et al. (2012) develop a simulation-based method for energy-efficient building design for manufacturing plants considering HVAC configurations and production characteristics. Moynihan et al. (2012) investigate the energy savings potential for a manufacturing facility by simulating the HVAC system and integrating it into the manufacturing plant's facility design. Ball et al. (2012) propose a framework for manufacturing plant design considering both the production system and building. Niefer and Ashton (1997) conduct a review of building related energy use for manufacturers by investigating the characteristics of the HVAC system and estimating energy intensity and energy saving potentials. While these studies are geared toward HVAC energy management in manufacturing facilities, they focus on the design stage and aim to identify the desired size, appropriate capability, and expected energy load of the HVAC system. Meanwhile, they fail to consider the operational states and integrated control of the two systems simultaneously.

In all, HVAC system management in manufacturing plants is typically performed independently from operating schedules of manufacturing production equipment. However, the production load is an internal heat load that must be considered in HVAC control strategies to achieve robust plant-level energy management; since the heat generated by the manufacturing production line may influence the HVAC load requirements. Although a simulation-based method integrating the two systems has been reported (Brundage et al., 2013); there lacks an analytical

model that can help manufacturers implement electricity DR by integrating scheduling frameworks for two interrelated systems.

1.2.3 Smart Grid Oriented Electricity and Natural Gas Demand Response for Manufacturers

The electric grid is a complex network of transmission lines, substations, and transformers that deliver electricity from power generation facilities to electricity end-users. Meanwhile, the SG moves the energy industry toward a more reliable and efficient power grid that promotes economic and environmental health. The SG provides energy stakeholders with the information and tools needed to make choices about energy use at both the supply and demand side through smart metering technology and DR programs. Nevertheless, while DR programs do offer guidelines for energy management, they cannot address dispatch and implementation needed to leverage the necessary information to realize the benefits of the SG. One method to do this is through DR research from the perspective of the energy end-user.

Many studies concentrating on DR from the perspective of energy end-users have been conducted. For example, in (Chai et al., 2014) the authors focus on end-user DR considering multiple utilities. They model residential energy users and utility companies using a two-level game. Through illustrative examples, they demonstrate that their proposed scheme is able to significantly reduce peak load and demand variation. In (Maharjan et al., 2016) the authors study DR for a large population regime. They introduce a hierarchical system model for decision making for multiple providers and customers, and establish a Stackelberg game between providers and end-users. The authors prove that there exists a unique number of providers that maximize profit and develop an iterative distribution algorithm. Next, in (Hansen et al., 2015) an aggregator-based residential DR tactic for SG resource allocation is developed. The aggregator must set an optimal schedule for residential customer assets. The aggregator profit is optimized using a heuristic

framework, which shows that the aggregator can achieve a desirable change in the load profile when optimizing their profit. More examples on DR can be found in (Vardakas et al., 2015), a survey paper on DR programs in Smart Gird with an emphasis on different pricing methods and optimization algorithms.

The aforementioned research focuses on residential and commercial electricity end-users rather than industrial energy users. More specifically, manufacturers have a large impact on the cost and environmental sustainability of power grid due to their large electricity demand (contributing to peak power) and large natural gas usage (due to the increasing dependency of the electricity sector on gas-fired generation). It is expected DR, for both electricity and natural gas, from large industrials can reap ancillary services at the transmission level (Cheng et. al, 2016 and Nistor, 2015). Some industrial sector specific DR driven production planning problems have been conducted (Bego et al., 2014; Sun et al., 2014; and Fernandez et al., 2013). Nevertheless, these papers either do not focus on the adaptability of such problems in the SG or consider a long term load scheduling approach defined by a set DR program. Hence, real-time and day to day input from the SG or changes in production are not considered. Also, these studies do not focus on the modeling complexity, problem solvability, and computational resources necessary for manufacturers to leverage the SG. Lastly, they fail to consider gas load management in the production and energy load scheduling models.

Natural gas is similar to electricity in that it goes through complex and limited distribution infrastructure. Moreover, gas utilities face supply and demand balancing challenges similar to those of electricity. Some studies on integrated electricity and natural gas supply and demand management have been conducted. In Zhang et al. (2016) the authors propose an integrated day-ahead scheduling model to dispatch hourly generation and load resources and deploy flexible

ramping for balancing intermittent renewable resources. Illustrative examples show that real-time natural gas delivery can directly impact hourly dispatch, flexible ramp deployment, and power system operation cost. Also, demand side participation can mitigate the dependency of electricity on natural gas by providing a viable option for flexible ramp when the natural gas system is inhibited. Zhang et al. (2017) present a planning model that minimizes cost for transmission lines and natural gas pipelines from interconnecting energy hubs based off of probabilistic reliability criteria. The authors find that, in contrast to single energy infrastructure planning, dually planning gas and electricity infrastructure enables a synergetic strategy to design multiple energy networks for optimizing the supply economics and satisfying reliability criteria. Next, in Qadrdan et al. (2017) the authors investigate the benefits of end-user DR in combined electricity and gas networks in Europe. They find that significant reduction in the capacity of new gas-fired power plants can be achieved due to electricity peak shaving. In turn, this reduces the need for imported gas by 90 million cubic meters of natural gas per day and leads to an estimated £60 billion in cost savings over a 50 year period. Furthermore, the authors stress that availability and cost of gas are crucial factors in power system planning. Finally, Li et al. (2013) develop a multi-agent problem for determining the TOU pricing structure for natural gas end-user load response for industrial and commercial gas customers. They find that optimally setting peak and valley prices for natural gas brings benefits to both the gas operator and gas users.

Inopportunely, these studies do not focus industrial end-users demand patterns as a function of production dynamics and constraints. While much research is present on DR, the current state of literature is not sufficient to realize promising benefits for industrial users and energy suppliers due to the following. First, most of the literature is not geared toward industrial energy customer's unique energy load dynamics. Current work is focused on residential and commercial type loads,

which cannot be used to describe manufacturing end-users. Modeling, solvability, and computation time are not considered in terms of SG needs for reactive decision making. Lastly, natural gas consuming manufacturing processes and their effect on supply/demand are not considered.

1.3 Research Framework and Thesis Organization

Based on the above motivation and literature review, the goal of this thesis is to provide manufacturers with a set of decision making tools for implementing cost effective production and energy management. Opportunities for sustainable manufacturing, from integrating DR programs and manufacturing production scheduling/operations decision making will be investigated, modeled, and optimized.

The proposed methodology and research framework integrates sustainable manufacturing, production scheduling, and electricity DR for manufacturers from three lenses, i.e., the manufacturing production system-level, the plant-level, and the utility-level. At the manufacturing production system-level, a comprehensive system level decision making strategy that considers production, energy, and maintenance is developed and analyzed. Meanwhile, the importance of including machine degradation dynamics and maintenance is illustrated. Next, for the plant-level lens, the system level perspective is broadened to consider the HVAC system. The HVAC energy consumption and production line heat load are studied and modeled. Finally, for the utility driven lens, a model that considers SG issued time-based and event based electricity and natural gas DR is presented. Figure 2 shows a schematic of the research framework.

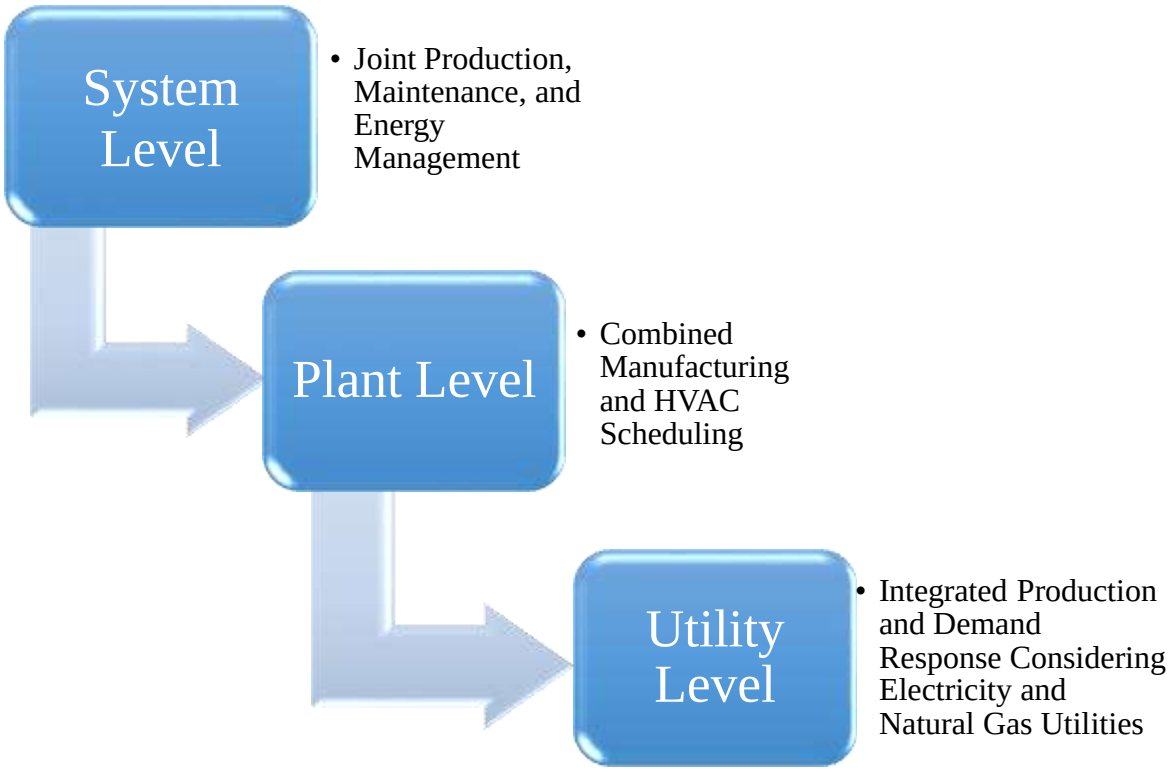

Figure 2 Research Framework

In all, the three proposed models provide a comprehensive set of tools for cost effective and sustainable production operations decision making models. This research will further advance the state of the art of research on joint energy and production decision making and provide manufacturers with analytical tools for implementing DR. Accordingly, the thesis is organized as follows. In Section 2, a model for joint production, maintenance, and energy management is presented. In Section 3, a combined manufacturing and HVAC scheduling model is developed and the heat generated by the production line is formulated. Furthermore, an integrated production and DR model considering electricity and natural gas utilities is developed in Section 4. A brief note to practitioners is presented in Section 5. Finally, the conclusions are drawn and future research tasks are discussed in Section 6.

2 Joint Production, Maintenance, and Energy Management

Parts of this chapter were previously published as: (1) “Sun, Zeyi, Fadwa Dababneh, and Lin Li. "Joint Energy, Maintenance, and Throughput Modeling for Sustainable Manufacturing Systems." *IEEE Transactions on Systems, Man, and Cybernetics: Systems* (2018). DOI: 10.1109/TSMC.2018.2799740.”. (2) “Dababneh, Fadwa, Lin Li, Rahul Shah, and Cliff Haefke. “Demand Response-Driven Production and Maintenance Decision-Making for Cost-Effective Manufacturing." *Journal of Manufacturing Science and Engineering* 140, no. 6 (2018): 061008.” and (3)“ Dababneh, Fadwa, Rahul Shah, Zeyi Sun, and Lin Li. "Framework and sensitivity analysis of joint energy and maintenance planning considering production throughput requirements." In *ASME 2017 12th International Manufacturing Science and Engineering Conference collocated with the JSME/ASME 2017 6th International Conference on Materials and Processing*, pp. V003T04A062-V003T04A062. American Society of Mechanical Engineers, 2017.”

with the JSME/ASME 2017 6th International Conference on Materials and Processing, pp. V003T04A062-V003T04A062. American Society of Mechanical Engineers, 2017.].

2.1 Objective and Overview

In this chapter, system level decision making methodology for serial and/or dependent manufacturing processes within manufacturing production lines that can represent DR frameworks, energy, production dynamics, and maintenance requirements simultaneously is presented. Since machine degradation and production capability are expected to have a significant impact on manufacturers' participation in DR, energy cost, and production throughput, they will be modeled analytically and the tradeoffs will be analyzed. Two models are presented. First a production scheduling model is formulated. Subsequently, an aggregate cost model is also presented.

For the production scheduling model, energy control and maintenance implementation are simultaneously considered to address the concerns of energy consumption, intelligent maintenance, and throughput improvement. Particle swarm optimization, with a local optimal avoidable mechanism and a time varying inertial weight, is used to solve the cost minimization problem and find a near optimal solution for the production and maintenance schedules. A numerical case study is implemented and the results show that the cost per unit production can be reduced significantly compared to the existing benchmark strategies. Meanwhile, for the aggregate cost model, production, maintenance, and DR parameters are considered in the same function and a factor analysis is performed.

The rest of this section is as follows. In Section 2.2 the joint energy, maintenance, and production scheduling problem is presented. Next, in Section 2.3 the aggregate cost model will is

derived. Meanwhile, Section 2.4 will present an illustrative case study and factor analysis. Lastly, Section 2.5 will conclude the chapter.

2.2 Methodology

To promote joint energy, production, and maintenance planning a demand response driven production and maintenance methodology is developed. A scheduling model is proposed and includes short term energy saving decision making and longer term maintenance decision making in the same optimization problem. Next, the aggregate cost model is derived from the proposed scheduling model and can be used to analyze the impact of various factors on the aggregate cost.

2.2.1 Nomenclature

Uppercase

B_{it}: buffer contents in buffer i at the beginning of interval t

C_i: maintenance cost of machine i per interval

$C^{ExtraCrew}$: cost of contracting one additional maintenance crew above MC per interval ($/crew)

$C^{Inventory}$: cost for storing one inventory unit ($/part)

C_{part}: cost per part produced ($/part)

$C^{Retrieval}$: the cost of retrieving one unit from an outside source ($/part)

CE: total electricity cost

CEM: total cost of extra maintenance crew resources ($)

CI: total inventory cost ($)

CR: total retrieved/outsourced products cost ($)

CM: total maintenance cost

CP: total benefit/cost of surpassing/falling short of the production target

CPD: power demand cost considering both production and maintenance activities

$CT_t(r(j_i))$: cumulative operation time that machine i stays in degradation state j_i with production efficiency $r(j_i)$ up to the beginning of interval t

CU_{it}^{IS} : cumulative inventory in the inventory space corresponding to buffer i during interval t (parts)

INV_{it} : amount of excess inventory incurred at buffer i during interval t (parts)

L: duration of the interval

$L(s)$: location matrix for an individual particle at iteration s from PSO

$L_{PB}(s)$: particle's best solution that has been identified up to the s^{th} iteration using PSO

$L_{GB}(s)$: global best solution that has been identified up to the s^{th} iteration using PSO

MC: number of maintenance crew resources

$MCEC$: total maintenance electricity consumption cost

MP_i: power consumption due to the maintenance tasks for machine i

MPD_t: total power demand due to maintenance tasks during time interval t

N: total number of machines in the production line

P_i: rated power of machine i

P^*: total number of particles in the swarm, i.e., total population in PSO

$P^* - p$: number of particles following avoidance PSO, i.e., population 2

PA: committed power limitation

$PCEC$: production electricity consumption cost

PD: power demand of the entire system

PPD_t: power demand from the machines due to production during time interval t

PR_i: production rate of machine i

REC_t: electricity consumption rate ($/kWh) for interval t

RET_{it}^{InBS} : number of units retrieved from an outside supplier (parts)

RET_{it}^{IS} : number of units retrieved from the inventory space (parts)

RPD: power demand rate ($/kW)

S_i: maximum capacity of buffer i

T: total number of time intervals in the planning horizon

TA: target production throughput

$TD(r(j_i))$: duration of the operation time that machine i stays in degradation state j_i before entering into next degradation state $(j+1)_i$

TP: production throughput of the manufacturing system for the entire production horizon

$V(s)$: velocity matrix for an individual particle at iteration s from PSO

Lowercase

a: penalty rate due to production loss

b: bonus rate due to additional production throughput

c_1 and c_2: learning factors from PSO

$l(s)$: avoidance coefficient during iteration s from PSO

p: number of particles following standard PSO, i.e., population 1 in PSO

r_{it}: production efficiency of machine i during interval t

r_i^{th}: threshold production capability of machine i at which maintenance task can be assigned (%)

$r(j_i)$: production efficiency of machine i in degradation state j_i

w_i: setup time of machine i after maintenance

w_1 and w_2: random real numbers between zero and one

Decision Variables

x_{it}: binary decision variable to denote the ON/OFF decision for machine i in interval t.

y_{it}: binary decision variable to represent the maintenance decision for machine i in interval t.

Greek Letters

$\alpha(s)$: inertial weight during iteration s for PSO

α_{max}: maximum inertial weight value for PSO

α_{min}: minimum inertial weight value for PSO

Δr_i: difference in the production efficiency between each pair of adjacent degradation states for machine i

δ_{it}: the percentage of time machine i is available to produce during interval t after considering setup time due to maintenance

$\gamma(s)$: avoidance rate during iteration s for PSO

Indices

i: index of machines

j_i: index of the degradation states of machine i

m: index representing the particles in population 1 of the PSO, $m \epsilon \{1,2,\ldots,p\}$

n: index representing the particles in population 2 of the PSO, $n \epsilon \{p+1,\ldots,P^*\}$

o: index representing the particles in total population of the PSO, $o \epsilon \{1,2,\ldots,P^*\}$

s: index of PSO iterations

s_{max}: index of the final iteration in the PSO
t: index of time intervals
Sets
OP: set of intervals that belong to on peak period

2.2.2 Problem Formulation

The problem is formulated according to the following. The manufacturer needs to determine a production schedule and maintenance plan under a TOU electricity DR program throughout the planning horizon considering energy cost, production throughput, and machine degradation. In the TOU electricity tariff program, the manufacturer is charged an electricity consumption rate ($/kWh) and power demand rate ($/kW/h). The electricity consumption rate varies over time depending on when peak demand hours occur. The power demand rate is applied to the maximum power demand (kW) of all the discretized intervals that occur during peak hours. Moreover, a maintenance cost is incurred each period that a maintenance task is scheduled ($/interval).

It is assumed that the manufacturing production line is a serial production line with N machines and N-1 buffers as shown in Figure 3. The production horizon is discretized into a set of intervals with a fixed duration L. All production and maintenance decisions are made at the beginning of each interval. Meanwhile, the degradation of the machines in the manufacturing system is described by the production efficiency, which is defined as the percentage of the actual production time (after deducting possible random failures due to degradations) per interval.

Figure 3 Serial Production Line

The degradation of the machine is reflected by the drop in production efficiency. We assume that such an efficiency decrease is known and deterministic throughout the time horizon; and follows the pattern shown in Figure 4. The machine's production efficiency will degrade to lower state with a lower production efficiency after staying at its current production efficiency for a given duration (in interval units). The production efficiency of each degradation state and the duration that the machine will operate in each degradation state are assumed to be known and deterministic. While simplified, this degradation model is widely used in industry due to its ease of understanding, available data, and straightforward modeling. The simplified degradation pattern can be obtained from historical or empirical data. Such a model is mainly geared toward the plants lacking high automation capabilities that are needed for sampling reliability related signals or features for building advanced degradation models.

Figure 4 Machine Degradation Illustration

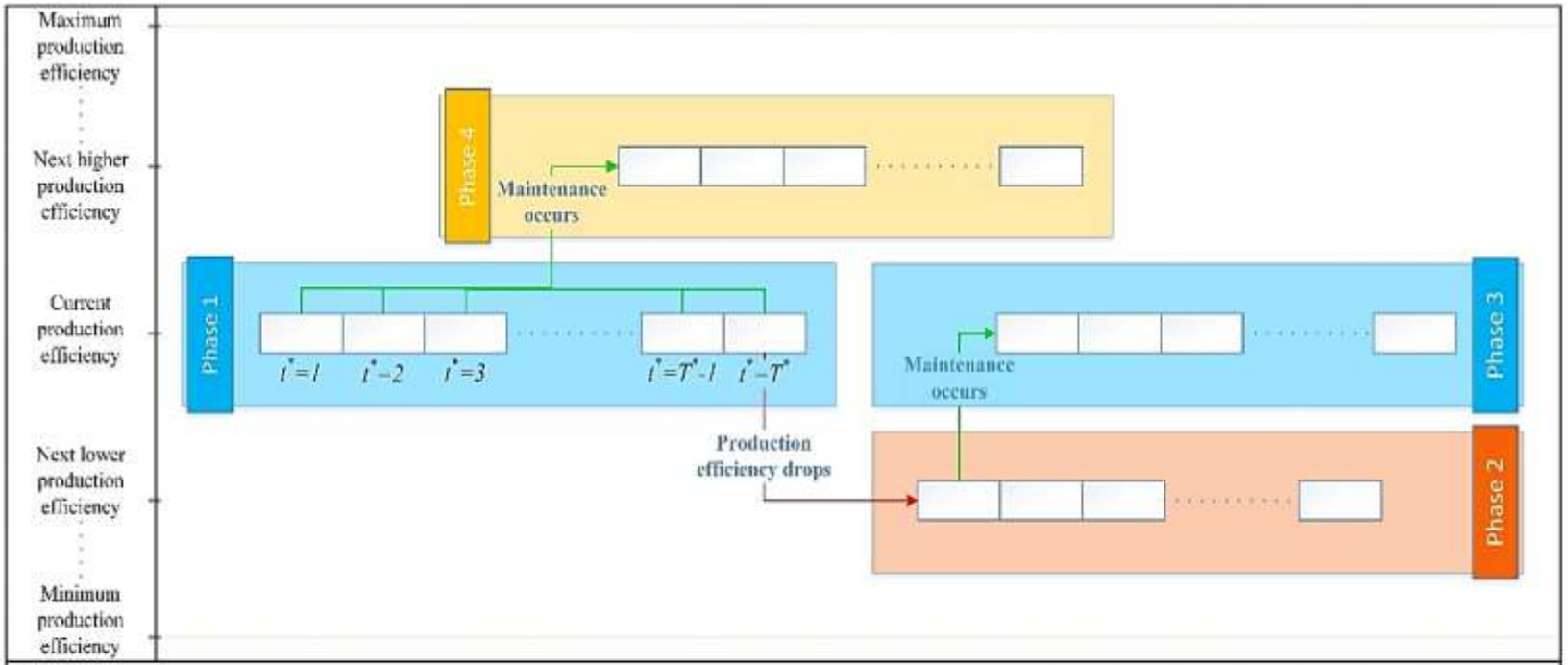

Key:
- **Phase 1:** is the phase where machine is in current production efficiency.
- **Phase 2:** is the phase where machine drops to next lower production efficiency if the machine in Phase 1 has operated for set number of intervals for current production efficiency.
- **Phase 3:** is the phase where machine can continue to stay in production efficiency of Phase 1 if maintenance operation is carried out at the beginning of Phase 2.
- **Phase 4:** is the phase where machine enters next higher production efficiency if maintenance operation is carried out at any interval in Phase 1.

In addition, we assume that the duration of the machines' random failures (or corrective maintenance) is relatively short compared to the duration of the slotted time interval. Moreover, we assume that corrective maintenance can restore the machine degradation state to the one before failure without influencing the production efficiency evolution of the machine. We also assume Δr_i, the difference in production efficiency between each pair of adjacent degradation states for machine i, is constant for machine i. Δr_i can be calculated by (2.1)

$$\Delta r_i = r((j-1)_i) - r(j_i), \quad j = 2, ..., J \tag{2.1}$$

Moreover, for simplicity, we also assume that the production efficiency improvement that can be achieved by maintenance for machine i in one interval is the same as Δr_i. The production efficiency of machine i during interval t, r_{it}, can be calculated by (2.2).

$$r_{it} = \begin{cases} r_{i(t-1)}, & if\ CT_t(r(j_i)) < TD(r(j_i)) \text{ and } y_{i(t-1)} = 0 \\ r_{i(t-1)} - \Delta r_i, & if\ CT_t(r(j_i)) = TD(r(j_i)) \text{ and } y_{i(t-1)} = 0 \\ r_{i(t-1)} + \Delta r_i, & if\ y_{i(t-1)} = 1 \end{cases} \tag{2.2}$$

In (2), $TD(r(j_i))$ is the number of operating intervals machine i stays in degradation state j_i before entering into the next degradation state $(j+1)_i$. The term operation time refers to the time the machine is not shut down for energy saving or maintenance activities. Hence, an operation interval includes both working and repair periods due to random failures. The cumulative operation time that machine i stays in degradation state j_i with a production efficiency of $r(j_i)$ up to the beginning of interval t, $CT_t(r(j_i))$, can be calculated by (2.3)

$$CT_t(r(j_i)) = \begin{cases} CT_{t-1}(r(j_i)) + 1 \cdot x_{i(t-1)}, & if\ CT_{t-1}(r(j_i)) < TD(r(j_i)) \text{ and } y_{i(t-1)} = 0 \\ 0, & if\ CT_t(r((j-1)_i)) = TD(r((j-1)_i)) \text{ or } y_{i(t-1)} = 1 \end{cases} \tag{2.3}$$

The initial conditions for r_{it} and $CT_t(r(j_i))$ are shown in (2.4) and (2.5), respectively.

$$r_{i1} = r(1_i), \quad \forall i \tag{2.4}$$

$$CT_1(r(1_i)) = 0, \forall i \tag{2.5}$$

Let x_{it} be the binary decision variable to denote the ON/OFF decision for machine i in interval t. It takes the value of one if machine i is on in interval t, and zero otherwise. Similarly, y_{it} is the binary decision variable that represents the maintenance decision. It takes the value of one if machine i is scheduled for maintenance in interval t, and zero otherwise. Maintenance can only be conducted when machine i is shut down. Two different problems are formulated as follows. Problem 1 aims to minimize the total cost including maintenance and electricity billing cost under the constraint of production throughput. Problem 2 relaxes the production target constraint and integrates it into the objective function, i.e., the objective is to minimize the overall cost including electricity billing cost, maintenance cost, and penalty cost due to throughput loss. Based on the above description and assumptions, **Problem 1** can be formulated by objective function (2.6) and constraints (2.7)-(2.13).

$$\min_{x_{it},\, y_{it}} (CM + CE) \tag{2.6}$$

$$s.t.\ \ PD \le PA \tag{2.7}$$

$$\sum_{i=1}^{N} y_{it} \le MC, \ \ \forall t \tag{2.8}$$

$$0 \le B_{it} \le S_i, \ \ i = 1, ..., N-1, \forall t \tag{2.9}$$

$$y_{it} \cdot x_{it} = 0, \forall i, \forall t \tag{2.10}$$

$$r(J_i) \le r_{it} \le r(1_i), \forall i, \forall t \tag{2.11}$$

$$(r_{it} - r_i^{th}) \cdot y_{it} \le 0, \ \ \forall i, \forall t \tag{2.12}$$

$$TP \ge TA \tag{2.13}$$

Similarly, **Problem 2** can be formulated by objective function (2.14) and constraints (2.7)-(2.12).

$$\min_{x_{it}, y_{it}} (CM + CP + CE) \tag{2.14}$$

$$s.t. \ \ PD \le PA \tag{2.7}$$

$$\sum_{i=1}^{N} y_{it} \le MC, \ \ \forall t \tag{2.8}$$

$$0 \le B_{it} \le S_i, \ \ i = 1, ..., N-1, \forall t \tag{2.9}$$

$$y_{it} \cdot x_{it} = 0, \forall i, \forall t \tag{2.10}$$

$$r(J_i) \le r_{it} \le r(1_i), \forall i, \forall t \tag{2.11}$$

$$(r_{it} - r_i^{th}) \cdot y_{it} \le 0, \ \ \forall i, \forall t \tag{2.12}$$

In (2.6) and (2.14), the maintenance cost, *CM*, is formulated as shown in (2.15).

$$CM = \sum_{t=1}^{T} \sum_{i=1}^{N} (1 - x_{it}) \cdot y_{it} \cdot C_i \tag{2.15}$$

The throughput cost, *CP*, formulated in (2.16), is defined as the benefit/penalty of surpassing/falling short of the production target. It can take a negative value if the target production throughput is exceeded.

$$CP = a \cdot \max(TA - TP, 0) - b \cdot \max(TP - TA, 0) \tag{2.16}$$

The throughput throughout the planning horizon, *TP*, can be formulated by (2.17).

$$TP = \sum_{t=1}^{T} (1 - y_{Nt}) \cdot x_{Nt} \cdot \delta_{Nt} \cdot PR_N \cdot r_{Nt} \cdot L \tag{2.17}$$

Meanwhile, the general formulation for δ_{Nt}, i.e., δ_{it}, is shown in (2.18).

$$\delta_{it} = \begin{cases} 1, \text{ if } y_{i(t-1)} = 0 \text{ and } y_{it} = 0 \\ 1 - \left(w_i / L \right), \text{ if } y_{i(t-1)} = 1 \text{ and } y_{it} = 0 \end{cases} \tag{2.18}$$

In (2.18) it is assumed that setup is required for a machine after undergoing maintenance; meanwhile, when the machine resumes operation after being shut down for energy savings, the setup time is assumed to be negligible.

Next, the electricity billing cost, *CE*, is shown in (2.19) and consists of the cost of electricity used by the machines for production, the cost of electricity consumption due to the maintenance tasks, and the cost due to the power demand.

$$CE = PCEC + MCEC + CPD \tag{2.19}$$

PCEC, *MCEC*, and *CPD* can be formulated by (20)-(22), respectively.

$$PCEC = \sum_{t=1}^{T} (REC_t \cdot L \cdot PPD_t) \tag{2.20}$$

$$MCEC = \sum_{t=1}^{T} (REC_t \cdot L \cdot MPD_t) \tag{2.21}$$

$$CPD = RPD \cdot \max_{t \in \mathbf{OP}} (PPD_t + MPD_t) \tag{2.22}$$

PPD_t and MPD_t can be calculated using (23) and (24) respectively.

$$PPD_t = \sum_{i=1}^{N} x_{it} \cdot P_i \cdot \delta_{it} \tag{2.23}$$

$$MPD_t = \sum_{i=1}^{N} MP_i \cdot y_{it} \tag{2.24}$$

Constraints (2.7)-(2.13) are explained as follows. Constraint (2.7) describes that the power demand, *PD,* during peak periods needs to be below the committed power demand, *PA*. *PD* can be calculated by

$$PD = \max_{t \in \mathbf{OP}} (PPD_t + MPD_t) \tag{2.25}$$

Constraint (2.8) describes that the total number maintenance tasks that can be performed in one interval cannot be larger than the number of maintenance resources available, *MC*. We assume that one maintenance resource can only conduct the maintenance task for one machine during a given interval. Constraint (2.9) describes that the buffer contents for each buffer location should be maintained in the range of zero and respective capacities. B_{it} can be calculated by (2.26)

$$B_{it} = B_{i(t-1)} + x_{i(t-1)} \cdot \delta_{i(t-1)} \cdot PR_i \cdot r_{i(t-1)} \cdot L - x_{(i+1)(t-1)} \cdot \delta_{(i+1)(t-1)} \cdot PR_{i+1} \cdot r_{(i+1)(t-1)} \cdot L \tag{2.26}$$

Constraint (2.9) and equation (2.26) are used to exclude the occurrence of "blockage" (when buffer stock reaches its capacity and the upstream machine cannot produce) and "starvation" (when buffer stock is zero and the downstream machine cannot produce). Here it is assumed that the machine will take the required amount of buffer contents in one batch from the upstream buffer at the beginning of each interval for the production of the entire interval. Meanwhile, the parts, after being processed by the machine, will be delivered to the downstream buffer, in one batch, at the end of the interval. Constraint (2.10) describes that the maintenance can only be implemented when machine *i* is shut down. Constraint (2.11) describes that the lower bound and upper bound

of the production efficiency of machine *i* cannot be exceeded. Constraint (2.12) describes that the maintenance task cannot be assigned if the production efficiency of the machine *i* has not reached a threshold value, r_i^{th}. Constraint (2.13) describes the production target, *TA*, needs to be satisfied in Problem 1.

Finally, to solve the Problems 1 and 2, Particle Swarm Optimization (PSO) is used to obtain a near optimal solution for the production and maintenance schedules. In the PSO search procedure, the entire swarm is divided into two populations based on avoidance rate, γ(*s*), which can be calculated iteratively using (27).

$$\gamma(s) = \begin{cases} rand(0,1), & \text{if } s < 0.75 \times s_{\max} \\ 1, & otherwise \end{cases} \tag{2.27}$$

The number of particles that perform the standard PSO, i.e., population 1 are shown by $p = round\left(P^* \times \gamma(s)\right)$. Meanwhile, the number of particles that perform local avoidable PSO, i.e., population 2, are shown by $P^* - p$. The velocities for the particles that belong to the two above populations are updated according to (2.28) and (2.29), respectively.

$$V_m(s+1) = \alpha(s)V_m(s) + c_1 w_1(L_{PB_m}(s) - L_m(s)) + c_2 w_2(L_{GB}(s) - L_m(s)) \quad \text{where } m \in \{1, 2, \ldots, p\} \tag{2.28}$$

$$V_n(s+1) = \alpha(s)V_n(s) - l(s)\{w_1(L_{PB_n}(s) - L_n(s)) + w_2(L_{GB}(s) - L_n(s))\} \quad \text{where } n \in \{p+1, \ldots, P^*\} \tag{2.29}$$

$\alpha(s)$ is the time varying inertial weight at iteration *s*. It is bounded by the minimum ($\alpha_{\min}$) and maximum ($\alpha_{\max}$) values. In the first iteration, $\alpha(s)$ is at the specified maximum and then with each iteration it drops according to equation (2.30) so that in the last iteration, it will take the value of the specified minimum. When the inertial weight is high, the search for the optimal solution is

more global and spread out until the general region where the optimal solution lies is determined. Then, as the inertial weight decreases, more localized search to find the optimal solution is conducted.

$$\alpha(s) = \alpha_{max} - \left(\frac{\alpha_{max} - \alpha_{\min}}{s_{max}} \right) s \tag{2.30}$$

$l(s)$ in (2.29) is defined as the "avoidance coefficient" and calculated according to (2.31).

$$l(s) = 2\left(1 - \frac{s}{s_{\max}}\right) \tag{2.31}$$

Additionally, the particles in the two populations update their positions using (2.32).

$$\begin{aligned} &L_o(s+1) = L_o(s) + V_o(s+1) \\ &\text{where } o \in \{1, 2, ..., P^*\} \end{aligned} \tag{2.32}$$

The initial velocity $V(s=1)$ for each particle is randomly generated from the set {-1, 0, 1}. Since both V and L are updated using real numbers, further steps as shown in (2.33) and (2.34) are needed to make V and L be in set {-1, 0, 1} and {0, 1}, respectively.

$$V(s+1) = \begin{cases} -1, & \text{if } V(s+1) < -0.5 \\ 0, & \text{if } -0.5 \le V(s+1) \le 0.5 \\ 1, & \text{if } V(s+1) > 0.5 \end{cases} \tag{2.33}$$

$$L(s+1) = \begin{cases} L(s) + V(s+1), \text{ if } 0 \le L(s) + V(s+1) \le 1 \\ 0, \text{ if } L(s) + V(s+1) < 0 \\ 1, \text{ if } L(s) + V(s+1) > 1 \end{cases} \tag{2.34}$$

The initialized energy control submatrix consists of all the elements with a value of one. Note that randomly drawing a number from the set {0, 1} to initiate the energy control submatrix may greatly decrease the number of feasible solutions due to constraint (2.9). Likewise, the initialized maintenance planning submatrix consists of all the elements with a value of zero. Note

that it is necessary to use zero due to constraint (2.10), otherwise the number of feasible solutions will be dramatically reduced.

The fitness function for individual particle is shown in (2.35) for Problem 1, with constraints (2.7)-(2.13) integrated as penalty terms. Similarly, for Problem 2, the fitness function is shown in (2.36), with constraints (2.7)-(2.12) integrated as penalty terms.

$$\begin{aligned} & CE + CM + A_1 \cdot [\min(PA - PD, 0)]^2 + A_2 \cdot \sum_{t=1}^{T} [\min(MC - \sum_{i=1}^{N} y_{it}, 0)]^2 \\ & + A_3 \cdot \sum_{t} \sum_{i=1}^{N-1} [\min(S_i - B_{it}, 0)]^2 + A_4 \cdot \sum_{t} \sum_{i=1}^{N-1} [\min(B_{it}, 0)]^2 \\ & + A_5 \cdot \sum_{t=1}^{T} \sum_{i=1}^{N} x_{it} \cdot y_{it} + A_6 \cdot \sum_{t=1}^{T} \sum_{i=1}^{N} [\min(r_{it} - r(J_i), 0)]^2 \\ & + A_7 \cdot \sum_{t=1}^{T} \sum_{i=1}^{N} [\max((r_{it} - r_i^{th}) \cdot y_{it}, 0)]^2 + A_8 \cdot [\min(TP - TA, 0)]^2 \\ & + A_9 \cdot \sum_{t=1}^{T} \sum_{i=1}^{N} [\min((r(1_i) - r_{it}), 0)]^2 \end{aligned} \tag{2.35}$$

$$\begin{aligned} & CM + CE + CP + A_1 \cdot [\min(PA - PD, 0)]^2 + A_2 \cdot \sum_{t=1}^{T} [\min(MC - \sum_{i=1}^{N} y_{it}, 0)]^2 \\ & + A_3 \cdot \sum_{t} \sum_{i=1}^{N-1} [\min(S_i - B_{it}, 0)]^2 + A_4 \cdot \sum_{t} \sum_{i=1}^{N-1} [\min(B_{it}, 0)]^2 \\ & + A_5 \cdot \sum_{t=1}^{T} \sum_{i=1}^{N} x_{it} \cdot y_{it} + A_6 \cdot \sum_{t=1}^{T} \sum_{i=1}^{N} [\min(r_{it} - r(J_i), 0)]^2 \\ & + A_7 \cdot \sum_{t=1}^{T} \sum_{i=1}^{N} [\max((r_{it} - r_i^{th}) \cdot y_{it}, 0)]^2 + A_8 \cdot \sum_{t=1}^{T} \sum_{i=1}^{N} [\min((r(1_i) - r_{it}), 0)]^2 \end{aligned} \tag{2.36}$$

where $A_1, A_2, \ldots$, and A_9 are nine large real numbers.

2.3 Aggregate Cost Model

The cost per part model can provide manufacturers and decision makers with a tool for assessing the performance of the above formulated joint energy, production, and maintenance scheduling model in an aggregate manner and aid higher level production decision making such

as determining annual production levels, TOU contracts, maintenance costs, etc. It can also be used to evaluate the impact of any deviations or changes in system parameter values due to system changes, limited data, and inaccurate parameter estimation. Accordingly, the aggregate cost model is derived from Problem 2 in Chapter 2.2.

The cost per part is denoted by C_{part} and formulated in (2.37), where inventory and additional maintenance crew cost functions are incorporated in the aggregate cost model.

$$C_{part} = \frac{CM + CE + CP + (CI + CR + CEM)}{TP} \tag{2.37}$$

CI, *CR*, and *CEM* are the inventory cost, retrieved/outsourced products cost, and the cost of extra maintenance crew resources, respectively. These cost functions are incorporated in the formulation for C_{part} to accommodate buffer or maintenance constraint violations; which are considered as non-strict constraints.

The inventory cost, *CI*, adjusts for excess inventory holding requirements that exceed buffer maximum capacities. The retrieved/outsourced cost, *CR*, is the cost of outsourcing due to empty buffer conditions. The extra maintenance crew cost, *CEM*, accounts for the cost when extra maintenance crew resources, above the level of *MC*, are required. Correspondingly, *CI* is shown by (38),

$$CI = \sum_{i=1}^{N-1} \sum_{t=1}^{T} INV_{it} \cdot C^{Inventory} \tag{2.38}$$

where $C^{Inventory}$ is the cost of storing one inventory unit and INV_{it} is the amount of excess inventory incurred at buffer *i* during interval *t*. INV_{it} is given by (39).

$$INV_{it} = \begin{cases} B_{it} - S_i, & if \ B_{it} > S_i \\ 0, & if \ 0 \le B_{it} \le S_i \end{cases} \tag{2.39}$$

Also, the cost of outsourced/retrieved parts due to buffer capacity shortage is given by (40), where $C^{Retrieval}$ is the cost of retrieving one unit from an outside source.

$$CR = \sum_{i=1}^{N-1} \sum_{t=1}^{T} RET_{it}^{InBS} C^{\text{Retrieval}} \tag{2.40}$$

RET_{it}^{InBS} represents the number of units retrieved from an outside supplier. For CR, additional production units are needed whenever the contents of buffer i during interval t fall below zero. However, the case in which additional units needed can be supplied (at no cost) from the inventory space incurred prior to interval t also needs to be considered. Accordingly, CU_{it}^{IS} represents the cumulative inventory in the inventory space corresponding to buffer i during interval t and is shown in (2.41),

$$CU_{it}^{IS} = CU_{i(t-1)}^{IS} + INV_{it} - RET_{it}^{IS} \tag{2.41}$$

where RET_{it}^{IS} is the number of units retrieved from the inventory space. When $CU_{it}^{IS} = 0$ the additional units needed are obtained from an outside supplier (outsourced). Thus, the number of units retrieved from the inventory space (RET_{it}^{IS}) and the number of units outsourced when the in-house inventory has depleted to zero (RET_{it}^{InBS}), are shown in (42) and (43), respectively.

$$RET_{it}^{IS} = \begin{cases} -B_{it}, & if\ B_{it} < 0 \text{ and } CU_{it}^{IS} \geq -B_{it} \\ CU_{it}^{IS}, & if\ B_{it} < 0 \text{ and } 0 < CU_{it}^{IS} < -B_{it} \\ 0, & if\ (B_{it} < 0 \text{ and } CU_{it}^{IS} = 0) \text{ or } 0 \leq B_{it} \leq S_i \end{cases} \tag{2.42}$$

$$RET_{it}^{InBS} = \begin{cases} -B_{it}, & if\ B_{it} < 0 \text{ and } CU_{it}^{IS} = 0 \\ -B_{it} - CU_{it}^{IS}, & if\ B_{it} < 0 \text{ and } 0 < CU_{it}^{IS} < -B_{it} \\ 0, & if\ (B_{it} < 0 \text{ and } CU_{it}^{IS} \geq -B_{it}) \text{ or } 0 \leq B_{it} \leq S_i \end{cases} \tag{2.43}$$

Because the buffer constraints have been incorporated in the aggregate cost model by considering inventory and outsourced product costs, B_{it} is permitted to assume negative values to represent buffer shortages. However, $RET_{it}^{IS} = -B_{it} \geq 0$ and $RET_{it}^{InBS} = -B_{it} \geq 0$ restrictions are emplaced. Finally, the cost of extra maintenance crew requirements is given in (2.44) and denoted by *CEM,* where $C^{ExtraCrew}$ is the cost of contracting one additional maintenance crew resource above *MC* per interval. Since the production schedule does not consider system parameter value uncertainty, *CI*, *CR*, and *CEM* are necessary to achieve feasible production plans.

$$CEM = \sum_{t=1}^{T} \max(0, \sum_{i=1}^{N} y_{it} - MC) \cdot C^{ExtraCrew} \tag{2.44}$$

2.3 Case Study, Results, and Analysis

In this section a case study to show the effectiveness of the proposed method is presented. First, the production scheduling case setup and PSO optimization procedure will be discussed. Next, the optimization results will be compared to baseline cases. Lastly, a factor analysis considering the aggregate cost model is presented.

2.3.1 Production Scheduling Case Setup

To illustrate the effectiveness of the proposed model, a numerical case study is implemented. We consider a manufacturing system that consists of five machines and four buffers. The parameters of each machine including the production rate, rated power, and setup time are shown in Table 1. The parameters of each buffer, including initial contents and buffer capacity, are shown in Table 2. The time horizon is an 8-hour shift (from 7:00 AM-3:00 PM) over the span of a 5-day week, slotted into 160 15-minute intervals. The peak period is from 1:00 PM to 3:00 PM for

all days of the week. The TOU tariff program consists of both a demand charge and a consumption charge as summarized in Table 3. Finally, the production target for the week is 1400 parts.

Table 1 Basic Machine Parameters for Chapter 2

Machine	Production Rate (parts/interval)	Rated Power (kW)	Setup Time (minutes)
1	12.5	15	3
2	12.5	17	2
3	12.5	24	2.5
4	12.5	17	4
5	12.5	21	2

Table 2 Basic Buffer Parameters for Chapter 2

Buffer	Initial	Capacity
1	70	160
2	70	145
3	50	140
4	75	160

Table 3 TOU Tariff Program for Chapter 2.3

Time of Day	Consumption Rate ($/kWh)	Demand Rate ($/kW)
7:00AM-1:00PM	0.08274	0
1:00PM-3:00PM	0.1679	18.8

The maintenance related parameters are set as follows. Δr_i is 0.05. The maximum and minimum production efficiencies are 0.95 and 0.65, respectively. The cost and the power required to perform a maintenance activity are shown in Table 4. Moreover, the initial production efficiency/degradation states, as well as maximum time that each machine can stay in each

degradation state are shown in Table 5 (for simplicity, we assume that this time is equal for all of the degradation states of a machine). The number of maintenance crew resources, *MC*, is 2.

Table 4 Maintenance Task Cost and Required Energy

Machine	Maintenance Cost per Interval ($/interval)	Power (kW)
1	15	1.5
2	25	2
3	20	2
4	18	1.5
5	22	2

Table 5 Machine Production Efficiency State Parameters

Machine	Initial Production Efficiency	Maximum Intervals Machine Can Stay in Each Degradation State
1	0.90	12
2	0.85	8
3	0.90	12
4	0.90	10
5	0.90	12

This case study considers the following five scenarios as shown in Table 6. For Scenario I, there is no dynamic energy control action implemented (all x_{it} are set to be one), while the maintenance is triggered by a threshold production efficiency. Next, Scenario II uses energy saving opportunities to implement maintenance. In other words, priority is given to energy saving actions while maintenance scheduling is secondary, i.e., all x_{it} will be determined by minimizing the electricity billing cost and the maintenance will be scheduled for those machines in off intervals. When the production efficiency of a machine drops to a value lower than a threshold value, the machine can be scheduled for maintenance. Scenario III implements the energy and maintenance

control separately. x_{it} will be obtained by minimizing the electricity billing cost under the constraint of production target, and the maintenance is triggered at a threshold production efficiency. Scenario IV implements the proposed joint production, maintenance, and energy model based on Problem 1. Scenario V implements the joint production, maintenance, and energy model based on Problem 2.

Table 6 Summary of Different Scenarios

Scenario	Description
I	No energy control, production efficiency triggered maintenance
II	Optimal energy control, maintenance will be confined to those off machines considering threshold production efficiency
III	Energy control and maintenance are implemented separately
IV	Joint energy, maintenance and throughput control using Problem 1
V	Joint energy, maintenance and throughput control using Problem 2

In a more practical sense, Scenario I can be considered a baseline model that is adopted by most industrial practitioners to maintain equipment reliability and improve productivity. Scenario II can be considered a naïve joint model, which tries to utilize the energy saving opportunities for maintenance. The energy driven production scheduling strategies for DR in both Scenarios II and III have been widely studied by academia due to the increasing concerns of environmental protection and climate change. As for industrial practitioners, the significance of the energy driven

scheduling method has also been gradually recognized and many manufacturers, especially those who are charged by typical TOU electricity rates, have started to adopt such methods. It is expected that energy driven production scheduling will be widely used in the near future. Therefore, these two scenarios as well as Scenario I are used as the benchmark to demonstrate the benefits from adopting the proposed model reflected by Scenarios IV and V.

For Scenarios I and III, the threshold production efficiency is 0.7 for all machines. Once the threshold value is reached, maintenance is triggered until the production efficiency is restored to 0.9. If more than two machines reach the threshold value of 0.7, the priority of maintenance will be determined randomly. For Scenario II, the threshold production efficiency is 0.7, which is applied to the machines that are shut down for energy saving; however, the production efficiency may not be restored to a production efficiency of 0.9 if the off intervals are not long enough. For both Scenarios IV and V, the maintenance threshold value, r_i^{th}, is set to 0.75 for all machines. Finally, the bonus rate of producing one more part after reaching the target throughput is \$3 and the penalty rate when falling one short of the target is \$5.

2.3.2 PSO Parameter Tuning

The problem was solved using the PSO method described in the previous section. The PSO swarm size used was 3000. The maximum iteration number, s_{max}, was set to 500. The learning factors, c_1 and c_2, were equal to 2. The inertial weight parameters $\alpha_{\max}$ and $\alpha_{\min}$ are set to start at 0.9 and end at 0.4, respectively. These PSO parameters are determined through literature (Arasomwan and Adewumi, 2013) and parameter tuning. For example, the PSO results due to different inertia weight configurations and learning factors are illustrated in Table 7 and Table 8, respectively. Note that this is a minimization problem. Accordingly, it can be seen that the adopted strategies can outperform the standard PSO.

Table 7 PSO Results Due to Different Inertia Weight Configurations

Inertia Weight (α)		PSO Population	
Type	Value	No split	With split
No Inertia Weight	--	2333.33	2319.994
Constant Inertia Weight	0.9	2307.172	2289.548
	0.7	2308.304	2303.533
	0.4	2310.572	2310.216
Linearly Decreasing Inertia Weight	0.9 to 0.4	2303.744	2254.613

*Tested using population size of 1000 over 100 iterations

Table 8 PSO Results Due to Different Learning Factors

Learning Factors (c_1 & c_2)	PSO Population	
	No Split	With Split
2	2303.744	2254.613
1.5	2302.866	2265.126
1	2304.738	2273.570
0.5	2310.237	2289.937
0	2335.037	2309.797

*Tested using population size of 1000 over 100 iterations
**Linearly decreasing inertial weight

2.3.3 Case Study Results

After solving the problem, the production and maintenance schedules for Scenarios IV and V are obtained; and are compared to Scenarios I-III. The throughput for each scenario is obtained as shown in Table 9. It is evident that all five scenarios reach the target throughout. It is also noted

that the throughput obtained in Scenarios IV and V is lower than some other scenarios since the proposed model is cost driven. Also note that the model does not take into account any material costs or holding. The resulting electricity consumption and power demand from the production line and the maintenance action are calculated as shown in Table 10.

Table 9 Production Throughput

Scenario	Throughput
I	1526
II	1405
III	1418
IV	1405
V	1419

Table 10 Electricity Consumption and Power Demand

Scenario	Production Electricity Consumption (kWh)	Maintenance Electricity Consumption (kWh)	Total Electricity Consumption (kWh)	Power Demand (kW)
I	3417.7	27.5	3445.2	94
II	3462.7	14.5	3477.2	79
III	3128.9	22.4	3151.3	79
IV	3429.6	10.5	3440.1	79
V	3439.3	10.9	3450.2	79

The electricity consumption (kWh) from production for Scenarios IV and V (proposed formulations) is higher than Scenario I (no energy control is implemented). Once again, the reason is that the proposed problem is cost driven. When considering the TOU program shown in Table III, the marginal price per kWh, compared to the marginal price per kW, is almost negligible.

Meanwhile, the consumption for Scenario I is lower, while the power demand (kW) is much higher than all other scenarios. Moreover, when comparing Scenario III to Scenarios IV and V (proposed formulations), the consumption is less, while the power demand is the same. Again, the reason is that the objective of this model is cost driven. Although the overall energy consumption is less for Scenario III, the maintenance cost is twice as much as that of Scenarios IV and V (see Figure 5). This is because the frequency of the maintenance tasks is reduced. It illustrates that the proposed model can also make maintenance scheduling more efficient.

Figure 5 summarizes the total cost and the non-energy related maintenance cost for each of the five scenarios. As expected, Scenarios I-III have a much higher total cost than Scenarios IV and V. This is due to the high non-energy related maintenance cost from Scenarios I-III. Thus, it shows that the combined model considering both Problems 1 and 2 is necessary and effective.

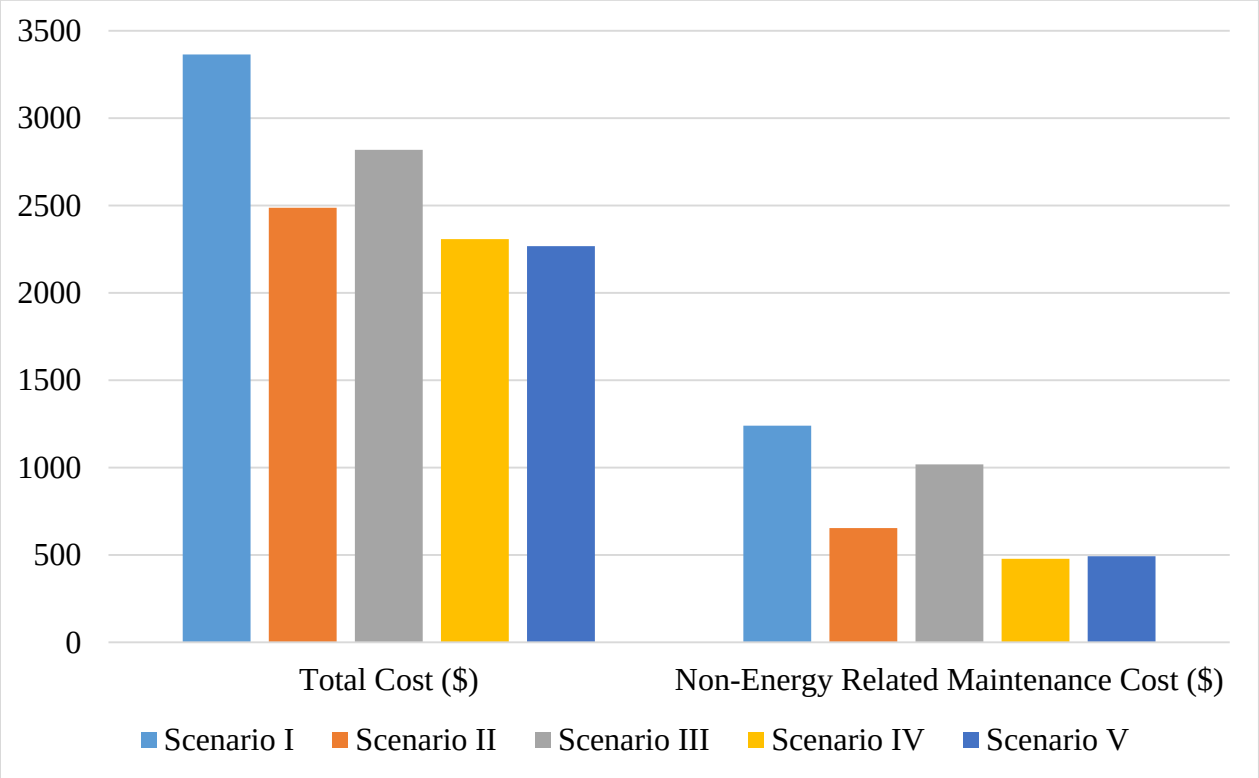

Figure 5 Energy and Maintenance Cost Comparison

Next, due to the difference in throughput among the scenarios, the cost per unit product produced is calculated and compared as shown in Table 11. The reduction of cost per unit produced when using the proposed model compared to Scenarios I, II, and III is illustrated in Table 12. Both Scenarios IV and V have a much lower cost per part than Scenarios I-III. Furthermore, Scenario V (Problem 2) achieves the lowest unit cost among all five scenarios. Hence, the objective of reducing the overall cost due to throughput loss, maintenance, and energy is realized by the proposed model. Accordingly, Problem 2 (i.e. Scenario V) is used as the reference case for the rest of this analysis in Section 2.3.4. Note that this is also the problem used to derive the aggregate cost model.

Table 11 Unit Cost per Part Produced

Scenario	Cost per Part ($)
I	2.205
II	1.770
III	1.989
IV	1.642
V	1.599

Table 12 Reduction of Unit Cost per Part Produced When Using Proposed Model

Comparison between Scenarios	Cost Reduction (%)
IV vs I	25.53%
IV vs II	7.23%
IV vs III	17.45%
V vs I	27.48%
V vs II	9.66%
V vs III	19.61%

2.3.4 Analysis and Discussion

An analysis is conducted to investigate the relationship between cost, energy consumption, production throughput, and maintenance using the aggregate cost model derived from Problem 2. The effect of different factors and their interactions are examined using DOE. Several samples of production and maintenance schedules, for each factor/parameter level, are obtained to better study the overall behavior of the production system as opposed to the behavior of a specific production schedule. A 3^6-factorial design with 32 replications is built. In all, the total number of observations is 23,328. The factors and factor levels are shown in Table 13. A graphical representation of these samples generated using the PSO algorithm is shown in Figure 6.

A simple 4-Step Monte Carlo sampling approach is adopted to obtain the replications (Sheehy and Martz, 2012):

- Step 1 identifies the transfer equation; i.e. the DR driven production and maintenance scheduling model.
- Step 2 requires the variable inputs to be defined. For the scope of this analysis, the machines' "on/off" states and the maintenance schedule throughout the production horizon will be the input values that need to be generated.
- Step 3 requires the dataset to be simulated in a randomized manner. The PSO method will be used to generate the dataset since it is an evolutionary algorithm that generates partially random samples (Zhong-Sheng et al., 2017).
- Step 4 analyzes the samples, which will be done using DOE factorial analysis methodology.

Table 13 Factor Levels

	Levels		
Factors	**1**	**2**	**3**
P_i	0.8	1.15	1.5
MP_i	0.8	1.15	1.5
PR_i	40	55	70
$r_{i(t=0)}$	0.7	0.8	0.9
$B_{i(t=0)}$	0	0.5	1
MC	1	3	5

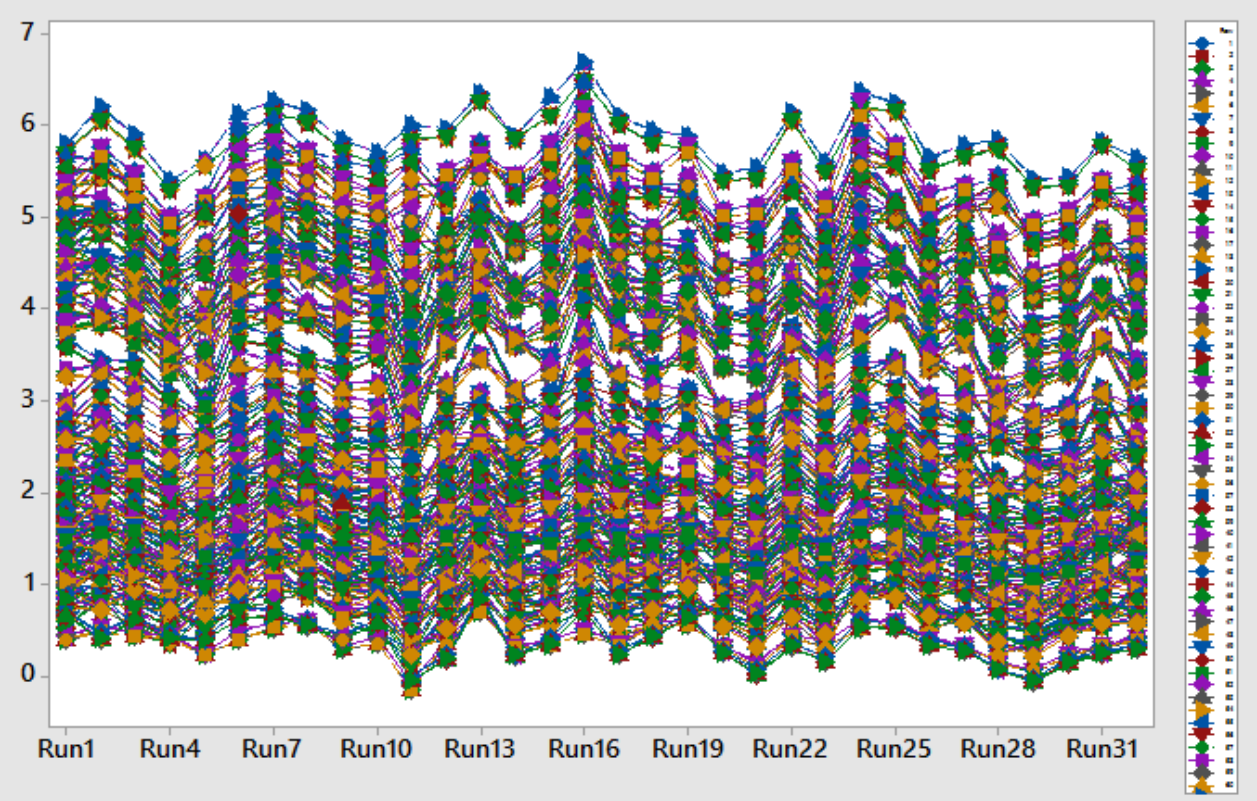

Figure 6 C_{part} for PSO Generated Samples

After running the factorial analysis considering all factors and higher order interactions, MP_i is found to be insignificant both in the linear model and in all higher order interactions. Additionally, all interactions higher than 2nd order interactions are not significant. Thus, MP_i and all interactions over 2nd order are disregarded. Finally, the interaction plot and ANOVA output are

shown in Figure 7 and Table 14, respectively. Meanwhile, Figure 8 shows the normal probability plot and histogram of the residuals.

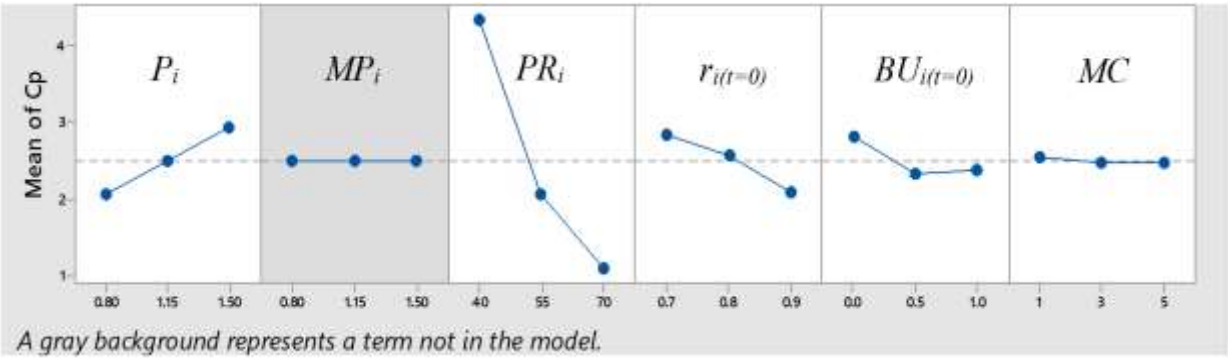

Figure 7 Main Effects Plot

Table 14 Reduced ANOVA Table

Source	DF	Adj SS	Adj MS	F-Value	P-Value
Model	50	50275.6	1005.5	11715.25	0.000
Linear	10	49721.6	4972.2	57930.87	0.000
P_i	2	3082.7	1541.3	17958.08	0.000
PR_i	2	43156.9	21578.5	251411.70	0.000
$r_{i(t=0)}$	2	2313.9	1156.9	13479.61	0.000
$B_{i(t=0)}$	2	1139.1	569.6	6636.13	0.000
MC	2	29.0	14.5	168.82	0.000
2-Way Interactions	40	553.9	13.8	161.35	0.000
P_i*PR_i	4	164.7	41.2	479.78	0.000
P_i*$r_{i(t=0)}$	4	6.8	1.7	19.86	0.000
PR_i*$r_{i(t=0)}$	4	365.0	91.2	1063.12	0.000
PR_i*$B_{i(t=0)}$	4	13.8	3.5	40.30	0.000
PR_i*MC	4	1.5	0.4	4.51	0.001
$r_{i(t=0)}$*$B_{i(t=0)}$	4	1.0	0.3	3.03	0.016
$r_{i(t=0)}$*MC	4	1.0	0.2	2.90	0.020
			R-sq	**R-sq(adj)**	**R-sq(pred)**
			96.18%	**96.17%**	**96.16%**

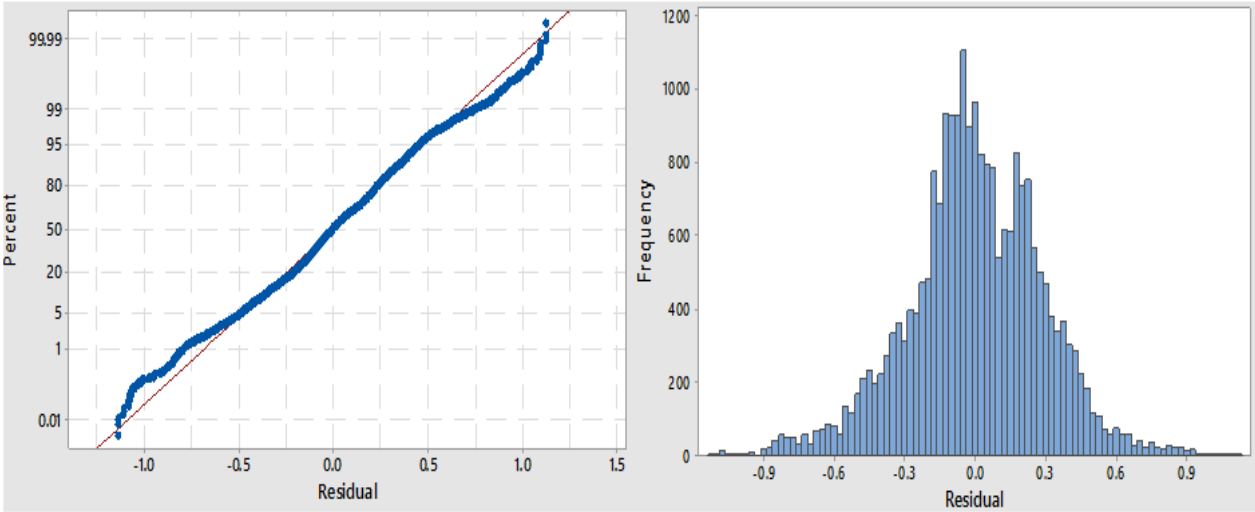

Figure 8 Normal Probability Plot and Histogram of Residuals for ANOVA Analysis

Next, assuming P_i, PR_i, $B_{i(t=0)}$, $r_{i(t=0)}$, and MC are all decision variables and the objective function is the aggregate cost per part function (minimize); the impact of the different system parameters can be further analyzed. A Response Surface model, which accounts for all statistically significant first order factors and second order interactions, is adopted. The corresponding results are illustrated in Figure 9 and suggest that the best outcomes are observed at the maximum production rate and minimum rated power. Meanwhile, the maintenance crew resources, initial machine production efficiency, and initial buffer inventory level fell into the middle range. The reason the initial machine production efficiency is not recommended to be at the maximum level is because it reduces maintenance scheduling flexibility since maintenance actions cannot be implemented when the production efficiency level is higher than the threshold level. Furthermore, it could lead to too many machines needing maintenance resources at the same time. Thus, leading to less flexibility in maintenance scheduling. In all, 69% reduction in C_{part} is achieved with the rated power is at 80%, production rate is 70, initial machine production efficiency is 0.85, initial buffer content level is at 69%, and maintenance crew resources is 3.

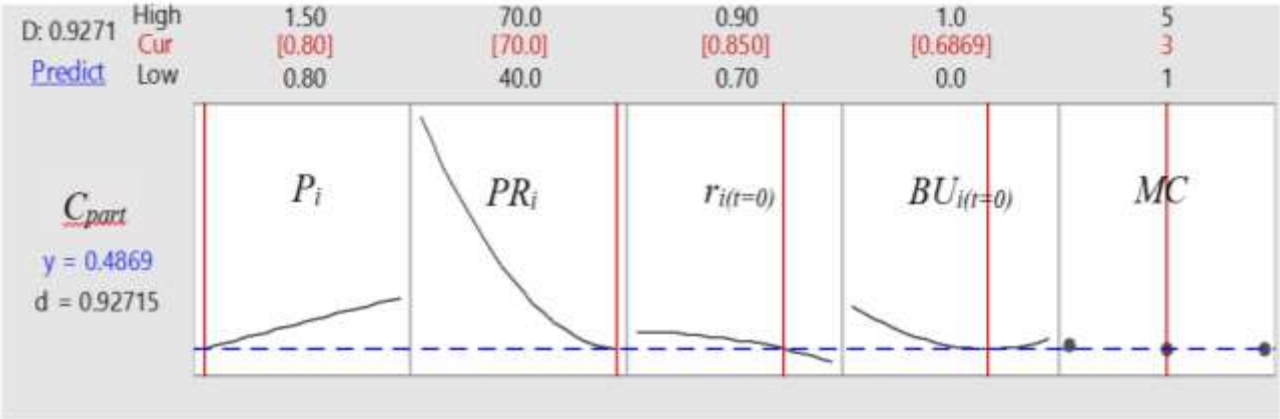

Figure 9 Response Optimizer

The savings due to parameter optimization for the aggregate cost model are compared to three baseline cased. The first baseline does not consider any dynamic energy control action (all machines are on unless the buffer constraints are violated), and the maintenance policy is set to be triggered by a threshold production capability level (Scenario I). The second baseline (Scenario II) implements an optimized production schedule such that all x_{it} are obtained by minimizing the electricity billing cost while considering TOU demand response. Meanwhile, the maintenance schedule is determined considering a threshold production capability policy similar to Scenario I. Scenario III implements an optimized maintenance schedule such that all y_{it} are obtained by minimizing the maintenance billing cost while TOU demand response driven decision making is not considered. Scenario IV represents the setup for the aggregate cost model derived from Problem 2. Note that the results for all four scenarios assume that the proposed system parameter changes are physically possible.

The percent savings due to parameter optimization for each of the scenarios is shown in Table 15. Dual scheduling and system parameter optimization can achieve 39-62% in savings compared to the baseline cases; indicating that iteratively optimizing energy and maintenance production scheduling with parameter optimization can have significant benefits.

Table 15 C_{part} after Parameter Optimization

Scenario	C_{part} without parameter optimization ($)	C_{part} with parameter optimization ($)	Percentage savings for C_{part}
I	2.40	1.4225	40.73
II	1.77	1.5899	10.18
III	1.88	1.2847	31.66
IV	1.60	0.4869	69.57

2. 4 Conclusion

In this Chapter, methodology for joint energy, maintenance, and throughput scheduling for typical manufacturing systems with multiple machines and buffers is proposed to guide operational activities on shop floors toward sustainable manufacturing. Multiple criteria from the perspective of sustainability are modeled and unified in a single cost minimization objective. The problems, with and without the production throughput constraint, are formulated to identify the optimal joint production, energy, and maintenance schedules that minimize the operational cost. Alongside to the proposed scheduling model, an aggregate cost model is established and can be used to determine the actual system performance in case of discrepancies or desired changes in system parameter values.

The proposed methodology can help determine the feasibility and promote flexible cost effective joint energy, production, and maintenance decision making. The results from the numerical case study illustrate the effectiveness with respect to the overall cost reduction when using the proposed joint model compared to the scenarios where energy and maintenance strategies are implemented separately. Moreover, the factor analysis indicates that there is a need to balance

production, maintenance, and electricity related factors simultaneously to ensure robust and attainable cost savings. While too few maintenance crew resources can lead to quickly degrading machine production efficiency and thus production loss; too many maintenance crew resources and maintenance activities can lead to unnecessary costs and production interruptions. This limits manufacturers' flexibility needed to leverage TOU tariff structures and hinders costs savings. In all, this research supports manufacturers in adopting demand-side energy management at the manufacturing system-level. .

3 HVAC Load Model in Manufacturing Facility Considering Manufacturing Operation for Peak Power Demand Reduction

3.1 Objective and Overview

Within a typical industrial manufacturing plant, the two main energy consumers are the manufacturing system and the HVAC system. Together these two systems can lead to high power demand profiles for manufacturers. Opportunely, using intelligent scheduling methods the total power demand due to the manufacturing operation and HVAC system can be reduced. This in turn results in economic and environmental sustainability benefits for manufacturers. Accordingly, a

method to reduce the power demand during peak periods using an HVAC work load model (which considers manufacturing heat sources) alongside to the manufacturing power demand model is proposed. The effect of the manufacturing operation on the indoor temperature and the HVAC working load is quantified by considering the heat transfer characteristics of the machines in the manufacturing system. A mathematical model is formulated using mixed integer nonlinear programming (MINLP) and solved using General Algebraic Modeling (GAMS). An optimal schedule for the manufacturing operation and control scheme for the HVAC temperature setpoints that can minimize the power demand during peak periods under the constraint of production throughput is identified. A numerical case study is used to illustrate the effectiveness of the proposed method.

The rest of the chapter is organized as follows. In Section 3.2 a preliminary simulation based study is implemented. Section 3.3 introduces the analytical electricity DR scheduling model for the combined HVAC and manufacturing system. Section 3.4 introduces a numerical case study. Finally Section 3.5 concludes the section.

3.2 Preliminary Simulation Based Method

A simulation model is built to study potential for implementing production and HVAC demand-side energy management. The simulation is built in two stages. The first part of the simulation deals with modeling the manufacturing system in ProModel, a discrete event simulation package that allows for a user-friendly interface. It can be used for the design, assessment, and optimization for both service and manufacturing settings. The manufacturing system can be modeled using the actual layout information, e.g., the number of machines, buffers, downtimes, and much more. Furthermore, different variables denoting different system performance measures

such as system throughput, energy consumption, and power demand can be defined by the users to make it easy to track and record all interested measures. Electricity DR can also be integrated accordingly to the method in Cuyler et. al (2014) where the different peak and off peak periods and prices can be configured. Next, the second part of the simulation is performed in EnergyPlus, an energy analysis and thermal load simulation program developed by Department of Energy based on DOE-2 and BLAST (DOE, 2012). It considers size and geometry, construction materials, internal heat loads, HVAC systems, and the environmental temperature to represent the thermal behavior of the building dynamically.

The obtained power consumption of the manufacturing system when electricity DR is implemented in ProModel can be used as internal heat source when integrated into the building model in EnergyPlus to establish a combined manufacturing and HVAC system simulation model. This internal heat source can be configured and adjusted in the combined simulation model to represent different production strategies, e.g., it can be set as zero for a 15-minute interval to simulate a production pause. With this combined simulation model, we will examine and compare three different DR policies for manufacturers as follows. The first policy (Policy I) is a baseline scenario where DR is not implemented for both the manufacturing system and HVAC system, i.e., the combined simulation is run without taking into account the DR event for both the HVAC and manufacturing systems. Hence, the energy and power consumption for the combined system can be obtained as a benchmark. The second policy (Policy II) considers the case when electricity DR is applied to the manufacturing system alone while allowing the HVAC to run at its standard demand. The third policy (Policy III) represents the case when both the HVAC and manufacturing systems are considered for DR.

The DR actions for the manufacturing system include ON and OFF decisions for the machines in the system to minimize the power demand during the DR event while maintaining the production throughput of the entire system. The optimal DR actions for the manufacturing system can be obtained using exhaustive search using the simulation model (Cuyler et. al, 2014). The control action for the HVAC includes ON and OFF actions while maintaining the indoor temperature in the desired range.

Using the joint simulation model, the influence of the manufacturing operation on the indoor temperature evolution can be investigated. Two indoor temperature curves, one with the manufacturing operation and the other one without manufacturing operation, can be obtained and compared. The power consumption of the combined system can also be examined from the combined simulation model and compared with the power consumption from the two exclusive simulation models, i.e., the manufacturing system model in ProModel, and the building HVAC model without the manufacturing operation in EnergyPlus.

The parameters of each machine including cycle time, mean time between failures (MTBF), mean time to repair (MTTR), and rated power are shown in Table 16. The parameters of each buffer including initial content level and buffer capacity are shown in Table 17.

.

Table 16 Basic Setting of Machines for Simulation Model

Machine	Cycle Time (min)	MTBF (min)	MTTR (min)	Rated Work (kW)
M1	0.5	100	4.95	21
M2	0.5	45.6	11.7	14
M3	0.5	98.8	15.97	20
M4	0.5	217.5	27.28	16
M5	0.5	109.4	18.37	13

Table 17 Basic Setting of Buffers for Simulation Model

Buffer	B1	B2	B3	B4
Initial Buffer Contents	50	8	22	28
Maximum Capacity of Buffer	70	40	30	42

The DR event is assumed to start at the 120th minute and end at the 150th minute of an 8-hour shift from 9:00AM to 17:00PM (i.e., from 11:00AM to 11:30AM). The DR action for the manufacturing system is obtained based on the work by Cuyler et. al (2014) as shown in Table 18 where 0 denotes shutdown and 1 denotes production. Meanwhile, each interval has a duration of 15-minutes.

Table 18 Demand Response Actions

	M_1	M_2	M_3	M_4	M_5
1st Interval (11:00-11:15AM)	0	1	0	0	0
2nd Interval (11:16-11:30AM)	0	0	1	1	0

The building that is demonstrated in the EnergyPlus is a one story, one thermal zone building in Chicago, Illinois. The typical information of one summer day and one winter day are used for the sizing of the model. The floor area of the building is 20m by 20m and the height of the building is 10m. Different materials were used for the construction of the building to best replicate a practical real world setting. The walls consist of wood fiberglass and plasterboard; the

roof is also made of fiberglass and plasterboard; and the floor consists of heavy concrete. Meanwhile, the target indoor temperature is from 20 to 24 (degrees Celsius) when the DR event does not occur and 20 to 27 (degrees Celsius) during the DR event. The fraction radiant of the electric equipment of the manufacturing system is set as 0.3 and the convection coefficient is 0.7 (Brundage et. al, 2013).

In addition, the HVAC system used in EnergyPlus is an Ideal Loads Air System. It is the simplest HVAC system that can be simulated because it does not require the user to specify the different operating components, such as air loops and water loops, of the HVAC system. This choice is usually used when the focus is on building performance and does not require very much detail on the functionality of HVAC system components.

Finally, to receive a report from EnergyPlus, objects, variables, and meters need to be specified. Objects represent the components in the target system. Variables report the value of any element of interest at different points in time. Meters are a special form of variables used to measure resource usage or generation in interval units (Siddiqui et al., 2008). Using the developed simulation model, three different DR policies are implemented as summarized in Table 19.

Table 19 Summary of Different Demand Response Policies

Policy	**HVAC**	**Manufacturing System**
I	Does not consider DR	Does not consider DR
II	Does not consider DR	Considers DR
III	Considers DR	Considers DR

The results are optioned and the power demand during peak periods under three different policies and corresponding carbon dioxide (CO_2) emission reduction for a winter day and summer day are summarized as shown in Table 20 and Table 21, respectively. Note that one kW reduction of power demand during peak periods translates to a 65 kWh reduction in electricity consumption (Siddiqui et al., 2008). Moreover, one kWh electricity generation may incur 1.52 pounds carbon dioxide (CO_2) emission (Environmental Protection Agency, 2014).). The power of the combined system throughout the time horizon of the two design days under the three polices is illustrated in Figure 10.

Table 20 Comparison of Three Demand Response Policies in Winter

Policy	Power Demand (kW)	Power Demand Reduction (%)	CO_2 Emission Reduction (lb.)
I	101	-	-
II	25.6	74.65	7450
III	24.5	75.74	7558

Table 21 Comparison of Three Demand Response Policies in Summer

Policy	Power Demand (kW)	Power Demand Reduction (%)	CO_2 Emission Reduction (lb.)
I	126.6	-	-
II	53.4	57.81	7232
III	24.5	80.64	10087

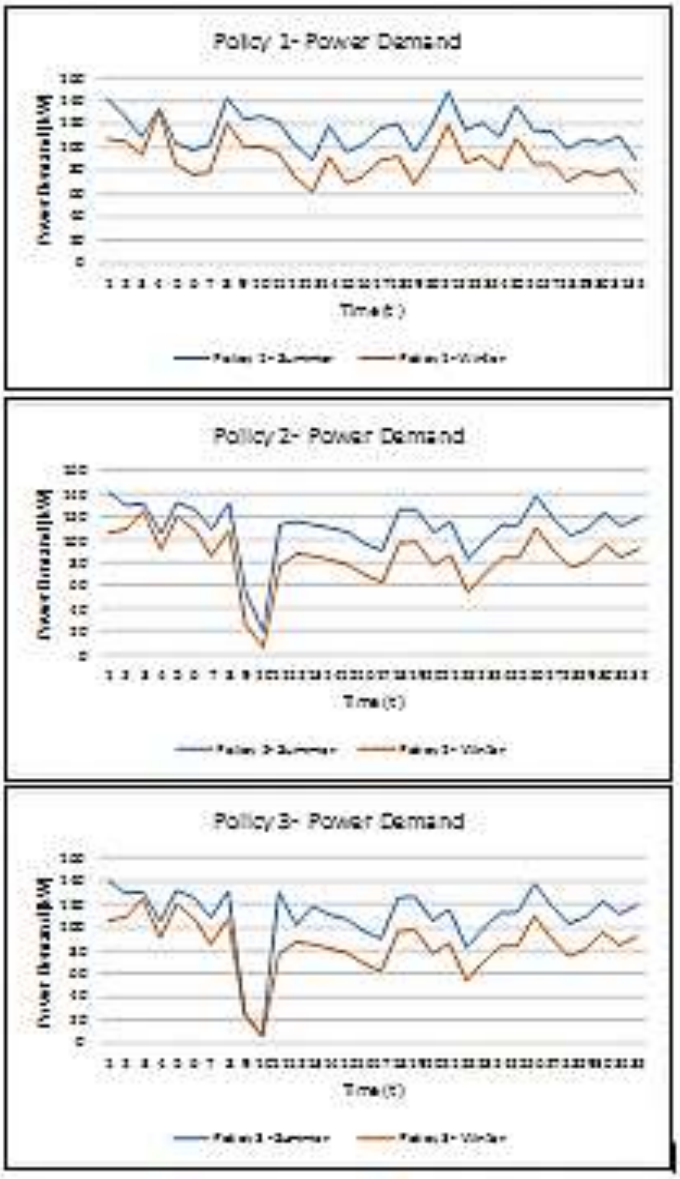

Figure 10 Power demand curves

It is evident from the results that HVAC system consideration alongside to DR driven production control for manufacturers can greatly improve the power consumption reduction of the combined system and also lead to more CO_2 emission reduction. Furthermore, it is interesting to note that the power demand for the winter day in Policies II and III are very close. This is because in the winter the heat generation due to the machines' being in an operating state can actually help

reduce the overall heating load required. This further suggests the importance of taking into account the relationship between the energy consumption from the production line and the HVAC system when designing facilities or studying building energy performance.

In the second part of the case study, the goal is to examine how the manufacturing operation's heat generation affects the room temperature on a summer day. Here the manufacturing operation is scheduled for 8 hours from 9:00AM to 5:00PM. The temperature curve for the building with and without the manufacturing operation when the HVAC system is completely shut down is shown in Figure 11. The purpose here is solely to illustrate the effects of the manufacturing operation on the room temperature and does not reflect the working conditions within the facility.

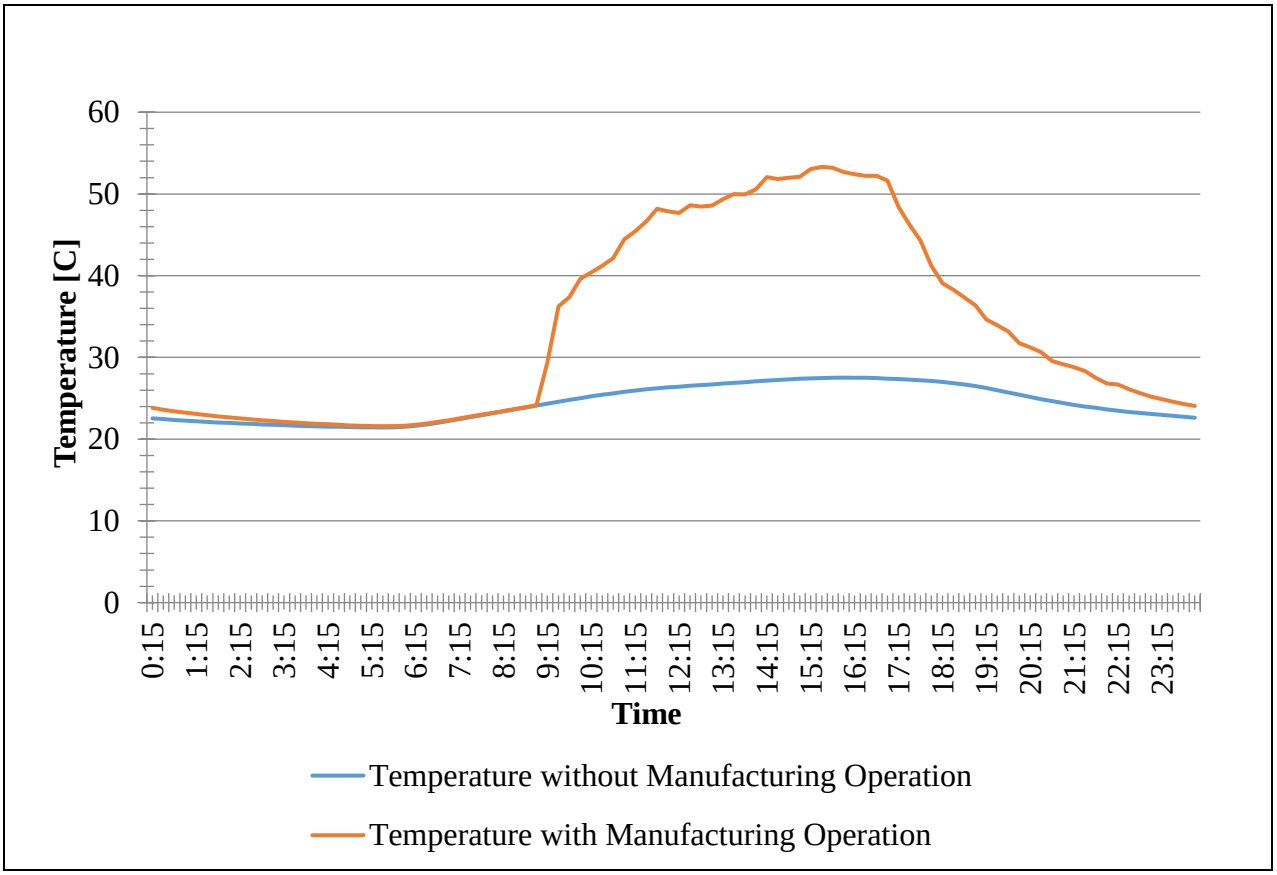

Figure 11 Indoor Temperature Curves with/without Manufacturing System

It is evident that the heat load generated by the machines plays a significant role in increasing the room temperature within a manufacturing plant. As a result, the HVAC requirement of a building is highly influenced by the power consumed and heat dissipated from the manufacturing system.

Next, the power consumption for the combined simulation model and two exclusive simulation models is compared. For the combined simulation model, the power consumption of the combined manufacturing and HVAC system, denoted as P_{total}, is recorded. For the manufacturing system model in ProModel and the building HVAC model without manufacturing operation in EnergyPlus, the power consumption for manufacturing system, denoted as P_{PL}, and the power consumption of the HVAC system without manufacturing operations, denoted as $P_{HVAC-BL}$, are obtained. The results are illustrated in Table 22.

Table 22 Power Consumption for Combined Model and Separated Models

Period	$P_{HVAC-BL}$ (kW)	P_{PL} (kW)	$P_{HVAC-BL} + P_{PL}$ (kW)	P_{total} (kW)
1	2.24	80.89	83.14	141.56
2	2.11	70.90	73.01	126.83
3	2.78	59.49	62.28	109.36
4	3.17	72.70	75.87	133.40
5	3.51	54.50	58.01	103.24
6	3.81	51.20	55.01	97.94
7	4.06	53.20	57.26	101.66
8	4.26	76.69	80.96	142.65

It can be seen that the power consumption of the combined system is not equal to the sum of the power consumption from two separated models as shown in (3.1). It implies that the optimal results from separated models may not be effective in finding an optimal energy control strategy.

$$P_{total} \neq P_{HVAC\text{-}BL} + P_{PL} \quad (3.1)$$

A more appropriate formulation would be described in (3.2).

$$P_{total} = P_{HVAC\text{-}BL} + P_{HVAC\text{-}PL} + P_{PL} \quad (3.2)(3.2)$$

where $P_{HVAC\text{-}PL}$ is the additional power required for the HVAC to work due to a change in the room temperature resulting from the heat generated by the manufacturing machines. It implies the necessity of an analytical model for the combined manufacturing and HVAC system

3.3 Methodology

3.3.1 Nomenclature

BU_{it}: the buffer contents in buffer i at the beginning of interval t

C_i : the capacity of buffer i

c_i: the convection fraction of machine i

C_p: the heat capacity (kWh/kgC) of the building

CQ: the heat transferred from the manufacturing operation during interval j

CQ_{Cj}: the instantaneous convective heat transferred from the manufacturing operation in interval j

CQ_{Rj}: the radiant heat transferred from the manufacturing operation up to the current interval j

CQ^*: the required HVAC load during interval j

EFF_i: the production efficiency of machine i

GQ_j: the heat generated due to manufacturing operation in interval j

H: the duration of the time interval

i: the index of the machines in the manufacturing system

j: the index of the slotted time intervals

k: the index of the radiant time series

M: total number of the time intervals in the planning horizon

N: the total number of the machines in the manufacturing system

$\boldsymbol{OP}$: the set of intervals that belong to peak periods

P_i: the rated power of machine i

PR_i: the production rate of machine i (unit per interval)

Q: the heat that needs to be added or removed when taking into account all of heat sources influencing the indoor temperature except for the manufacturing operation during the interval j

s_k: the radiant time series coefficients

TP: the production throughput of the manufacturing system throughout the planning horizon

TP^*: the production target of the planning horizon

T_j: the forecasted temperature of the building (when HVAC is off) considering all heat sources except for the manufacturing operation

T_{max}: upper bound of acceptable indoor temperature

T_{min}: lower bound of acceptable indoor temperature

V: the volume of the building (m^3)

w_j: the coefficient of performance (COP) of the HVAC

x_{ij}: binary decision variable to denote the ON/OFF decision for machine in interval j

y_j: decision variable for the HVAC temperature setpoint in interval j

Z_j^1: binary variable reflecting the heating state of the HVAC system

Z_j^2: binary variable reflecting the cooling state of the HVAC system

α: conversion factor that converts a unit of temperature to the unit of heat in the building

ρ : the density of air (kg/m3)

ΔT_j : the temperature difference between T_j and the temperature setpoint

η_i : the motor efficiency of machine i

3.3.2 Problem Formulation

Assume a serial production line with N machines and N-1 buffers. Let i be the index of the machines (i=1, …, N) and the buffers (i=1, …, N-1) in the system. The production horizon is slotted into a set of intervals with the same duration H. Let j=1, …, M be the index of the discretized intervals. These intervals can belong to either peak or off-peak periods. The manufacturer needs to identify an optimal schedule for the manufacturing system and HVAC system to minimize electricity demand during peak periods. For the production schedule the manufacturer must decide if the station will be turned on or off for energy savings. For the HVAC system the manufacturer must decide on a temperature setpoint schedule for the manufacturing plant.

The HVAC system is modeled as a single object, and is such that its performance measure represent the aggregate performance across all system components. It has two mutually exclusive states, heating and cooling, for each given period. The heating state is defined as the state during which the HVAC has to add heat into the room to maintain the temperature to be at or above the instated temperature setpoint. The required HVAC load is the amount of heat that needs to be added to the room to maintain the temperature. Conversely, the cooling state is when the HVAC system has to remove heat from the building to maintain the temperature to be below or at the temperature setpoint. The required HVAC load is defined as the amount of heat that must be removed from the building to maintain the temperature setpoints. The temperature setpoints at any time must be within the allowable temperature range. It is also assumed that the temperature has no effect on the productivity within the plant.

Among the loads that must be considered for the HVAC system is the internal heat load from the manufacturing production system machines. The machines generate heat at a rate proportional to the motor inefficiency. Also, the heat transferred to the surroundings corresponds

to the convective and radiative split ratio of each machine. Meanwhile, conduction is assumed to be negligible. The convective portion of the heat generated is immediate transfer into the room is added to the surroundings as an instantaneous load (Hosni et al., 1999). Conversely, the radiative portion of the heat generated is absorbed by its surrounding surfaces in the manufacturing plant, which is eventually dissipated to the surrounding air over time (Hosni et al., 1999). The radiant time series approach in (Spitler et al., 1997) is adopted to model this delay in radiant heat dissipation by giving weights that dictate the percentage of the radiant heat that is absorbed by the room at each time-interval. This delay in heat transfer from the radiant fraction of the heat explains why the heat generated by the machines may not be equal to the cooling load required by the HVAC system when operating in the cooling state (Wilkins and Hosni, 2000). Figure 12 shows a brief illustration of the behavior of the convective and radiant heat transfer at each interval.

Figure 12 Illustration of Convective and Radiant Heat Transfer Due to Manufacturing Operation in Different Intervals

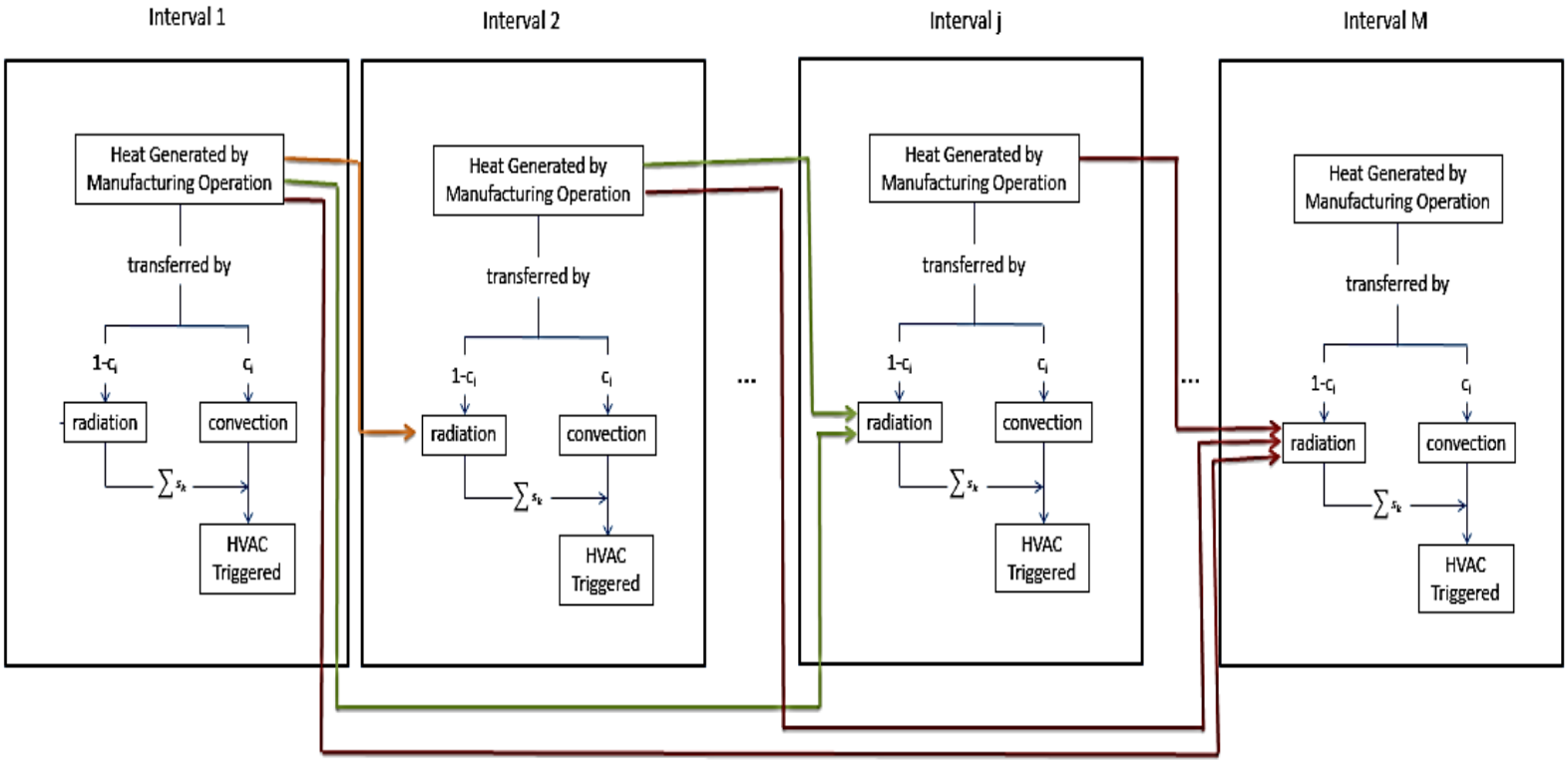

Accordingly, the optimization problem is formulated as follows. Let x_{ij} be the binary decision variable to denote the production schedule, which takes the value of one if machine i is scheduled to produce during interval j, and zero otherwise. Let y_j be the indoor temperature setpoint for the building for interval j. Let **OP** be the set of the intervals that belong to the peak period. Let P_i be the rated power of machine i. The proposed method can be formulated with the objective function (3.3) and the constraints (3.4)-(3.7).

$$\min_{x_{ij},\, y_j}\left(\max_{j\in\mathbf{OP}}\left(\sum_i x_{ij}P_i+\left(\frac{\left|CQ_j^*\right|w_j}{H}\right)\right)\right) \tag{3.3}$$

$$Z_j^1+Z_j^2\le 1 \tag{3.4}$$

$$0\le BU_{ij}\le C_i \tag{3.5}$$

$$TP\ge TP^* \tag{3.6}$$

$$T_{\min}\le y_j\le T_{\max} \tag{3.7}$$

In (1), w_j is the coefficient of performance (COP) of the HVAC system. It is used to describe the efficiency of the HVAC system. It takes into account all factors influencing HVAC performance (i.e. outdoor temperature and the required HVAC load) and quantifies how much energy is needed by the HVAC system to add or remove one unit of heat. Meanwhile, CQ_j^* is the required HVAC load during interval j that can maintain the indoor temperature.

CQ_j^*, the required HVAC load during interval j that can maintain the indoor temperature, can be calculated by (3.8)

$$CQ_j^*=Z_j^1(Q_j-CQ_j)+Z_j^2(CQ_j+Q_j) \tag{3.8}$$

where CQ_j is the heat transferred from the manufacturing operation during interval j. Z_j^1 and Z_j^2 are the binary variables reflecting the heating or cooling state of the HVAC system, respectively. They take the value of one if the HVAC is in a heating or cooling state, respectively; and zero otherwise. Q_j represents the heat that needs to be added (when in the heating state) or removed (when in the cooling state) when taking into account all of heat sources influencing the indoor temperature except for the manufacturing operation during the interval j.

CQ_j can be calculated by taking into account the convective (c_i) and radiative split ($1-c_i$) of each machine. Let GQ_j be the heat generated due to manufacturing operation in interval j, which can be calculated by (3.9).

$$GQ_j = H(\sum_{i=1}^{N} P_i x_{ij}(1-\eta_i)) \tag{3.9}$$

where η_i is the motor efficiency of machine i. Let CQ_{Cj} be the instantaneous convective heat transferred from the manufacturing operation in interval j. It can be formulated by (3.10)

$$CQ_{Cj} = c_i \cdot GQ_j \tag{3.10}$$

The radiant heat transfer with a ratio of $1\text{-}c_i$ is considered non-instantaneous with accumulative effects. Therefore, the radiant time series approach is applied to the radiant portion of the heat that is to be transferred into the room. The radiant heat fraction can be represented by the radiant time series s_k, $k = 1, ..., j$. It is obvious that $s_1 \succ s_2 \succ ... \succ s_j$. It represents the fact that the radiant heat gradually attenuates, and thus it will influence not only the present time interval but also the later ones. Let CQ_{Rj} be the radiant heat transferred from the manufacturing operation up to the current interval j. It can be formulated as (3.11)

$$CQ_{Rj} = H(\sum_{k=j}^{1}\sum_{j'=1}^{j}\sum_{i=1}^{N}(1-c_i)s_k P_i x_{ij'}(1-\eta_i)) \tag{3.11}$$

Therefore, CQ_j can be calculated by (3.12).

$$CQ_j = CQ_{Cj} + CQ_{Rj} \tag{3.12}$$

After introducing CQ_j, Z_j^1 and Z_j^2, and Q_j. Z_j^1 and Z_j^2 can be formulated by (3.13) and (3.14), respectively.

$$Z_j^1 = \begin{cases} 1, & if \quad y_j - \left(T_j + \dfrac{CQ_j}{\alpha}\right) > 0 \\ 0, & otherwise \end{cases} \tag{3.13}$$

$$Z_j^2 = \begin{cases} 1, & if \left(T_j + \dfrac{CQ_j}{\alpha}\right) - y_j > 0 \\ 0, & otherwise \end{cases} \tag{3.14}$$

where α is a conversion factor that converts a unit of temperature to the unit of heat. α can be calculated by (3.15).

$$\alpha = C_p \cdot \rho \cdot V \tag{3.15}$$

In (45) C_p is the specific heat capacity of air (kWh/kgC), ρ is the density of air (kg/m^3), and V is the volume of the building (m^3). T_j is the forecasted temperature of the building (when the HVAC system is off) considering all heat sources except for the manufacturing operation, during interval j. Using T_j, we can calculate the temperature difference between T_j and the temperature setpoint y_j using (3.16)

$$\Delta T_j = Z_j^1(y_j - T_j) + Z_j^2(T_j - y_j) \tag{3.16}$$

Thus, Q_j in (6) can be calculated by (3.17).

$$Q_j = \alpha \cdot \Delta T_j \tag{3.17}$$

The calculation of the power consumption for each interval in the objective function considering both manufacturing operation and HVAC working load can be briefly summarized as shown in Figure 13.

Meanwhile, BU_{ij} represents the buffer contents in buffer *i* at the beginning of interval *j*; and can be calculated by (3.18).

$$BU_{ij} = BU_{i(j-1)} + x_{i(j-1)} \cdot PR_i \cdot EFF_i \cdot H - x_{(i+1)(j-1)} \cdot PR_{i+1} \cdot EFF_{i+1} \cdot H$$
$$i = 1, ..., N-1;\ j = 1, ..., M \tag{3.18}$$

where PR_i is the production rate of the machine *i*; and EFF_i denotes the production efficiency of machine *i*.

TP is the production throughput of the manufacturing system throughout the planning horizon and TP^* is the production target for the planning horizon. *TP* can be calculated by (3.19).

$$TP = \sum_j (x_{Nj} \cdot PR_N \cdot EFF_N \cdot H) \tag{3.19}$$

Figure 13 Flowchart to Calculate Power Demand

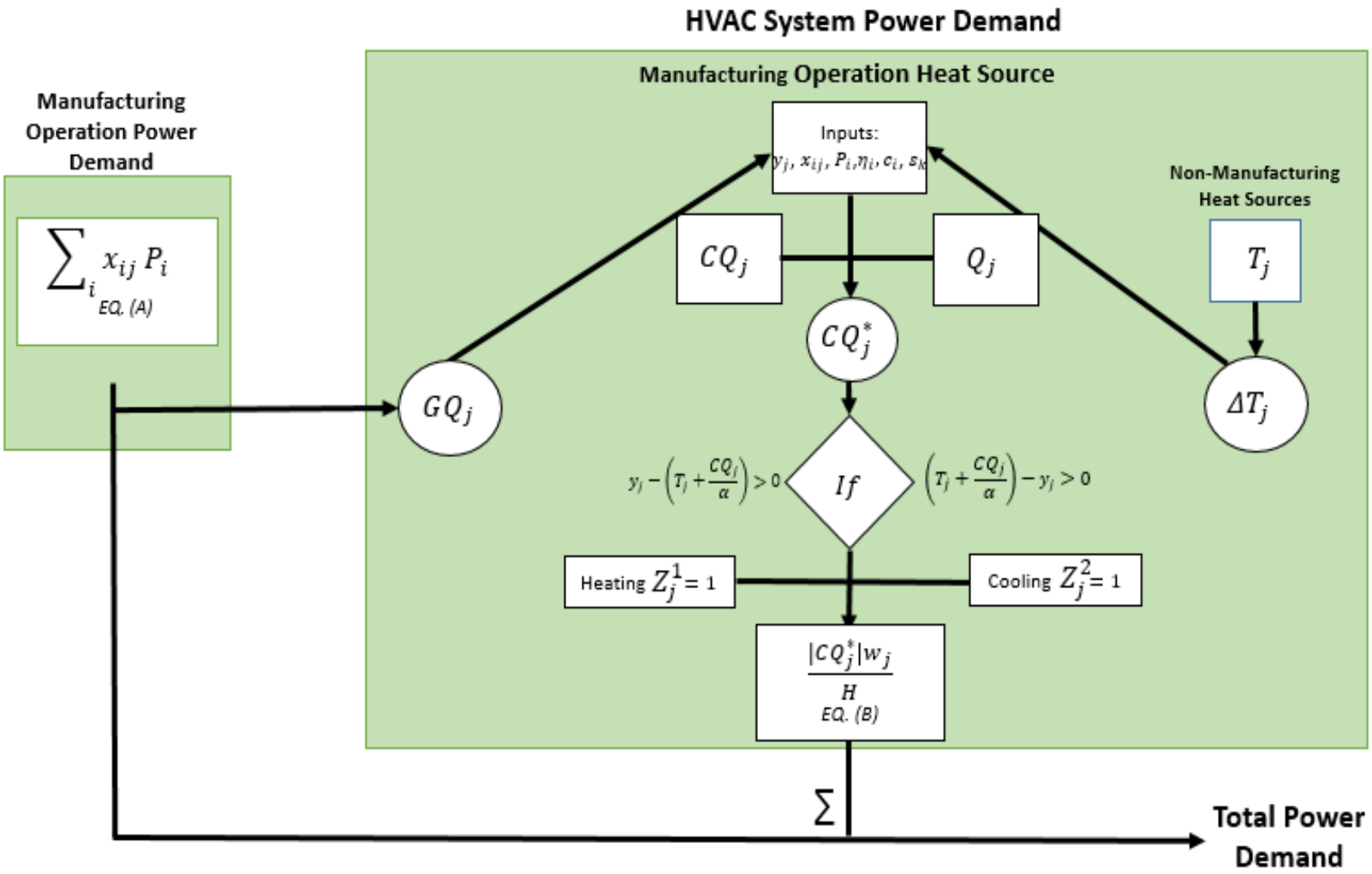

3.4 Case Study Results and Analysis

To illustrate the effectiveness of the proposed electricity DR model for the combined manufacturing and HVAC system, a numerical case study is implemented. The case study considers the following three control scenarios. The first scenario (Scenario I) is a baseline model that is used as the benchmark, i.e., no DR is considered. In the second scenario (Scenario II), the objective function is to minimize the power demand during peak hours solely due to the manufacturing operation, while the HVAC is controlled according to the allowable temperature range separately. Finally, the third scenario (Scenario III) utilizes the proposed combined manufacturing and HVAC model.

Two different days, i.e., a summer day and a winter day, are considered in the study. For the summer day, all three scenarios have the same allowable temperature setpoints such that the target indoor temperature must be from 20 to 25 degrees Celsius. Similarly, for the winter day the allowable temperature setpoints are such that the target indoor temperature has to be from 18 to 22 degrees Celsius.

Meanwhile, a manufacturing system that consists of five machines and four buffers, is considered. The parameters of each machine including production rate, rated power, production efficiency, and motor efficiency are shown in Table 23. The parameters of each buffer, including initial contents and buffer capacity, are shown in Table 24. The time horizon is an 8 hour shift (from 9:00a.m.-5:00p.m.) that is slotted into 32 15-minute intervals, where the peak periods begin at 12:00p.m. and last until the end of the shift (i.e., intervals 13 through 32). The production target for this shift is 320 parts. Referring to (Brundage et al., 2013) the radiant and convective fraction of the machines are 0.3 and 0.7 respectively.

Table 23 Basic Machine Setup for Chapter 3

Machine	Production Rate (per 15min)	Rated Power	Production Efficiency	Motor Efficiency
M1	12.5	15	0.9	0.85
M2	12.5	17	0.9	0.85
M3	12.5	24	0.8	0.80
M4	12.5	17	0.9	0.85
M5	12.5	21	0.9	0.80

Table 24 Basic Buffer Setup for Chapter 3

Buffer	B1	B2	B3	B4
Initial Buffer Contents	70	70	50	75
Maximum Capacity of Buffer	160	145	140	160

The outdoor temperature profile for a winter day in January and a summer day in July for Chicago, Illinois is obtained from EnergyPlus. EnergyPlus is used to provide the temperature data based on specific parameters such as date, location, etc. It can also describe the thermal behavior of a building dynamically while considering building size, geometry, construction materials, internal heat loads, and environmental temperature. For the summer day, the outdoor temperature values range from a minimum 22 degrees Celsius to a maximum of is 33 degrees Celsius. Similarly, for the winter day, the outdoor temperature values range from a minimum -23 degrees Celsius to a maximum of is -15 degrees Celsius.

The indoor temperature of the building considering everything but the manufacturing operation, T_j , is also obtained using EnergyPlus as shown in Figure 14. The building considered in the case study is a one-story building with the floor area of 20m by 20m. The height of the

building is 10m. Different materials were used for the construction of the building to best replicate a practical real world setting and are as follows. The walls consist of wood fiberglass and plasterboard. The roof is also made of fiberglass and plasterboard. Meanwhile, the floor is constructed from heavy concrete.

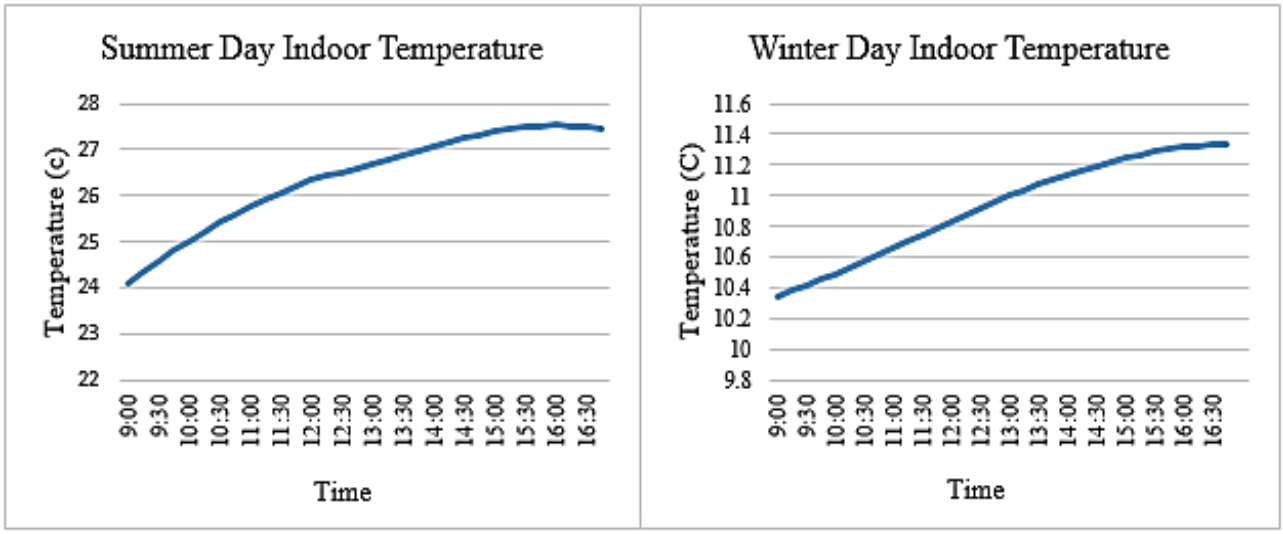

Figure 14 Indoor Temperature Considering Everything but Manufacturing Operation

The radiant time series s_k coefficients from Bruning (2004) are adopted and shown in Figure 15. The COP of the HVAC system is assumed to have a nameplate value of 3.6 for an ideal HVAC system. In this case, the only factor affecting the COP that is considered is the outdoor temperature. The COP at each interval *j*, i.e., w_j, is calculated by increasing the nameplate value by 2% for every degree Celsius change of outdoor temperature. For simplicity w_j is assumed to be the same for both the summer day and the winter day and is shown in Figure 16.

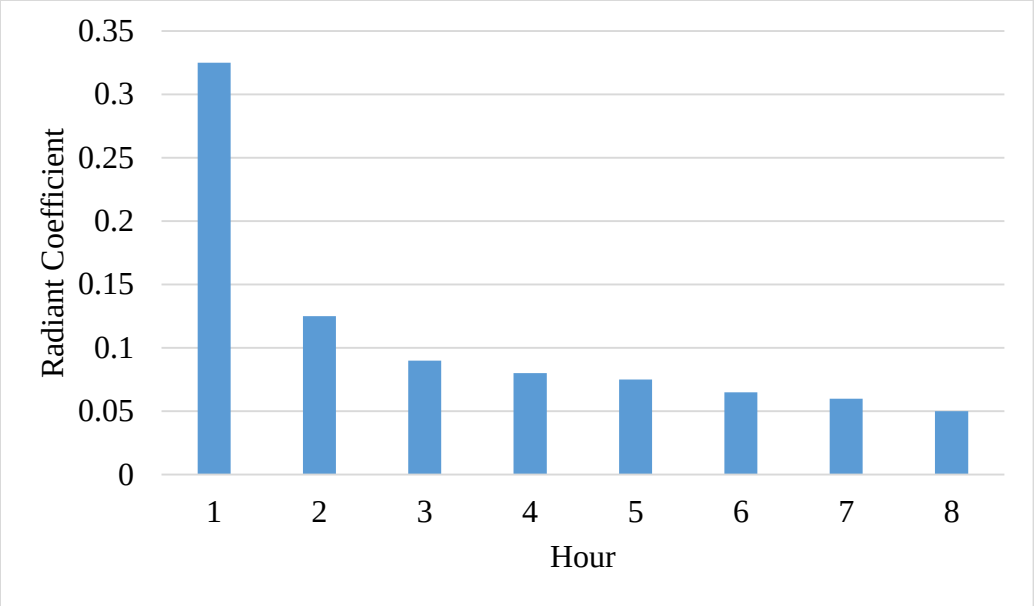

Figure 15 Radiant Time Series Coefficients

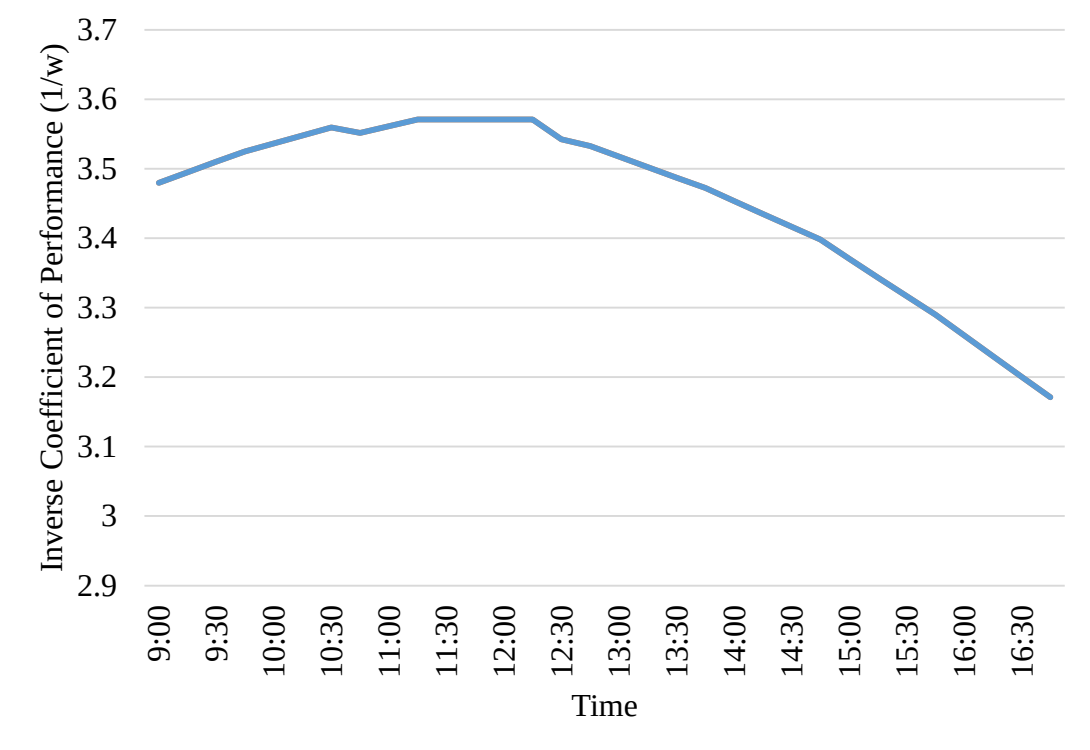

Figure 16 HVAC Coefficient of Performance

The production schedule and HVAC setpoints are identified by solving the objective function (3.3) with constraints (3.4)-(3.7) using General Algebraic Modeling (GAMS). GAMS is an advanced optimization program which is integrated with a large variety of solvers towards complex and large-scale modeling applications (Rosenthal, 2004). The DICOPT solver is selected to solve the proposed combined manufacturing and HVAC scheduling problem. This problem is a mixed integer nonlinear programing (MINLP) problem with integer and binary variables, and linear and nonlinear continuous variables. The DICOPT algorithm solves the problem by dividing it into a series of nonlinear programming (NLP) and mixed integer programming (MIP) sub-problems. The solvers CONOPT and LINDOGLOBAL are used to solve NLP and MIP sub-problems, respectively. The solved production schedule, buffer contents, and the HVAC temperature setpoints for Scenario III are shown in Figure 17, Figure 18, and Figure 19. It takes five and 16 minutes to solve the winter and summer cases, respectively using a desktop that has an AMD A8-6410 APU with AMD Radeon R5 Graphics 2.00GHz processor with 6GB memory.

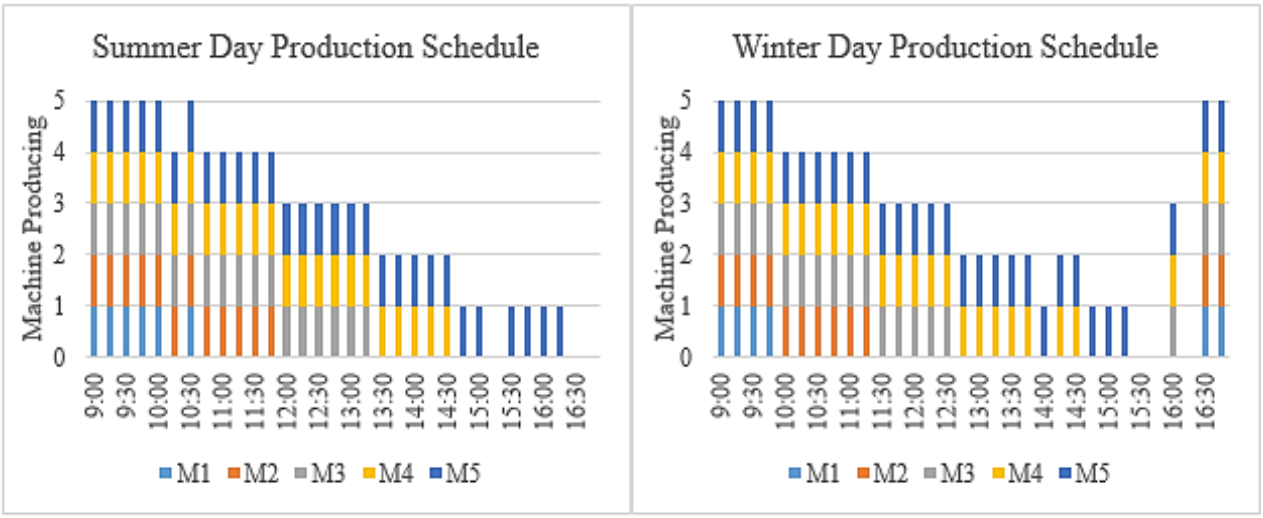

Figure 17 Production Schedule for Scenario III

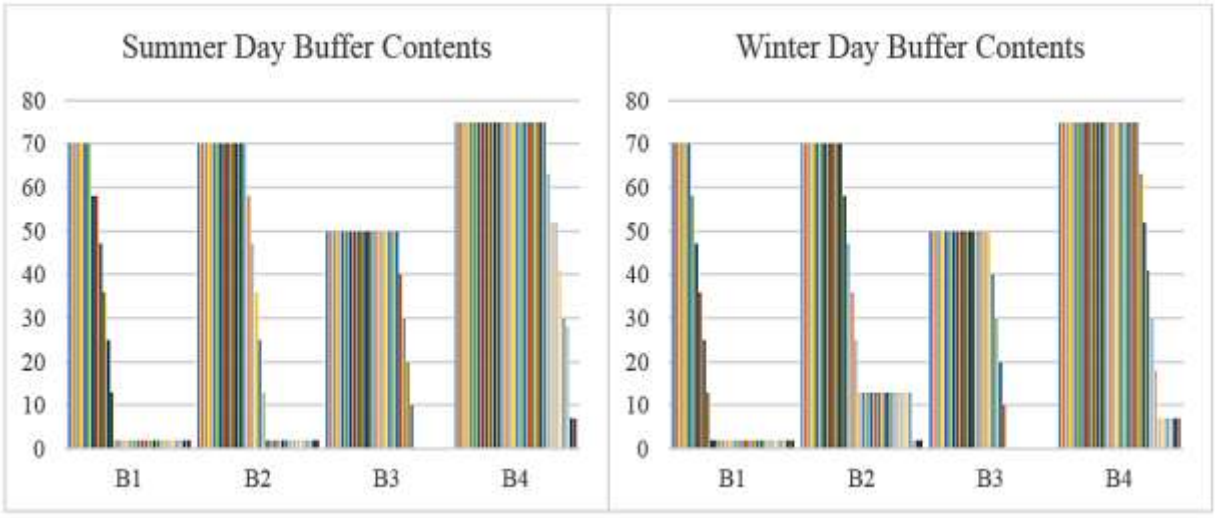

Figure 18 Buffer Contents for Scenario III

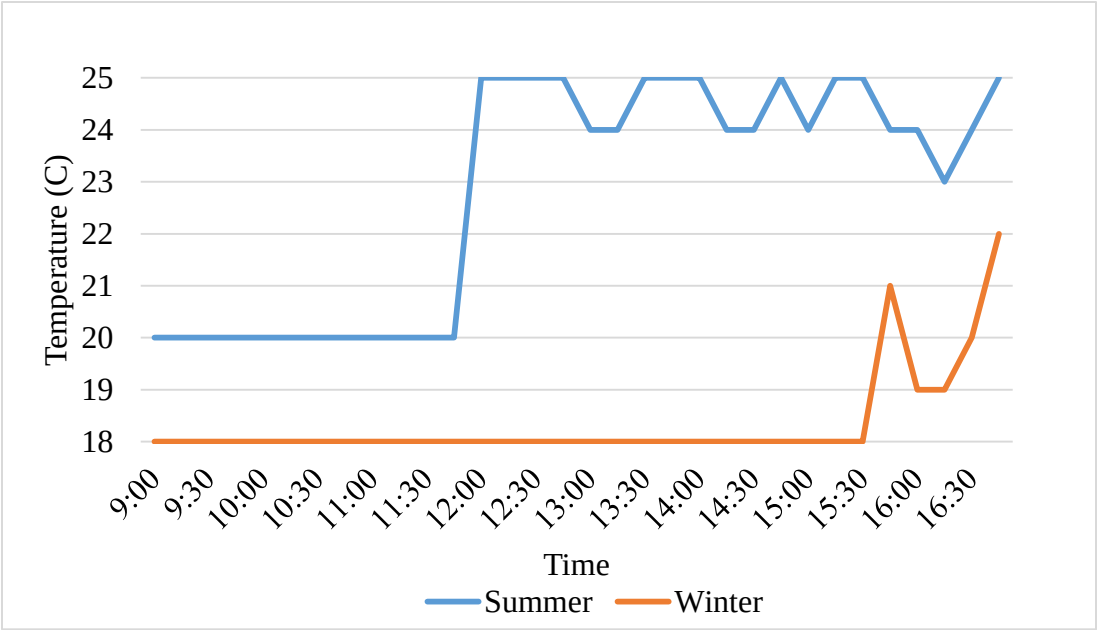

Figure 19 HVAC Temperature Setpoints for Scenario III

The profile of the total power consumption in Scenario III can be found in in Figure 20, where the power profiles of Scenarios I and II are also graphed for comparison. It can be seen that in Scenario III that the power consumption during off peak periods is much higher than in peak periods; thus, the energy consumption during peak periods can be successfully shifted to the off

peak periods. It also illustrates that the maximum power consumption during peak periods can be reduced compared to Scenarios I and II, which demonstrates that the objective of this research, i.e., reduce the maximum power consumption during peak periods, can be effectively achieved. Note that there is significant difference in the summer and winter power profiles since the heat generated by the machines can actually be used to help heat the building.

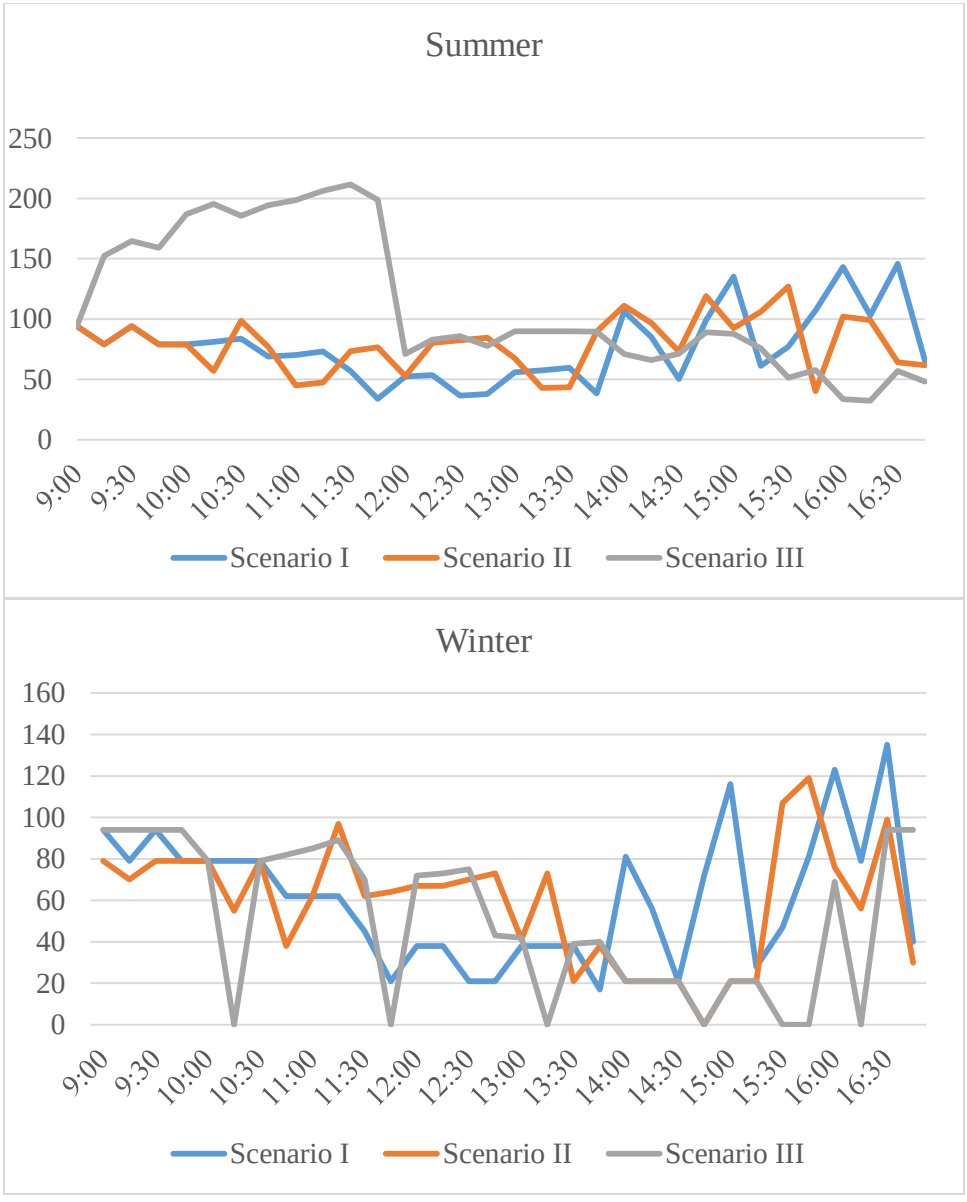

Figure 20 Summer and Winter Power Profile

Table 25 lists the power demand during peak periods and the "peak-to-average" ratio of the three scenarios. Meanwhile, Table 26 shows the power demand reduction percentages compared to the baseline scenarios.

Table 25 Peak Power Demand and Peak-to-Average Ratio

	Summer		Winter	
	Peak Power Demand (kW)	Peak-to-Average Ratio*	Peak Power Demand (kW)	Peak-to-Average Ratio*
Scenario I	145.9	1.8	135.4	2.2
Scenario II	127	1.6	119.2	2
Scenario III	89.9	0.8	94	1.7

* The peak-to-average ratio is calculated by dividing the maximum power during peak hours by the average power throughout the entire production horizon.

Table 26 Peak Power Demand Reduction Comparison

	Power Demand Reduction in Peak Periods	
	Summer	**Winter**
Scenarios III vs I	38.4%	30.6%
Scenarios III vs II	29.3%	21.1%

It can be seen from Table 26 that the power demand during peak periods for the summer day under Scenario III is about 38% and 29% less than Scenarios I and II, respectively. Similarly, the power demand during peak periods for the winter day under Scenario III is about 30% and 21% less than Scenarios I and II, respectively.

To examine the cost effectiveness of the proposed method, we also compare the cost reduction percentages of the three scenarios in Table 27 and Table 28. The proposed method during

the summer day, can achieve approximately 10% and 7% in cost reductions compared with Scenarios I and II, respectively. Correspondingly, during the winter day approximately 29% and 21% in cost reductions can be achieved compared with Scenarios I and II, respectively. It is interesting to note that the winter day results in much greater cost savings then the summer day. This is most likely due to the advantage of the winter day's ability to use the heat generated by the machines to reduce the HVAC heating load.

Table 27 Electricity Billing Cost

	Electricity Cost ($)	
	Summer	Winter
Scenario I	4878.9	4373.7
Scenario II	4618.5	3952.9
Scenario III	4387.5	3096.3

Table 28 Electricity Billing Cost Reduction

	Electricity Cost Reduction	
	Summer	**Winter**
Scenario III vs Scenario I	10.0%	29.2%
Scenario III vs Scenario II	7.0%	21.2%
Scenario II vs Scenario I	5.3%	9.6%

3.5 Conclusion

In this Chapter, an integrated production and HVAC system scheduling model is developed and aims to minimize the peak power demand for the manufacturing plant. A HVAC work load model, considering the heat generated by the manufacturing operation, is proposed. Meanwhile, the production line and HVAC power demand are formulated. The model is formulated as a mixed integer nonlinear programming (MINLP) problem. General Algebraic Modeling (GAMS) is used

to solve the problem and identify the schedule for the manufacturing system and determine the HVAC temperature setpoints that can minimize the power demand during peak periods. The case study shows that significant peak power demand reduction can be achieved compared to minimizing the power demand of the manufacturing system and HVAC system exclusively.

4 Integrated Electricity and Natural Gas Demand Response for Manufacturers in the Smart Grid

Parts of this chapter were previously published as: “Dababneh, Fadwa, and Lin Li. "Integrated Electricity and Natural Gas Demand Response for Manufacturers in the Smart Grid." *IEEE Transactions on Smart Grid* (2018). DOI: 10.1109/TSG.2018.2850841.”.

4.1 Objective and Overview

The SG opens many opportunities for electricity suppliers and customers to maintain grid stability, reduce electricity cost, and promote environmentally sustainable operation. Unfortunately, these benefits cannot be fully realized from industrial energy customers due to inadequate manufacturing decision making methodology that can consider manufacturers and energy suppliers simultaneously through real-time electricity, gas, and production control. Hence, in this chapter, a real-time electricity and natural gas driven production scheduling model for manufacturers is established. The model considers time-based and event-based electricity and gas DR. A Modified Simulated Annealing algorithm is proposed to solve the problem in reaction to real-time supply notifications so that the interaction between manufacturers and energy providers is promoted. Numerical case studies are implemented and illustrate that 66-68% in energy cost savings for the manufacturer can be achieved when using the proposed model compared to baseline scenarios. Meanwhile, the Modified Simulated Annealing algorithm outperforms various solution methods in solving the proposed problem.

The rest of the chapter is organized as follows. The proposed integrated EDR and GDR driven production scheduling model is presented in Section 4.2. The solution approach and real-time scheduling procedure are discussed in Section 4.3. Section 4.4 shows illustrative and numerical cases for the proposed method. Lastly, Section 4.5 concludes the chapter.

4.2 Integrated EDR and GDR Driven Production Scheduling Model

An integrated EDR and GDR driven production scheduling model is developed. The scheduling problem aims to minimize the manufacturer's production line energy cost while considering energy and production constraints. The global input parameters are the DR programs, production target, and planning horizon duration. The local station/buffer input parameters are the production rate, production efficiency, rated energy demand, initial buffer contents, etc.

4.2.1 Nomenclature

Model Indices

i: index of the stations in the production line

t: index of the intervals throughout the planning horizon

Model Parameters

CP_i: specific heat capacity of the medium in the furnace

ew_i: setup time for station i

GA_{event}: upper bound for gas demand during GDR event

g_i: gas steady state usage rate for station i

gs_{it}: startup gas requirement for station i during interval t

H: length of the decision interval in hours

Int_{it}: integer part of L_{it}

L_{it}: number of intervals station i performs setup as of interval t

$NRDR$: gas incentive rate for GDR event ($/(MMBTU/hr))

PA_{TOU}: upper bound for power demand during TOU peak hours

PA_{event}: upper bound for power demand during EDR event

PD_t: power demand for the production line during interval t

p_i: motor startup power for station i

PR_i: production rate of station i

ps_{it}: steady state power for station i during interval t

REC_t: electricity consumption rate during interval t ($/kWh)

RDR: power demand incentive rate for the EDR event ($/kW)

RGC_t: natural gas usage rate ($/MMBTU)

RPD: power demand rate ($/kW)

rf_{it}: maintenance indicator equal to one if station i is being repaired in interval t and zero otherwise.

S_i: buffer capacity corresponding to station i

ST_i: required temperature for station i

TA: target production yield for the entire planning horizon

V_i: chamber volume of station i

α_i: heat from one-unit increase in temperature

ρ_i: density of medium (i.e., air) in station i

Model Variables

B_{it}: buffer content level for station i during interval t

DS_{it}: percent of time station i is performing setup in interval t

$Frac_{it}$: fractional part of L_{it}

GD_t: gas demand for the production line during interval t

$TELE$: total electric energy consumption

$TGAS$: total natural gas consumption

CE_{event}: incentive payment for participating in the EDR event

C_{ELE}: total cost of electricity

CE_{TOU}: cost of electricity under the electricity TOU program

CG_{event}: incentive payment for GDR curtailment

CG_{TOU}: cost of gas under the natural gas TOU program

C_{NG}: total cost of natural gas

TA_i: minimum number of parts to be outputted by station i

T_{it}: temperature at station i during interval t

TP: total production throughput for the entire planning horizon

TP_t: production throughput during interval t
x_{it}: binary decision variable denoting a station's on/off state
Simulated Annealing Variables
AP_p: probability of accepting a positive transition in SA
$H(X,Y)$: hamming distance between solution X and solution Y
N_X: neighborhood of solution X in SA
p: positive transition in SA
$penTP$: target throughput penalty
$penPD$: peak power limit penalty
$penBUmin$: minimum buffer content penalty
$penBUmax$: maximum buffer capacity penalty
q_1- q_4: binary penalizing indicators
S: random set of positive transitions
TPR: temperature parameter
λ_{f1}- λ_{f7}: penalties in the fitness function
χ: acceptance probability
$\varepsilon_{TP}, \varepsilon_{PD}, \varepsilon_{BU}, \varepsilon_{PEN0}$: number of elements randomly chosen from $I \times T$ matrix, corresponding to constraints violated

4.2.2 Problem Formulation

Consider the discrete serial, I station and I-1 buffer, production line as shown in Figure 21. The stations in the serial production line can consume either electricity or gas. The planning horizon is discretized into a set of fixed finite intervals with duration H. Let i, i=1, ..., I, be the index of the stations and t, t=1, ..., T, be the index of the intervals. x_{it} denotes the state of station i during interval t, which equals one if station i is scheduled for production, and zero otherwise.

Figure 21 *I* Station *I*-1 Buffer Serial Production Line

Once parts are processed at a given station they will be stored in the downstream buffer. For a station to be able to process parts, the station needs to first take parts from its corresponding upstream buffer. Meanwhile, it is assumed that the first machine is never starved and the last machine is never blocked. Buffers are typically used in manufacturing settings to provide more robust and resilient production. Typically, in the case of station failures or required maintenance tasks, the buffers can help mitigate production loss and open up opportunities for energy and cost savings using intelligent scheduling methods. The production throughput, *TP*, and the buffer contents, B_{it}, can be calculated as follows.

$$TP_t = H \cdot (1 - DS_{It}) \cdot PR_I \cdot \eta_I \cdot x_{It} \quad \forall t \tag{4.1}$$

$$TP = \sum_{t=1}^{T} TP_t \tag{4.2}$$

$$B_{it} = B_{i(t-1)} + H \cdot \left(1 - DS_{i(t-1)}\right) \cdot PR_i \cdot \eta_i \cdot x_{i(t-1)} - H \cdot \left(1 - DS_{(i+1)(t-1)}\right) \cdot PR_{(i+1)} \cdot \eta_{(i+1)} \cdot x_{(i+1)(t-1)} \quad \forall\, i \,\&\, \forall t \tag{4.3}$$

PR_i and η_i are the production rate and efficiency of station *i*, respectively. DS_{it} is the percentage of time station *i* is performing setup during interval *t* and is calculated in (4.4)-(4.8).

$$L_{it} = \left[ew_i \cdot x_{it} \cdot (1 - x_{i(t-1)})\right] \div (60 \cdot H) \; \forall\, i \,\&\, \forall t \tag{4.4}$$

$$Int_{it} = \lfloor L_{it} \rfloor \quad \forall\, i \,\&\, \forall t \tag{4.5}$$

$$Frac_{it} = L_{it} - Int_{it} \quad \forall\, i \,\&\, \forall t \tag{4.6}$$

$$Int_{it} = \sum_{t}^{t=t+Int_{it}-1} DS_{it} \quad \forall\, i \,\&\, \forall t \tag{4.7}$$

$$DS_{i(t+Int_{it})} = Frac_{it} \quad \forall\, i \,\&\, \forall t \tag{4.8}$$

L_{it} is the total time needed for setup for station *i* starting from interval *t* and is in interval units. ew_i is the setup time, in minutes, for station *i*. Int_{it} is the integer part of L_{it}, and is the number of whole

intervals starting from interval t that station i is in setup. Finally, $Frac_{it}$ is the fractional part of L_{it}, representing the setup time that will be incurred by station i during interval $t+Int_{it}$.

Next, event-based EDR and GDR programs are employed to encourage manufacturers to decrease their energy load for monetary incentives. Notifications of electricity and gas supply reduction events are assumed to be monitored in real-time. The manufacturer will be informed one decision interval before the event. All energy saving actions and utility notifications can only be made at the beginning of each interval. Event driven electricity and gas supply reduction events are denoted by dr_t and ng_t, respectively. dr_t is equal to one if there is a notification that an EDR event will occur in interval $t+1$ and zero otherwise. Similarly, ng_t is equal to one if a GDR event will occur in interval $t+1$ and zero otherwise. CE_{event}, the total incentive (negative cost) for partaking in the EDR event, is shown in (4.9).

$$CE_{event} = \min[0, dr_t \cdot RDR \cdot (PD_{t+1} - PA_{event})] \tag{4.9}$$

RDR is the incentive rate (\$/kW); PD_{t+1} is the power demand for the entire production line in interval $t+1$, and PA_{event} is the committed power limitation level during the event. CG_{event} , the incentive (negative cost) for GDR events, is shown in (4.10).

$$CG_{event} = \min[0, ng_t \cdot NRDR \cdot (GD_{t+1} - GA_{event})] \tag{4.10}$$

$NRDR$ is the incentive rate (\$/[MMBTU/hr]); GD_{t+1} is the gas flow (MMBTU/hr) for the entire production line during interval $t+1$, and GA_{event} is the committed gas usage limit.

Moreover, both electricity and natural gas TOU programs are considered. In the electricity TOU program, the manufacturer is charged an electricity consumption rate (\$/kWh) and power demand rate (\$/kW). The electricity consumption rate varies over time. During peak hours, a higher consumption rate and demand rate (to the maximum power demand of all the intervals in peak hours) are applied. The cost function is shown below.

$$CE_{TOU} = \sum_{t=1}^{T} (H \cdot REC_t \cdot PD_t) + RPD \cdot \max_{t \in EOP} PD_t \tag{4.11a}$$

EOP is a subset of *t* denoting electricity peak hours. PD_t is the manufacturer's electricity demand during interval *t*; REC_t is the electricity consumption rate during interval *t* ($/kWh); and *RPD* is the power demand rate ($/kW). The "max" function in (4.11a) expresses the maximum power flow in peak hours which is a nonsmooth exogenous operator and leads to many computational challenges when solving the problem. Hence, the "softmax" function is used to approximate the "max" function (Bishop, 2006) as shown in the revised equation in (4.11b), where S_e is a constant in the "softmax" approximation.

$$CE_{TOU} = \sum_{t=1}^{T} (H \cdot REC_t \cdot PD_t) + RPD \cdot ln\left(\sum_{t \in EOP} e^{S_e \cdot PD_t}\right)/S_e \tag{4.11b}$$

Next, the gas TOU program is considered. The manufacturer is charged different usage rates corresponding to peak, valley, and flat rate hours ($/MMBTU). The cost function is shown below.

$$CG_{TOU} = \sum_{t=1}^{T} (H \cdot RGC_t \cdot GD_t) \tag{4.12}$$

GD_t is the manufacturer's gas demand during interval *t* and RGC_t is the gas usage rate ($/MMBTU) during interval *t*.

Subsequently, it is necessary to model the energy demand and consumption. PD_t, the total electric power demand for the production line during interval *t* and GD_t, the total natural gas usage rate for the production line during interval *t*, are shown in (4.13) and (4.14), respectively. *ES* and *NGS* are subsets of *i* denoting stations that use electricity or natural gas, respectively.

$$PD_t = \sum_{i \in ES} [(ps_i \cdot DS_{it}) + (x_{it} \cdot p_i \cdot (1 - DS_{it})] \ \ \forall t \tag{4.13}$$

$$GD_t = \sum_{i \in NGS} [(gs_{it} \cdot DS_{it}) + (x_{it} \cdot g_i \cdot (1 - DS_{it})] \ \ \forall t \tag{4.14}$$

ps_i is the motor startup power for station *i*; p_i is the steady state power; gs_{it} is the gas startup usage

rate for station *i* during interval *t*; and g_i is the gas steady state usage. The total energy consumption functions are shown in (4.15) and (4.16).

$$TELE = \sum_t H \cdot PD_t \tag{4.15}$$

$$TELE = \sum_t H \cdot PD_t \tag{4.16}$$

It is assumed that the startup power for electric equipment and motors is known and deterministic. However, if natural gas consuming stations require heating, the startup energy requirements for process heating will depend on the initial temperature before startup occurs. Several factors may influence this, such as ambient air conditions, volume, heat loss, etc. Assuming that natural gas consuming stations are producing heat, the station startup time is fixed, and the gas flow rate can be adjusted, gs_{it} can be calculated by (17).

$$gs_{it} = \begin{cases} \int_{T_{it}}^{ST_i} \alpha_i \cdot o_i \cdot dT_{it}, & if\ T_{it} < ST_i \\ 0, & otherwise \end{cases} \tag{4.17}$$

$$\forall\, i \in NGS\ \&\ \forall t$$

o_i (MMBtu/C) is the gas required to increase the temperature by one degree Celsius; ST_i is the station's target temperature; T_{it} is the station's actual temperature in interval *t*; and α_i converts a unit temperature into heat. α_i can be calculated by (4.18).

$$\alpha_i = CP_i \cdot \rho_i \cdot V_i \quad \forall\, i \in NGS \tag{4.18}$$

CP_i is the specific heat capacity of the station; ρ_i is the density of air; and V_i is the volume. gs_{it} provides a simple method for calculating the startup gas requirement for the station. Finally, an optimization problem is developed based on the production, energy, and DR cost models. The objective is to minimize the total cost of the energy purchased by the manufacturer under the DR programs described previously. Meanwhile, x_{it} is the binary decision variable that defines the

production schedule. The manufacturer needs to determine a production schedule that considers energy costs and production throughput. Accordingly, the question can be formulated as a nonlinear combinatorics problem and is described by objective function (4.19) and constraints (4.20)–(4.23).

$$\min_{x_{it}}[C_{ELE} + C_{NG}] \tag{4.19}$$

$$TP \geq TA \tag{4.20}$$

$$PD_t \leq PA \quad \forall\, t \in EOP \tag{4.21}$$

$$0 \leq B_{it} \leq S_i \quad \forall\, i = (1,2,\dots,I-1) \tag{4.22}$$

$$x_{it} + rf_{it} \leq 1 \quad \forall\, i \,\&\, \forall\, t \tag{4.23}$$

From (4.19), C_{ELE} and C_{NG} are the total cost of electricity and natural gas and can be formulated by (4.24) and (4.25), respectively.

$$C_{ELE} = CE_{event} + CE_{TOU} \tag{4.24}$$

$$C_{NG} = CG_{event} + CG_{TOU} \tag{4.25}$$

Constraint (4.20) enforces that the target throughput level is met. Constraint (4.21) imposes that the power demand during peak periods is within the committed level during on-peak hours. Constraint (4.22) maintains the buffer contents to be within zero and the maximum buffer capacity. Finally, constraint (4.23) turns the stations off when repair is scheduled.

Due to the exponentially growing search space as the number of machines or intervals increase ($2^{I\times T}$), constraints (4.26) and (4.27) are incorporated into the problem to tighten the search space. These constraints give a lower bound for the least number of intervals station *i* must be on throughout the production horizon to ensure production throughput.

$$\sum_{t=1}^{T} x_{it} \geq \frac{TA_i - B_{i(t=1)}}{H \cdot PR_I \cdot \eta_I} \quad \forall i = (1,2,\dots,I-1) \tag{4.26}$$

$$\sum_{t=1}^{T} x_{It} \geq (TA/H \cdot PR_I \cdot \eta_I) \tag{2.27}$$

4.3 Solution Approach and Real-Time Implementation Procedure

The proposed problem is a nonlinear combinatorics problem with $I \times T$ variables and $2^{I \times T}$ possible solutions. As the number of stations and intervals increase, the nonlinear combinatorics problem increases exponentially. For the proposed problem to be able to realize the benefits of DR events, a production schedule needs to be determined within a decision interval's duration. Exact solution methods can guarantee the optimality of a solution; however, metaheuristics can provide "good" solutions (that lead to energy cost savings) in real-time.

Hence, the fitness function in (4.28) is used to represent the problem. Constraints are mapped as penalties. $CE_{TOU} + CG_{TOU}$ is used in place of $C_{ELE} + C_{NG}$ since CE_{event} and CG_{event} are added iteratively as event notifications occur.

$$\begin{aligned} & CE_{TOU} + CG_{TOU} + \lambda_{f1}[\min(TP - TA, 0)]^2 + \lambda_{f2}[\min(PA - \max(PD_{t \in EOP}), 0)]^2 \\ & + \lambda_{f3} \sum_{t=1}^{T} \sum_{i=1}^{I-1} [\min(S_i - B_{it}, 0)]^2 + \lambda_{f4} \sum_{t=1}^{T} \sum_{i=1}^{I-1} [\min(B_{it}, 0)]^2 \\ & + \lambda_{f5} \sum_{t=1}^{T} \sum_{i=1}^{I} (Int_{it} \cdot x_{it}) + + \lambda_{f6} \sum_{t=1}^{T} \sum_{i=1}^{I} (Int_{it} \cdot rf_{it}) + \\ & + \lambda_{f7} \sum_{t=1}^{T} \sum_{i=1}^{I} (x_{it} \cdot rf_{it}) \end{aligned} \tag{4.28}$$

4.3.1 Simulated Annealing

Simulated Annealing (SA) is used to solve the proposed problem. SA is an efficient and powerful tool for finding near optimal solutions for large scale nonlinear problems. The algorithm

can accept a fraction of "bad" solutions, which allows it to escape local optimal regions in the neighborhood structure (Henderson et al., 2003). The SA procedure starts with an initial solution X and moves to a new solution, Y, within the neighborhood, N_X, if its objective function value is not greater than (minimization problem) the incumbent solution. If the objective function value is greater than the incumbent solution, the inferior solution may still be accepted with a probability of $exp(-(f(Y) - f(X))/TPR)$. Swap, insertion, and reversion methods are typically used for defining the neighborhood of a solution (Shedden, 1990; and Jolai et al., 2012); however, they are not robust for problems with high dimensionality. Thus, the hamming distance (HD) is used and provides an efficient permutation method with robust exploration capability (Yao, 1992).

Definition 1: *The "Hamming" distance between two permutations* $X=[x_1, x_2, \ldots, x_n]$ *and* $Y=[y_1, y_2, \ldots, y_n]$ *is* ε *if there are exactly* ε *different elements between them.*

SA relies heavily on a temperature schedule; thus, a cooling schedule that balances global and local search needs to be determined. Let m be the number of outer loop iterations that the temperature (TPR_m) is reduced at, and v be the number of inner loop iterations. The temperature for the next outer loop TPR_{m+1}, is obtained by $TPR_{m+1} = \alpha \cdot TPR_m$ such that the current temperature is multiplied by a constant α and $\alpha \in (0,1)$.

The ability of SA to escape the local minimum depends on the average probability of accepting "bad" moves, which depends on the temperature. Determining a robust initial temperature requires a sample of positive transitions and estimating the acceptance probability, $\chi^*(TPR) = \chi_0$, that can reach TPR_0. A novel procedure is proposed to determine the initial temperature (TPR_0) in (Ben-Ameur, 2004), where the acceptance ratio of increasing cost moves (χ) is set to a specified value χ_0.

Definition 2: *Positive transition p requires E_{max}>E_{min}, where E_{max_p} and E_{min_p} are energies (objective costs) at the states after transition max_p and min_p.*

Definition 3: *Let, δ_p=$Emax_p$-E_{min_p} and* $\chi(TPR) = \sum_p \pi_{min_p} \frac{1}{|N(min_p)|} exp\left(\frac{-\delta_p}{TPR}\right) \div \sum_p \pi_{min_p} \frac{1}{|N(min_p)|}$; $\pi_{min_p}/|N(min_p)|$ *is the probability to generate a transition p when the energy states follow the stationary distribution,* $\pi_k = |N(k)|\exp\left(\frac{-E_k}{TPR}\right)/\sum_j |N(j)|\exp\left(\frac{-E_j}{TPR}\right)$, *and N(.) is the set of neighbors for the state.*

A modified estimation of the acceptance probability, based on a random set *S* of positive transitions, for computing the initial temperature, is proposed in (4.29); where $AP_p = exp(-(E_{max\_p} - E_{min\_p})/TPR)$ is the probability of accepting a positive transition.

$$\hat{\chi}(TPR) = \sum_{p \in S} AP_p / \|S\| \tag{4.29}$$

4.3.2 Penalty Driven Hamming Distance Function

The neighborhood function can leverage the problem structure to speed up and enhance the search. However, many studies assign a fixed neighborhood size at the beginning (Yao, 1992), limiting SA's ability to search at different scales and stages. Since SA attempts to combine exploration of a space and exploitation of a sub-space into the same algorithm, the neighborhood size should be adjusted at different search stages relative to the current temperature for faster convergence. Leveraging important problem specific features (i.e., station type and on/off-peak intervals) in the neighborhood definition and SA procedure can amplify these benefits.

Thus, a penalty guided HD function, directing the computational resources on the highest impact variables in the search, is proposed. The HD will target specific areas of the $I \times T$ matrix depending on the constraints being violated. The HD is scaled using the penalty incurred from λ_{f1}-λ_{f7}, while integrating constraint priorities with the objective function. Let *penTP* be the target throughput penalty; *penPD* be the penalty when the power during peak intervals exceeds the committed power limit; penalty *penBUmin* be the penalty when the buffer contents of a station fall below zero; and *penBUmax* be the penalty when buffer contents exceed the maximum capacity. These penalties are formulated as shown in (4.30)-(4.33).

$$penTP = \lambda_{f1}[\min(TP - TA, 0)]^2 \tag{4.30}$$

$$penPD = \lambda_{f2}[\min(PA - \max(PD_{t \in EOP}), 0)]^2 \tag{4.31}$$

$$penBUmin = \lambda_{f4} \sum_{t=1}^{T} \sum_{i=1}^{I-1} [\min(B_{it}, 0)]^2 \tag{4.32}$$

$$penBUmax = \lambda_{f3} \sum_{t=1}^{T} \sum_{i=1}^{I-1} [\min(S_i - B_{it}, 0)]^2 \tag{4.33}$$

Moreover, let q_1, q_2, q_3 and q_4 be binary penalizing indicators for the throughput constraint, peak power demand constraint, minimum buffer capacity constraint, and maximum buffer capacity constraint, respectively. These indicators take a value of one if the corresponding constraint is violated and zero otherwise as shown in equations (4.34)-(4.37).

$$q_1 = \begin{cases} 1, & if\ penTP > 0 \\ 0, & otherwise \end{cases} \tag{4.34}$$

$$q_2 = \begin{cases} 1, & if\ penPD > 0 \\ 0, & otherwise \end{cases} \tag{4.35}$$

$$q_3 = \begin{cases} 1, & if\ penBUmin > 0 \\ 0, & otherwise \end{cases} \tag{4.36}$$

$$q_4 = \begin{cases} 1, & if\ penBUmax > 0 \\ 0, & otherwise \end{cases} \tag{4.37}$$

For a combinatorial optimization problem with a large countable permutation space Ω, each $X \in \Omega$ can be denoted by an $I \times T$ matrix. The neighborhood N_X of permutation X is d_{XY} distance away from X and is defined by equation (4.38).

$$N_X = \{Y | Y \in \Omega, d_{XY} = H(X,Y)\} \tag{4.38}$$

where $X \notin N_X$ and $X \in N_Y$ if $Y \in N_X$. The HD between the current permutation,X, and the next one, Y, governs the neighborhood function. The HD is denoted by $H(X,Y)$ and calculated in (4.39), which gives the total number of elements that need to be inverted in the current permutation, X, to obtain the new permutation, Y, in the neighbourhood of X, N_X.

$$\begin{aligned} H(X,Y) = {} & q_1 \cdot \varepsilon_{TP} + q_2 \cdot \varepsilon_{PD} + q_3 \cdot \varepsilon_{BU} + q_4 \cdot \varepsilon_{BU} + (1-q_1) \cdot (1-q_2) \cdot (1-q_3) \\ & \cdot (1-q_4) \cdot \varepsilon_{PEN0} \end{aligned} \tag{4.39}$$

where ε_{TP}, ε_{PD}, and ε_{BU} correspond to the number of elements randomly chosen from specific areas of the $I \times T$ matrix depending on the constraint being violated. ε_{PEN0} denotes the number of elements randomly chosen from the $I \times T$ matrix when none of the constraints are violated. These elements, when inverted, result in a new permutation in the neighborhood of X. The procedure to calculate $H(X,Y)$ is shown as follows.

Step 1: SET the HD evolution, ε = [ε_1, ε_2, ..., ε_m], where ε_1, ε_2, ..., ε_m are the HD at temperature levels 1, 2, ..., *m,* respectively

Step 2: **IF** ($q_1 > 0$)
SELECT randomly $\varepsilon_{TP} = f(\varepsilon)$ number of elements from row $i=I$ of the matrix and
INVERT the elements. (for e.g. $\varepsilon_{TP} = max(\varepsilon - \lambda_1, \lambda_2)$)

ELSE IF ($q_2 > 0$)
SELECT randomly $\varepsilon_{PD} = f(\varepsilon)$ number of elements from rows $i \in ES - \{I\}$ and columns $t \in EOP$ of the IxT matrix and
INVERT the elements. (for e.g. $\varepsilon_{PD} = \varepsilon + \lambda_3$)

ELSE IF ($q_3 > 0$) || ($q_4 > 0$)
SELECT randomly $\varepsilon_{BU} = f(\varepsilon)$ number of elements from rows $i=1, \ldots, I\text{-}1$ of the IxT matrix and
INVERT the elements. (for e.g. $\varepsilon_{BU} = \varepsilon + \lambda_4$)
ELSE IF ($q_1 = 0$) && ($q_2 = 0$) && ($q_3 = 0$) && ($q_4 = 0$)
SELECT randomly $\varepsilon_{PEN0} = f(\varepsilon)$ number of elements from rows $i=1, \ldots, I\text{-}1$of IxT matrix and
INVERT the elements. (for e.g. $\varepsilon_{PEN0} = max(\varepsilon + \lambda_5, \lambda_6)$)
Step 3: COMPUTE $H(X, Y)$

Step 4: END

4.3.3 Modified Simulated Annealing (MSA) Algorithm

The MSA algorithm using the penalty driven HD is formulated as follows. At a given iteration in the MSA procedure, the HD is used to create neighbors for the incumbent solution and a different HD is defined for each type of constraint. The iterations remain constant within a given temperature level and are updated when progressing to different levels. The HD will target specific regions in the incumbent solution's decision matrix based on the violated constraint. If there are not any violated constraints, the HD targets the entire decision matrix of the incumbent solution.

Let trg_{TP} represent $I \times T$ matrix elements targeted during the neighborhood search using the penalty driven HD when the throughput constraint is violated, $trg_{TP} = \{i = I, t = 1, \ldots, T\}$; trg_{PD} represent the target elements when the power demand constraint is violated, $trg_{PD} = \{i \in ES - \{I\}, t \in EOP\}$; trg_{BU} represent the target elements when buffer constraints are violated, $trg_{BU} = \{i = 1, \ldots, I, t = 1, \ldots, T\}$; and trg_{PEN0} represent the target elements when none of the constraints are violated, $trg_{PEN0} = \{i = 1, \ldots, I - 1, t = 1, \ldots, T\}$. The MSA algorithm is shown below.

Step 0: GENERATE trg_{TP}, trg_{PD}, trg_{BU}, trg_{PEN0}
Step 1: GENERATE an initial solution $X = X_0$ using and
ASSIGN best solution $X^* = X_0$
Step 2: SELECT m, $v = [v_1, v_2, \ldots, v_m]$ and number of neighbors
NS, and GENERATE an initial temperature $TPR = TPR_0$
Step 2.1: **(a)** FOR Iteration j such that $j = 1{:}m$
(b) FOR Iteration k such that $k = 1{:}v_j$
(c) FOR Iteration l such that $l = 1{:}NS$
Randomly SELECT solution Y_l based on current solution
X from the neighborhood N_X specified by $H(X, Y_l)$
Step 2.2: CHECK IF $f(Y_l) \leq f(X)$
THEN accept Y_l as new solution; SET $X = Y_l$
CHECK IF $f(Y_l) \leq f(X^*)$
THEN accept Y_l as best solution; SET $X^* = Y_l$; END IF
ELSE accept Y_l as new solution with probability
$\exp(-(f(Y_l) - f(X))/TPR_j)$; END IF
Step 2.3: CHECK IF $l = NS$
THEN end LOOP of iteration l, UPDATE $k = k+1$ and
GOTO Step 2.1 (c); END IF
Step 2.4: CHECK IF $k = v_j$
THEN end LOOP of iteration k, calculate $TPR_{j+1} = \alpha TPR_j$
UPDATE $j = j + 1$ and GOTO Step 2.1 (b); END IF
Step 2.5: CHECK IF $j = m$
THEN end LOOP of iteration j; END IF
Step 3: SET $\sigma_p = X^*$; END

The MSA algorithm utilizes the dynamic neighborhood structure through the penalty driven HD, which can easily be adapted to any addition or relaxation of constraints. Figure 22 shows an example of the matrix operations when the HD targets peak power periods due to a power limitation violation.

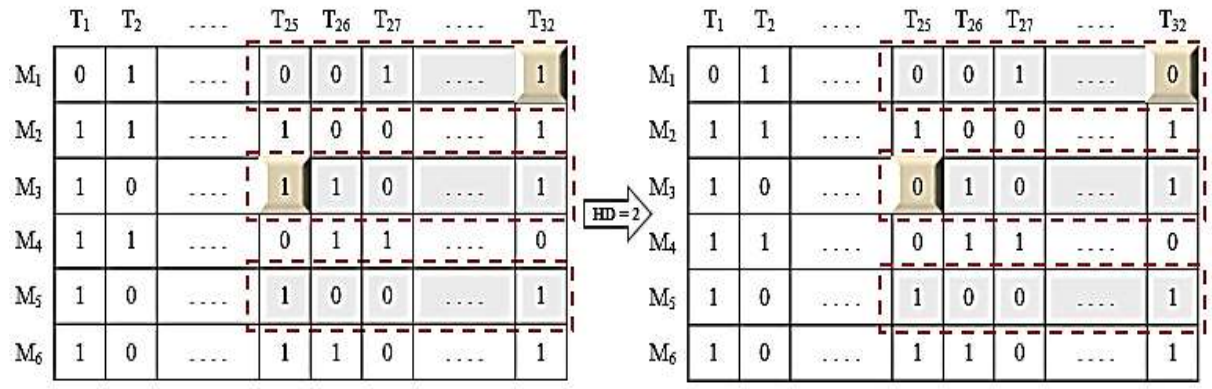

Figure 22 Hamming Distance Operations Due to Power Limitation Violation

The MSA algorithm will converge to a near optimal solution in polynomial time if it is *asserting* and *infeasible diminishing* (Mendivil and Shonkwiler, 2010). The SA chain is *asserting* if there is some probability greater than zero of obtaining a feasible solution in the neighborhood N_X of solution X. Next, the SA chain is *infeasible diminishing* if the probability of transition to an infeasible solution from the present solution decays to zero as the time steps approach infinity. For a combinatorial optimization problem with a large permutation space Ω, the MSA algorithm will start with an initial solution X_0 and as the temperature changes, a sequence of solutions is constructed, where $\{X_0, X_1, X_2, \dots\} \subset \Omega$. For each step in this chain, an $H(X, Y)$ amount of change occurs to move from a solution X to a neighboring solution Y. If this change improves the fitness, the change is accepted, otherwise the change is rejected with a probability. Such a stochastic construction of *Xs* is defined as a Markov chain and forms the basis of the SA algorithm. Moreover, since the problem is a constrained optimization problem, a large penalty is assigned to treat the infeasible solutions as feasible. The penalty attenuates the fitness of infeasible solutions so that they will perform poor in comparison to any feasible solution. Hence, the HD will allow reaching a feasible solution from an infeasible one with some positive probability, thus assuring that the MSA algorithm will be *asserting*. Meanwhile, since the acceptance probability of positive

transition reduces to zero as the temperature levels fall, the MSA algorithm is also *infeasible diminishing*. Therefore, it may be concluded that the MSA algorithm will converge to a near optimal solution in a polynomial time.

4.3.4 Real-Time Implementation Procedure

Due to the need to process DR events from the SG or gas utility promptly, it is vital to solve the proposed problem in real-time. Once notifications for electricity or gas supply reduction events are received, a new production schedule needs to be computed before the next decision interval starts. This may be in as little as 15 or 30 minutes.

At the beginning of the production horizon, the first production schedule, σ_p^*, is obtained under the TOU program. Next, as EDR and GDR events occur and feedback enters the optimization loop, the scheduling process is triggered and the procedure repeats until the end of the production horizon. Upon compilation, *TA* and *T* are reset. The real-time production scheduling strategy to implement this is shown as follows.

Step 1: FOR $dr_t = 1$ or $ng_t = 1$; SET $t^* = t$
Step 2: $TA = TA - TP_t$, $T = T - t$
Step 2.1: CHECK IF $dr_t = 1$
THEN IF $\sigma_p^*(i \in ES, t+1) = 0$ STOP
ELSE IF $\sigma_p^*(i \in ES, t+1) \neq 0$
THEN $CE = CE + [dr_t \cdot RDR \cdot (PD_{t+1} - PA_{DR})]$
Step 2.2: CHECK IF $ng_t = 1$
THEN IF $\sigma_p^*(i \in NGS, t+1) = 0$ STOP
ELSE IF $\sigma_p^*(i \in NGS, t+1) \neq 0$
THEN $CG = CG + [ng_t \cdot NRDR \cdot (GD_{t+1} - GA_{DR})]$
Step 3: RECOMPILE Schedule $\sigma_{p,new}^*$
Step 4: SET $\sigma_p^* = \begin{cases} \sigma_p^*, & if\ t \leq t^* \\ \sigma_{p,new}^*, & if\ t > t^* \end{cases}$
Step 5: STOP

4.4 Case Study

An illustrative case to show the effectiveness of the proposed model is conducted and numerical experiments on the solution quality of the MSA algorithm are presented.

4.4.1 Illustrative Case Study

Consider a manufacturing system with 6 stations and 5 buffers. The planning horizon is from 7am-3pm (32 15-minute intervals per day). Table 29 shows the station parameters. Table 30 shows the TOU tariffs. The production target is 8,100/month.

Table 29 Parameter Values for Chapter 4

Parameter	Description	Value
station	ES (1) /NGS (2)	[1, 2, 1, 2, 1, 1]
η_i	station efficiency	[0.8, 0.8, 0.8, 0.8, 0.8, 0.8]
p_i	rated power (kW)	[150, 0, 240, 0, 210, 170]
g_i	gas usage (MMBTU/hr)	[0, 10, 0, 10, 0, 0]
PR_i	production rate (parts/hr)	[50, 50, 50, 50, 50, 50]
$BU_{i(t=0)}$	initial buffer capacity (parts)	[70, 70, 50, 75, 60]
S_i	max buffer capacity (parts)	[160, 145, 140, 160, 145]
ew_i	station setup time (min)	[3, 2, 2.5, 4, 2, 2.5]
PA	peak power limitation	56 kW
PA_{event}	DR event demand limitation	40 kW

Table 30 Electricity and Gas TOU Programs

Natural Gas		
Peak	8am-12pm; 4-7pm	10.43 $/MMBTU
Flat	6-8am; 12-4pm; 7-10pm	8.48 $/MMBTU
Valley	10pm-6am	4.24 $/MMBTU
Electricity		
Off-Peak	7am-1pm	0.08274 $/kWh
On-Peak	1-3pm	0.1679 $/kWh & 18.8 $/kW

Three scenarios are considered. Scenario 1 does not enforce any DR programs using production scheduling. Stations are "on" unless buffer constraints are violated. Scenario 2 is a heuristic approach, during electricity peak hours stations are randomly turned off. Buffer constraints are handled similar to Scenario 1 and GDR is not considered. Scenario 3 uses the integrated EDR and GDR driven production model.

Accordingly, the gas and power profiles for the baseline cases and proposed method are simulated and shown in Figure 23. The corresponding monthly billing cost and energy consumption values are shown in Table 31. Scenario 3 leads to savings of about 68% and 66% compared to Scenarios 1 and 2, respectively. Meanwhile, the most significant savings come from natural gas cost reduction. This further illustrates the need to include GDR considerations in traditional EDR driven production scheduling problems.

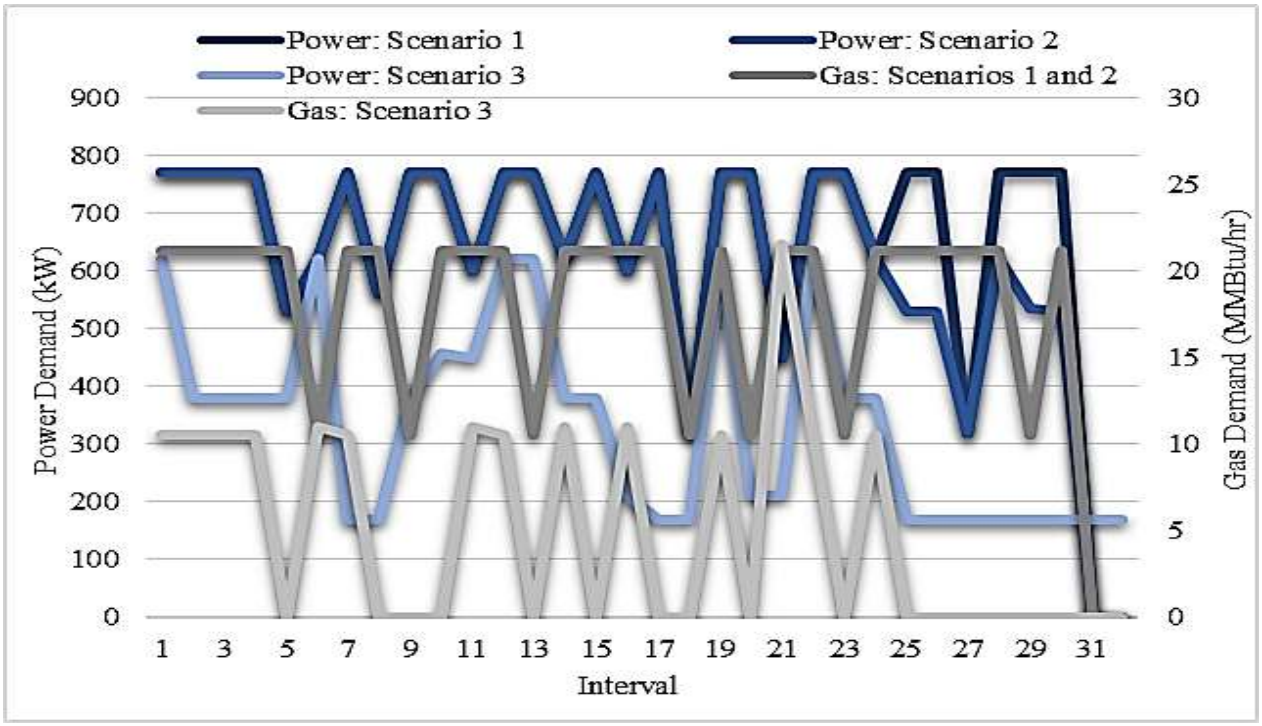

Figure 23 Energy Use Profiles

Table 31 Scenario Comparison under TOU Programs

Production Line's Energy Cost Profile			
Source/Type	**Scenario 1**	**Scenario 2**	**Scenario 3**
Monthly electric use (kWh)	5,160.00	4,883.63	2,680.50
Peak power demand (kW)	770.00	620.00	170.00
Monthly gas use (MMBTU)	139.92	132.00	40.13
Electric consumption ($)	15,471.60	14,079.30	7,522.20
Peak Power demand ($)	14,476.00	11,656.00	3,196.00
Gas use ($)	39,765.60	39,765.60	11,314.50
Total Cost ($)	**69,713.20**	**65,500.90**	**22,032.70**

Next, assuming a gas curtailment event occurs in interval 8 and electricity curtailment event occurs in interval 28 in the same day, the final production schedule after applying the real-time scheduling strategy is shown in Figure 24. If these events are to occur 10 times a year, the real-time scheduling strategy can lead to an added cost savings of $24,260/ year.

Figure 24 Flow Chart of Real-Time Production Scheduling

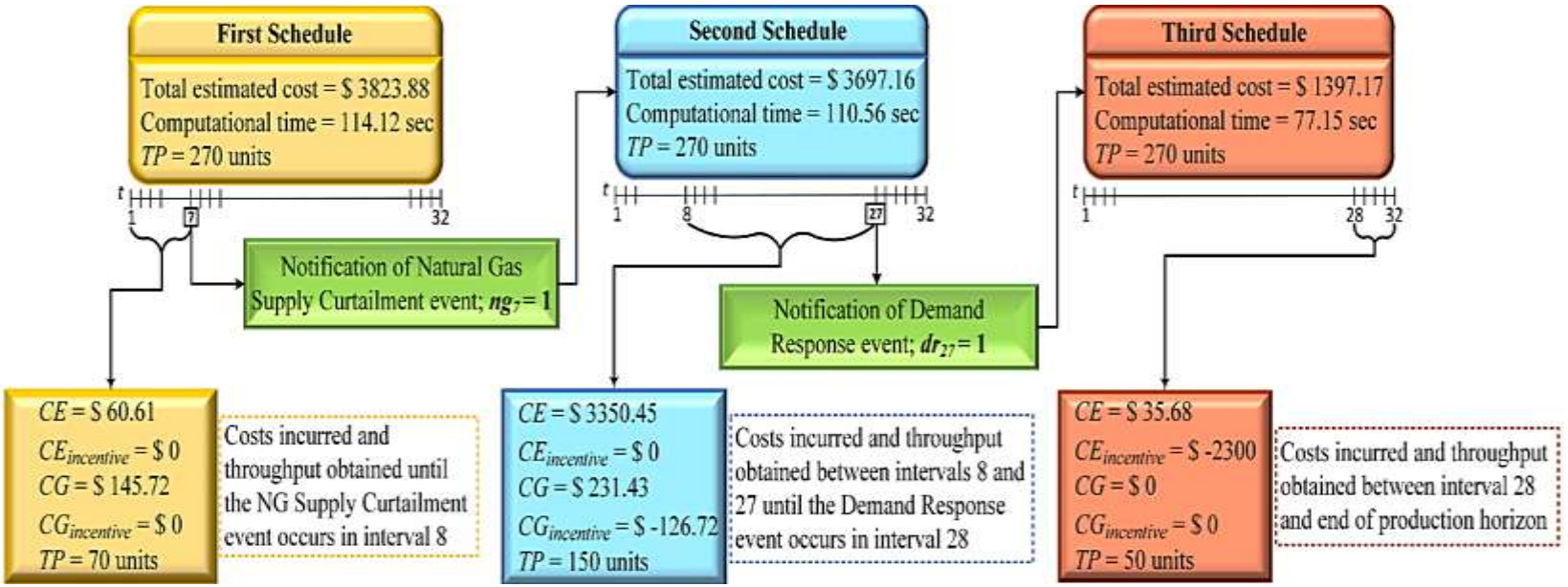

Moreover, in Scenario 3 (i.e. proposed model), profit loss due to production is assumed to be zero since the production target constraint ensures that production goals are met. However, if manufacturers are willing to sacrifice production for potential cost savings, loss of production when participating in DR programs needs to be analyzed. Hence, the production throughput constraint is relaxed and integrated into the objective function cost as a throughput cost such that $TPC = penalty \cdot \max(TA - TP, 0) - benefit \cdot \max(TP - TA, 0)$. Consequently, the penalty and benefit terms will dictate the tradeoff between production loss and cost savings. The cost and throughput for different unit benefit and unit penalty values are shown in Table 32. The best observed case is with a unit penalty of $50 and unit benefit of $20, which leads to a throughput of 8,340 (higher than in Scenario 3) and 18.5% in cost savings compared to Scenario 3. The worst throughput case is with a penalty of $5 and benefit of $10, which achieves an additional 10.97% in cost savings compared to Scenario 3 but with a throughput of 6,000. The worst cost case is with a penalty of $50 and benefit of $10, which leads to the throughput falling to 6,300 and a 29.08% cost increase compared to Scenario 3. Hence, for Scenario 3, the energy cost savings significantly outweigh the production cost.

Table 32 Results after Relaxing Production Throughput Constraint

(Penalty, Benefit)	Cost	Throughput	Cost/Part
(50, 20)	$17,956.44	8,340	$2.15
(200, 10)	$21,045.78	8,400	$2.51
(10, 200)	$21,613.01	8,040	$2.69
(100, 10)	$22,726.88	7,740	$2.94
(5, 10)	$19,614.78	6,000	$3.27
(50, 10)	$28,439.43	6,300	$4.51

When the throughput target is relaxed, manufacturers and researchers must carefully set penalty and benefit terms. These parameters have a significant impact on the cost and throughput levels and are typically unknown or cannot be easily calculated.

4.4.2 Operational Cost Benefits for Power Providers

GDR is expected to benefit power providers due to the rise in gas-fired power generation. Hence, potential cost savings for power providers through manufacturer participation in GDR are estimated according to the following assumptions. Natural gas demand reduction in gas peak hours is allocated to be used for conventional gas generators in place of coal-fired generators. The heat rate for the gas plant is 12,000 Btu/kWh. The coal combustion turbine cost is assumed to be $95/kW and gas combustion turbines cost is $66/kW. The gas demand profile from Scenarios 1 and 2 (GDR is not implemented) is compared to Scenario 3 (GDR is implemented), and the resulting "gas reduction" and "electricity from gas fired generation" daily profiles are shown in Table 33. The results suggest that over a 5-year period (with 261 working days per year), this individual manufacturer's participation in GDR can lead to $207,146 in cost savings for power providers.

Table 33 Gas Reduction and Electricity Generation Profiles

Gas Reduction Profile (MMBTU/interval)	[5.28, 0, 2.64, 5.28, 2.64, 5.28, 2.5343472, 2.64 2.64, 2.5343472, 5.28, 2.5343472, 5.28, 2.64, 2.64 2.64, 0, 2.64, 2.64, 2.64]
Electricity from Gas Fired Generation (kWh/interval)	[0.44, 0, 0.22, 0.44, 0.22, 0.44, 0.21, 0.22, 0.22, 0.21, 0.44, 0.21, 0.44, 0.22, 0.22,0.22, 0, 0.22, 0.22, 0.22, 0.44]

4.4.3 Evaluation of Alternate Solution Approaches

The effectiveness of the MSA algorithm compared to BARON [43], SA, and PSO is studied. Production lines with 6, 12, 25, and 50 stations are considered. The results are shown in Table 34. The MSA algorithm obtains the best solution in the least time; SA beats PSO but is inferior to MSA; BARON, in theory, will obtain the global optimal solution if ran indefinitely.

Table 34 Algorithm Performance for Solution Methods

Method	Stations	6	12	25	50
MSA	Cost ($)	$22,033	$21,228	$17,267	$14,158
	time (sec)	114.12	204.28	274.56	428.39
SA	Cost ($)	$24,161	$29,057	$28,052	$67,842
	time (sec)	900	900	900	900
PSO	Cost ($)	$42,002	$42,318	$77,916	$116,782
	time (sec)	900	900	900	1,400
BARON	Cost ($)	$23,392	$22,788	$13,814	$14,571
	time (sec)	3,600	36,000	36,000	36,000

Moreover, to better investigate the convergence of the MSA algorithm compared to traditional SA, the cost for each inner loop iteration, for the first 1000 iterations, is plotted in Figure 24. It can be seen that MSA algorithm moves towards the region with the global optimal solution faster than traditional SA.

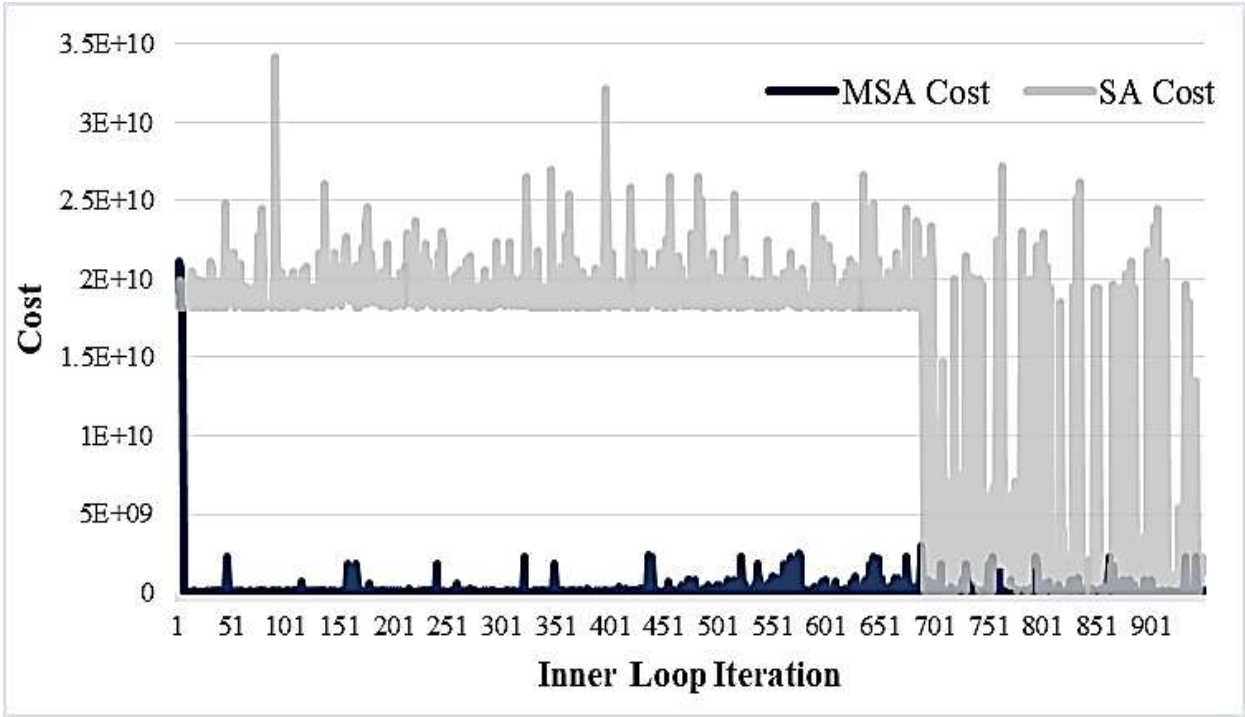

Figure 25 Inner Loop Iteration Costs of MSA and SA

4.5 Conclusion

In this chapter, an electricity and gas DR driven production scheduling model for manufacturers is established. The model considers time-based and event-based DR. A MSA algorithm is proposed to solve the problem in response to real-time supply notifications to promote the interaction between manufacturers and energy providers. A case study is conducted and the simulated cases show that 66-68% in energy cost savings for the manufacturer can be achieved using the proposed integrated TOU DR model. Moreover, an added $24,260/year can be saved using the real-time scheduling strategy. Lastly, $207,146 in savings from power generation may be possible (over a 5 year period) solely from this single manufacturer's participation in GDR.

5 Note to Practitioners

Before implementing the proposed cost effective joint energy and production operations decision making methodology for sustainable manufacturing systems, the following four criteria must be satisfied to promote the feasibility of applying demand response in manufacturing.

- The machines and/or manufacturing equipment need to be physically capable of being turned on and off or set to a lower rated power level. For example, variable speed drives can be used to control production equipment's' operating states while avoiding high initial startup power requirements.
- The production line needs to be flexible and provide opportunities in which production equipment can be manipulated without affecting the production system stability or leading to throughput loss. Such flexibility is observed with production lines that have inherent idle times and/or buffers.
- Expected demand response incentive needs to be attainable and significant. An example of this would be a time-of-use program with a short on peak period and significant difference between on-peak and off-peak rates.
- A method for controlling the production line (for example programmable control), to implement the proposed joint energy and production schedules, is necessary. Several commercial products facilitating energy management on the multi-machine level have emerged in the market and can enable this.

6 Summary and Future Work

Three joint energy and production planning models for manufacturers are presented (i.e. an integrated energy and maintenance production planning model, a combined manufacturing and HVAC system scheduling model, and demand response driven real-time decision making model considering natural gas and electricity). The proposed models provide a comprehensive set of tools for cost efficient joint energy and production operations decision making toward economically and environmentally sustainable manufacturing. This research will further advance the state of the art of research on sustainable manufacturing and end-user demand response; and provide manufacturers with analytical tools for implementing joint energy and throughput management for sustainable manufacturing systems.

In the future, some research extensions that can be conducted are as follows. The joint production and HVAC model can be advanced to also include natural gas consuming components and costs. Additionally, joint production and energy decision making can be extended to include onsite energy generation and energy storage. Finally, the gap among energy end-users and suppliers can be bridged by integrating DR bidding and direct load control for manufacturers.

References

Arasomwan, M.A. and Adewumi, A.O., 2013. On the performance of linear decreasing inertia weight particle swarm optimization for global optimization. *The Scientific World Journal*, *2013*.

Ball, P.D., Despeisse, M., Evans, S., Greenough, R.M., Hope, S., Kerrigan, R., Levers, A., Lunt, P., Oates, M., Quincey, R. and Shao, L., 2012, April. Modelling buildings, facilities and manufacturing operations to reduce energy consumption. In *Proceedings of the Production and Operations Management Society (POMS) international conference, Chicago, USA*.

Bego, A., Li, L. and Sun, Z., 2014. Identification of reservation capacity in critical peak pricing electricity demand response program for sustainable manufacturing systems. *International Journal of Energy Research*, *38*(6), pp.728-736.

Ben-Ameur, W., 2004. Computing the initial temperature of simulated annealing. *Computational Optimization and Applications*, *29*(3), pp.369-385.

Bhushan, R.K., 2013. Optimization of cutting parameters for minimizing power consumption and maximizing tool life during machining of Al alloy SiC particle composites. *Journal of Cleaner Production*, *39*, pp.242-254.

Bishop, C.M., 2006. Pattern recognition and machine learning (information science and statistics) springer-verlag new york. *Inc. Secaucus, NJ, USA*.

Boyd, G., Dutrow, E. and Tunnessen, W., 2008. The evolution of the ENERGY STAR® energy performance indicator for benchmarking industrial plant manufacturing energy use. *Journal of cleaner production*, *16*(6), pp.709-715..

Braun, J.E. and Chaturvedi, N., 2002. An inverse gray-box model for transient building load prediction. *HVAC&R Research*, *8*(1), pp.73-99.

Braun, J.E., 1990. Reducing energy costs and peak electrical demand through optimal control of building thermal storage. *ASHRAE transactions*, *96*(2), pp.876-888.

Brundage, M.P., Chang, Q., Chen, D. and Yu, V., 2013b, June. Energy Savings Opportunities of an Integrated Facility and Production Line. In *ASME 2013 International Manufacturing Science and Engineering Conference collocated with the 41st North American Manufacturing Research Conference* (pp. V002T04A008-V002T04A008). American Society of Mechanical Engineers.

Brundage, M.P., Chang, Q., Li, Y., Xiao, G. and Arinez, J., 2013a, August. Energy efficiency management of an integrated serial production line and HVAC system. In *Automation Science and Engineering (CASE), 2013 IEEE International Conference on* (pp. 634-639). IEEE.

Chai, B., Chen, J., Yang, Z. and Zhang, Y., 2014. Demand response management with multiple utility companies: A two-level game approach. *IEEE Transactions on Smart Grid*, *5*(2), pp.722-731.

Chai, B., Chen, J., Yang, Z. and Zhang, Y., 2014. Demand response management with multiple utility companies: A two-level game approach. *IEEE Transactions on Smart Grid*, *5*(2), pp.722-731.

Chang, Q., Ni, J., Bandyopadhyay, P., Biller, S. and Xiao, G., 2007. Maintenance opportunity planning system. *Journal of Manufacturing Science and Engineering*, *129*(3), pp.661-668.

Chang, Q., Xiao, G., Biller, S. and Li, L., 2013. Energy saving opportunity analysis of automotive serial production systems. *IEEE Transactions on Automation Science and Engineering*, *10*(2), pp.334-342.

Chen, Z., Wu, L. and Fu, Y., 2012. Real-time price-based demand response management for residential appliances via stochastic optimization and robust optimization. *IEEE Transactions on Smart Grid*, *3*(4), pp.1822-1831..

Chen, Z.S., Zhu, B., He, Y.L. and Yu, L.A., 2017. A PSO based virtual sample generation method for small sample sets: Applications to regression datasets. *Engineering Applications of Artificial Intelligence*, *59*, pp.236-243.

Cheng, M., Wu, J., Galsworthy, S.J., Ugalde-Loo, C.E., Gargov, N., Hung, W.W. and Jenkins, N., 2016. Power system frequency response from the control of bitumen tanks. *IEEE Transactions on Power Systems*, *31*(3), pp.1769-1778.

Chupka, Marc W., Robert Earle, Peter Fox-Penner, and Ryan Hledik. "Transforming America's Power Industry." *The Brattle Group, para The Edison Foundation, www. eei. org* (2008).

Coit, D.W., 1997. System-reliability confidence-intervals for complex-systems with estimated component-reliability. *IEEE Transactions on Reliability*, *46*(4), pp.487-493.

Corno, F. and Razzak, F., 2012. Intelligent energy optimization for user intelligible goals in smart home environments. *IEEE transactions on Smart Grid*, *3*(4), pp.2128-2135.

Dong, M. and He, D., 2007. A segmental hidden semi-Markov model (HSMM)-based diagnostics and prognostics framework and methodology. *Mechanical systems and signal processing*, *21*(5), pp.2248-2266.

Duflou, J.R., Sutherland, J.W., Dornfeld, D., Herrmann, C., Jeswiet, J., Kara, S., Hauschild, M. and Kellens, K., 2012. Towards energy and resource efficient manufacturing: A processes and systems approach. *CIRP Annals-Manufacturing Technology*, *61*(2), pp.587-609.

Duflou, J.R., Sutherland, J.W., Dornfeld, D., Herrmann, C., Jeswiet, J., Kara, S., Hauschild, M. and Kellens, K., 2012. Towards energy and resource efficient manufacturing: A processes and systems approach. *CIRP Annals-Manufacturing Technology*, *61*(2), pp.587-609.

Erickson, V.L. and Cerpa, A.E., 2010, November. Occupancy based demand response HVAC control strategy. In *Proceedings of the 2nd ACM Workshop on Embedded Sensing Systems for Energy-Efficiency in Building* (pp. 7-12). ACM.

Erickson, V.L., Achleitner, S. and Cerpa, A.E., 2013, April. POEM: Power-efficient occupancy-based energy management system. In *Proceedings of the 12th international conference on Information processing in sensor networks* (pp. 203-216). ACM.

Ernst & Young-EY. 2018. *Energy: More than just an operating expense?*. [online] Available at: https://www.ey.com/Publication/vwLUAssets/ey-energy-more-than-just-an-operating-expense/$File/Energy%20more%20than%20just%20an%20operating%20expense.pdf [Accessed 13 Jul. 2018].

Feng, L., Mears, L. and Schulte, J., 2016b, October. Key variable analysis and identification on energy consumption of automotive manufacturing plant. In *Technologies for Sustainability (SusTech), 2016 IEEE Conference on* (pp. 162-168). IEEE.

Feng, L., Mears, L., Beaufort, C. and Schulte, J., 2016a. Energy, economy, and environment analysis and optimization on manufacturing plant energy supply system. *Energy Conversion and Management*, *117*, pp.454-465.

Fernandez, M., Li, L. and Sun, Z., 2013. "Just-for-Peak" buffer inventory for peak electricity demand reduction of manufacturing systems. *International Journal of Production Economics*, *146*(1), pp.178-184.

Frenk, H., Dekker, R. and Kleijn, M., 1997. A unified treatment of single component replacement models. *Mathematical Methods of Operations Research*, *45*(3), pp.437-454.

Frigerio, N. and Matta, A., 2015. Energy-efficient control strategies for machine tools with stochastic arrivals. *IEEE Transactions on Automation Science and Engineering*, *12*(1), pp.50-61.

Ghislain, J.C. and McKane, A.T., 2006. *Energy efficiency as industrial management practice: The Ford production system and institutionalizing energy efficiency* (No. 2006-01-0829). SAE Technical Paper.

Hansen, T.M., Roche, R., Suryanarayanan, S., Maciejewski, A.A. and Siegel, H.J., 2015. Heuristic Optimization for an Aggregator-Based Resource Allocation in the Smart Grid. *IEEE Trans. Smart Grid*, *6*(4), pp.1785-1794.

Hansen, T.M., Roche, R., Suryanarayanan, S., Maciejewski, A.A. and Siegel, H.J., 2015. Heuristic Optimization for an Aggregator-Based Resource Allocation in the Smart Grid. *IEEE Trans. Smart Grid*, *6*(4), pp.1785-1794.

He, D., Li, R., Zhu, J. and Zade, M., 2011. Data mining based full ceramic bearing fault diagnostic system using AE sensors. *IEEE Transactions on Neural Networks*, *22*(12), pp.2022-2031.

Hemmecke, R., Kppe, M., Lee, J. and Weismantel, R., 2010. Nonlinear integer programming. In 50 Years of Integer Programming 1958-2008 (pp. 561-618).

Henderson, D., Jacobson, S.H. and Johnson, A.W., 2003. The theory and practice of simulated annealing. In *Handbook of metaheuristics* (pp. 287-319). Springer, Boston, MA.

Heng, A., Zhang, S., Tan, A.C. and Mathew, J., 2009. Rotating machinery prognostics: State of the art, challenges and opportunities. *Mechanical systems and signal processing*, *23*(3), pp.724-739.

Henze, G.P., Felsmann, C. and Knabe, G., 2004. Evaluation of optimal control for active and passive building thermal storage. *International Journal of Thermal Sciences*, *43*(2), pp.173-183.

Herrmann, C. and Thiede, S., 2009. Process chain simulation to foster energy efficiency in manufacturing. *CIRP journal of manufacturing science and technology*, *1*(4), pp.221-229.

Herrmann, C., Thiede, S., Kara, S. and Hesselbach, J., 2011. Energy oriented simulation of manufacturing systems–Concept and application. *CIRP Annals-Manufacturing Technology*, *60*(1), pp.45-48.

Hosni, M.H., Jones, B.W. and Xu, H., 1999. Experimental results for heat gain and radiant/convective split from equipment in buildings. *ASHRAE Transactions*, *105*(2), pp.527-539.

Houwing, M., Negenborn, R.R. and De Schutter, B., 2011. Demand response with micro-CHP systems. *Proceedings of the IEEE*, *99*(1), pp.200-213.

Jardine, A.K., Lin, D. and Banjevic, D., 2006. A review on machinery diagnostics and prognostics implementing condition-based maintenance. *Mechanical systems and signal processing*, *20*(7), pp.1483-1510.

Jolai, F., Rabiee, M. and Asefi, H., 2012. A novel hybrid meta-heuristic algorithm for a no-wait flexible flow shop scheduling problem with sequence dependent setup times. *International Journal of Production Research*, *50*(24), pp.7447-7466.

Kintner-Meyer, M., Schneider, K. and Pratt, R., 2007. Impacts assessment of plug-in hybrid vehicles on electric utilities and regional US power grids, Part 1: Technical analysis. *Pacific Northwest National Laboratory*, *1*.

Lee, S., Li, L. and Ni, J., 2013. Markov-based maintenance planning considering repair time and periodic inspection. *Journal of Manufacturing Science and Engineering*, *135*(3), p.031013.

Li, L. and Sun, Z., 2013. Dynamic energy control for energy efficiency improvement of sustainable manufacturing systems using Markov decision process. *IEEE Transactions on Systems, Man, and Cybernetics: Systems*, *43*(5), pp.1195-1205.

Li, L., Ambani, S. and Ni, J., 2009. Plant-level maintenance decision support system for throughput improvement. *International Journal of Production Research*, *47*(24), pp.7047-7061.

Li, L., Chen, X.D., Tseng, M.L., Wang, C.H., Wu, K.J. and Lim, M.K., 2017. Effective power management modeling of aggregated heating, ventilation, and air conditioning loads with lazy state switching. *Journal of Cleaner Production*, *166*, pp.844-850.

Li, L., Gong, C., Wang, D. and Zhu, K., 2013. Multi-agent simulation of the time-of-use pricing policy in an urban natural gas pipeline network: A case study of Zhengzhou. *Energy*, *52*, pp.37-43.

Li, L., Gong, C., Wang, D. and Zhu, K., 2013. Multi-agent simulation of the time-of-use pricing policy in an urban natural gas pipeline network: A case study of Zhengzhou. *Energy*, *52*, pp.37-43.

Li, L., Sun, Z., Yang, H., and Gu, F., 2012. A simulation based approach to energy efficiency improvement study of sustainable manufacturing systems, in *Proceedings of the 2012 ASME International Manufacturing Science and Engineering Conference (MSEC), June 4-8, 2012, Notre Dame, IN, U.S.,* paper number MSEC 2012 – 7242

Liang, Y., Levine, D.I., and Shen, Z.J., 2012, Thermostats for the smart grid: Models, benchmarks, and insights, Energy Journal, 33(4), 61-95.

Liao, R., Li, G., Miao, S., Lu, Y., Zhu, J. and Shen, L., 2012, November. Weather-clustering based strategy design for dynamic demand response building HVAC control. In *Proceedings of the Fourth ACM Workshop on Embedded Sensing Systems for Energy-Efficiency in Buildings* (pp. 33-35). ACM.

Liu, H., Zhao, Q., Huang, N. and Zhao, X., 2013. A simulation-based tool for energy efficient building design for a class of manufacturing plants. *IEEE Transactions on Automation Science and Engineering*, *10*(1), pp.117-123.

Maharjan, S., Zhu, Q., Zhang, Y., Gjessing, S. and Başar, T., 2016. Demand response management in the smart grid in a large population regime. *IEEE Transactions on Smart Grid*, *7*(1), pp.189-199.

Maharjan, S., Zhu, Q., Zhang, Y., Gjessing, S. and Başar, T., 2016. Demand response management in the smart grid in a large population regime. *IEEE Transactions on Smart Grid*, *7*(1), pp.189-199.

Mendivil, F. and Shonkwiler, R., 2010. Annealing a genetic algorithm for constrained optimization. *Journal of optimization theory and applications*, *147*(2), pp.395-410.

Mobley, R.K., 2011. *Maintenance fundamentals*. Elsevier.

Moldavska, A. and Welo, T., 2017. The concept of sustainable manufacturing and its definitions: A content-analysis based literature review. *Journal of Cleaner Production*, *166*, pp.744-755.

Motegi, N., Piette, M.A., Watson, D.S., Kiliccote, S. and Xu, P., 2007. Introduction to commercial building control strategies and techniques for demand response. *Lawrence Berkeley National Laboratory LBNL-59975*.

Mouzon, G. and Yildirim, M.B., 2008. A framework to minimise total energy consumption and total tardiness on a single machine. *International Journal of Sustainable Engineering*, *1*(2), pp.105-116.

Moynihan, G.P. and Triantafillu, D., 2012. Energy savings for a manufacturing facility using building simulation modeling: A case study. *Engineering Management Journal*, *24*(4), pp.73-84.

Nguyen, T.A. and Aiello, M., 2013. Energy intelligent buildings based on user activity: A survey. *Energy and buildings*, *56*, pp.244-257.

Niefer, M.J. and Ashton, W.B., 1997. *An analysis of buildings-related energy use in manufacturing* (No. PNNL--11499). Pacific Northwest National Lab., Richland, WA (United States).

Nistor, S., Wu, J., Sooriyabandara, M. and Ekanayake, J., 2015. Capability of smart appliances to provide reserve services. *Applied Energy*, *138*, pp.590-597.

Qadrdan, M., Cheng, M., Wu, J. and Jenkins, N., 2017. Benefits of demand-side response in combined gas and electricity networks. *Applied energy*, *192*, pp.360-369.

Qadrdan, M., Cheng, M., Wu, J. and Jenkins, N., 2017. Benefits of demand-side response in combined gas and electricity networks. *Applied energy*, *192*, pp.360-369.

Ramírez-Márquez, J.E. and Jiang, W., 2006. Confidence bounds for the reliability of binary capacitated two-terminal networks. *Reliability Engineering & System Safety*, *91*(8), pp.905-914.

Rapier, Robert. "The Price of Energy." *Forbes Magazine*. (2011). www.forbes.com/sites/energysource/2010/01/26/the-price-of-energy/#69e9076367b1

Rosenthal, R.E., 2004. GAMS--a user's guide.

Shedden, J.S., 1990. *An evaluation of a modified simulated annealing algorithm for various formulations* (No. AFIT/CI/CIA-90-020D). Air Force Inst of Tech Wright-Patterson AFB OH.

Sheehy, P. and Martz, E., 2012. Doing monte carlo simulation in minitab statistical software. In *ASQ Lean Six Sigma Conference, Phoenix, AZ, Feb* (pp. 27-28).

Siddiqui, O., Hurtado, P. and Parmenter, K., 2008. *The Green Grid Energy Savings and Carbon Emissions Reductions Enabled by a Smart Grid*.

Spitler, J.D., Fisher, D.E. and Pedersen, C.O., 1997. The radiant time series cooling load calculation procedure. *Transactions-American Society of Heating Refrigerating and Air Conditioning Engineers*, *103*, pp.503-518.

Sun, Z. and Li, L., 2013. Opportunity estimation for real-time energy control of sustainable manufacturing systems. *IEEE Transactions on Automation Science and Engineering*, *10*(1), pp.38-44.

Sun, Z., Li, L., Fernandez, M. and Wang, J., 2014. Inventory control for peak electricity demand reduction of manufacturing systems considering the tradeoff between production loss and energy savings. *Journal of cleaner production*, *82*, pp.84-93..

Thiede, S., 2012. *Energy efficiency in manufacturing systems*. Springer Science & Business Media.

Thiede, S., Herrmann, C. and Kara, S., 2011. State of Research and an innovative Approach for simulating Energy Flows of Manufacturing Systems. In *Glocalized Solutions for Sustainability in Manufacturing* (pp. 335-340). Springer, Berlin, Heidelberg.

U.S. Department of Energy, 2006. Benefits of demand response in electricity markets and recommendations for achieving *them. Washington, DC, USA, Tech. Rep.*

U.S. Department of Energy, 2010. Manufacturing energy & carbon footprint for all manufacturing sector (NAICS 31-33). *Energy Efficiency & Renewable Energy.*

U.S. Energy Information Administration, 2017. Electricity Customers. Energy and the Environment. (2017).

U.S. Environmental Protection Agency, 2014. Calculations and Reference, Washington D.C., U.S. http://www.epa.gov/cleanenergy/energy-resources/refs.html

U.S. Federal Energy Regulatory Commission, 2013. Federal Energy Regulatory Commission. *"*A National Assessment & Action Plan on Demand Response Potential."

Vardakas, J.S., Zorba, N. and Verikoukis, C.V., 2015. A survey on demand response programs in smart grids: Pricing methods and optimization algorithms. *IEEE Communications Surveys & Tutorials*, *17*(1), pp.152-178.

Vardakas, J.S., Zorba, N. and Verikoukis, C.V., 2015. A survey on demand response programs in smart grids: Pricing methods and optimization algorithms. *IEEE Communications Surveys & Tutorials*, *17*(1), pp.152-178.

Wang, H. and Pham, H., 1999. Some maintenance models and availability with imperfect maintenance in production systems. *Annals of Operations Research*, *91*, pp.305-318.

Wang, H., 2002. A survey of maintenance policies of deteriorating systems. *European journal of operational research*, *139*(3), pp.469-489.

Wang, L., Wang, Z. and Yang, R., 2012. Intelligent multiagent control system for energy and comfort management in smart and sustainable buildings. *IEEE transactions on smart grid*, *3*(2), pp.605-617.

Wang, Y., Brzezinski, A.J., Qiao, X. and Ni, J., 2017. Heuristic feature selection for shaving tool wear classification. *Journal of Manufacturing Science and Engineering*, *139*(4), p.041001.

Wang, Y., Li, L. and Huang, S., 2012. Derivation of reliability and variance estimates for multi-state systems with binary-capacitated components. *IEEE Transactions on Reliability*, *61*(2), pp.549-559.

Wilkins, C. and Hosni, M.H., 2000. Heat gain from office equipment. *Ashrae Journal*, *42*(6), p.33.

Winter, M., Li, W., Kara, S. and Herrmann, C., 2014. Determining optimal process parameters to increase the eco-efficiency of grinding processes. *Journal of Cleaner Production*, *66*, pp.644-654.

Yao, X., 1992. Dynamic neighbourhood size in simulated annealing. In *Proc. of Int'l Joint Conf. on Neural Networks (IJCNN'92)* (Vol. 1, pp. 411-416).

Yao, X., Sun, Z., Li, L. and Shao, H., 2015, June. Joint maintenance and energy management of sustainable manufacturing systems. In *ASME 2015 International Manufacturing Science and Engineering Conference* (pp. V002T04A008-V002T04A008). American Society of Mechanical Engineers.

Yao, X., Sun, Z., Wei, D. and Wang, L., 2016, June. Joint maintenance and energy management in manufacturing systems: prospect discussion, challenge analysis, and a case study. In *ASME 2016 11th International Manufacturing Science and Engineering Conference* (pp. V002T04A041-V002T04A041). American Society of Mechanical Engineers.

Yi, P., Dong, X., Iwayemi, A., Zhou, C. and Li, S., 2013. Real-time opportunistic scheduling for residential demand response. *IEEE Transactions on smart grid*, *4*(1), pp.227-234.

Yildirim, M.B. and Mouzon, G., 2012. Single-machine sustainable production planning to minimize total energy consumption and total completion time using a multiple objective genetic algorithm. *IEEE transactions on engineering management*, *59*(4), pp.585-597.

Yuan, G. and Ghanem, B., 2016. Binary Optimization Via Mathematical Programming With Equilibrium Constraints. *arXiv preprint arXiv:1608.04425*

Zhang, X., Che, L., Shahidehpour, M., Alabdulwahab, A. and Abusorrah, A., 2016. Electricity-natural gas operation planning with hourly demand response for deployment of flexible ramp. *IEEE Transactions on Sustainable Energy*, *7*(3), pp.996-1004.

Zhang, X., Che, L., Shahidehpour, M., Alabdulwahab, A. and Abusorrah, A., 2016. Electricity-natural gas operation planning with hourly demand response for deployment of flexible ramp. *IEEE Transactions on Sustainable Energy*, *7*(3), pp.996-1004.

Zhang, X., Che, L., Shahidehpour, M., Alabdulwahab, A.S. and Abusorrah, A., 2017. Reliability-based optimal planning of electricity and natural gas interconnections for multiple energy hubs. *IEEE Transactions on Smart Grid*, *8*(4), pp.1658-1667.

Zhang, X., Che, L., Shahidehpour, M., Alabdulwahab, A.S. and Abusorrah, A., 2017. Reliability-based optimal planning of electricity and natural gas interconnections for multiple energy hubs. *IEEE Transactions on Smart Grid*, *8*(4), pp.1658-1667.

VITA

****

EDUCATION

Ph.D. in Industrial Engineering and Operations Research, University of Illinois at Chicago (UIC), **01/2015-08/2018**

M. S. in Industrial Engineering and Operations Research, University of Illinois at Chicago (UIC), **01/2015-08/2016**

B. S. in Industrial Engineering and Operations Research, University of Illinois at Chicago (UIC), **08/2011-12/2014**

AWARDS

- Institute for Environmental Policy and Science Predoctoral Fellowship, 2017
- Provost Award for Graduate Research, 2016

RESEARCH EXPERIENCE

Sustainable Manufacturing Systems Research Laboratory, UIC

- **Research Assistant** (11/2016-8/2018): U.S. Department of Energy Industrial Assessment Center: Energy Efficiency, Smart Manufacturing, and Cyber Security (DE-EE0007722; $2,087,872)
- **Research Assistant** (10/2013-8/2018): NSF GOALI Collaborative Research (with General Motors): Cost-Effective Energy Efficiency Management of Sustainable Manufacturing Systems (CMMI-1131537; $246,355)

Mechanical and Industrial Engineering Department, UIC

- **Editorial Assistant** (12/2012-7/2015): International Journal of Heat and Mass Transfer, Numerical Heat Transfer, and International Communication in Heat and Mass Transfer

JOURNAL PUBLICATIONS

Sun, Z., Li, L., Bego, A. and **Dababneh, F.**, 2015. Customer-side electricity load management for sustainable manufacturing systems utilizing combined heat and power generation system. *International Journal of Production Economics*, *165*, pp.112-119.

Sun, Z., Li, L. and **Dababneh, F.**, 2016. Plant-level electricity demand response for combined manufacturing system and heating, venting, and air-conditioning (HVAC) system. *Journal of cleaner production*, *135*, pp.1650-1657.

Dababneh, F., Li, L. and Sun, Z., 2016. Peak power demand reduction for combined manufacturing and HVAC system considering heat transfer characteristics. *International Journal of Production Economics*, *177*, pp.44-52.

Dababneh, F., Li, L., Shah, R. and Haefke, C., 2018. Demand Response-Driven Production and Maintenance Decision-Making for Cost-Effective Manufacturing. *Journal of Manufacturing Science and Engineering*, *140*(6), p.061008.

Sun, Z., **Dababneh, F.** and Li, L., 2018. Joint Energy, Maintenance, and Throughput Modeling for Sustainable Manufacturing Systems. *IEEE Transactions on Systems, Man, and Cybernetics: Systems*. DOI:10.1109/TSMC.2018.2799740.

Dababneh, F. and Li, L., 2018. Integrated Electricity and Natural Gas Demand Response for Manufacturers in the Smart Grid. *IEEE Transactions on Smart Grid*. DOI: 10.1109/TSG.2018.2850841.

Li, L., **Dababneh, F.** and Zhao, J., 2018. Cost-effective supply chain for electric vehicle battery remanufacturing. *Applied Energy*, *226*, pp.277-286.

CONFERENCE PAPERS

Dababneh, F., Atanasov, M., Sun, Z. and Li, L., 2015, June. Simulation-based electricity demand response for combined manufacturing and HVAC system towards sustainability. In *ASME 2015 International Manufacturing Science and Engineering Conference* (pp. V002T05A009-V002T05A009). American Society of Mechanical Engineers.

Dababneh, F., Shah, R., Sun, Z. and Li, L., 2017, June. Framework and sensitivity analysis of joint energy and maintenance planning considering production throughput requirements. In *ASME 2017 12th International Manufacturing Science and Engineering Conference collocated with the JSME/ASME 2017 6th International Conference on Materials and Processing* (pp. V003T04A062-V003T04A062). American Society of Mechanical Engineers.

Ge, Y., **Dababneh, F.** and Li, L., 2017. Economic Evaluation of Lignocellulosic Biofuel Manufacturing Considering Integrated Lignin Waste Conversion to Hydrocarbon Fuels. *Procedia Manufacturing*, *10*, pp.112-122.

WHITE PAPERS

Restructuring Recharged, The Superior Performance of Competitive Electricity Markets 2008-2016, *RESA-Retail Energy Supply Association*, Phillip R. O'Connor, April 2017.

SERVICE

Conference Co-Chair:

- Session on "Additive Manufacturing: Processing & Materials", ASME 2017 International Conference on Manufacturing Science and Engineering (MSEC), Los Angeles, CA, USA, June 8th, 2017.

Journal Reviewer:

- International Journal of Production Economics
- Journal of Cleaner Production
- Reliability Engineering & System Safety
- International Journal of Energy Sector Management
- Transportation Research Part E: Logistics and Transportation Review
- Utilities Policy

Conference Reviewer:

- Proceedings of American Society of Mechanical Engineering, Manufacturing Science and Engineering Conference (ASME MSEC)
- Proceedings of Complex Adaptive Systems, Engineering Cyber Physical Systems Conference

****

Appendix

ASME Copyright
https://journaltool.asme.org/Help/AuthorHelp/WebHelp/Guidelines/Rights_and_Permissions.htm

“

Assignment of Copyright
ASME requests that authors/copyright owners assign copyright to ASME in order for a journal paper to be published by ASME. Authors exempt from this request are direct employees of the U.S. Government, whereby papers are not subject to copyright protection in the U.S., or non-U.S. government employees, whose governments hold the copyright to the paper.

For more information on copyright, please view the Copyright Transfer information page.

Retained Rights of Authors
Authors retain all proprietary rights in any idea, process, procedure, or articles of manufacture described in the Paper, including the right to seek patent protection for them. Authors may perform, lecture, teach, conduct related research, display all or part of the Paper, and create derivative works in print or electronic format. Authors may reproduce and distribute the Paper for non-commercial purposes only. Non-commercial applies only to the sale of the paper per se. For all copies of the Paper made by Authors, Authors must acknowledge ASME as original publisher and include the names of all author(s), the publication title, and an appropriate copyright notice that identifies ASME as the copyright holder.

Permissions
Once your paper has been published by ASME, you may wish to submit it for inclusion in a non-ASME publication or to incorporate some or all of its elements in another work. Since ASME is the legal holder of copyright for its papers, it will be necessary for you to secure the permission of the copyright holder to have its material published in another source.

In this case, for permission to have your paper - in whole or in part, as is or adapted - published elsewhere, please submit your request here

Questions
The ASME Publishing staff is available to discuss current ASME policy on permissions and rights. Please feel free to contact us with any questions or comments at: permissions@asme.org.
”

Dear Prof. Dababneh,
It is our pleasure to grant you permission to use **all or any part of** the ASME paper

- Framework and Sensitivity Analysis of Joint Energy and Maintenance Planning Considering Production Throughput Requirements, by Fadwa Dababneh, Rahul Shah, Zeyi Sun and Lin Li, Paper No. MSEC2017-2936
- Simulation-Based Electricity Demand Response for Combined Manufacturing and HVAC System Towards Sustainability, by Fadwa Dababneh, Mariya Atanasov, Zeyi Sun and Lin Li, Paper No. MSEC2015-9278

- Demand Response-Driven Production and Maintenance Decision-Making for Cost-Effective Manufacturing, by Fadwa Dababneh; Lin Li; Rahul Shah; Cliff Haefke, J. Manuf. Sci. Eng. 2018; 140(6)

cited in your letter for inclusion in a Doctoral Thesis entitled Cost Effective Joint Energy and Production Operations Decision Making for Sustainable Manufacturing Systems to be published by University of Illinois at Chicago.

Permission is granted for the specific use as stated herein and does not permit further use of the materials without proper authorization. Proper attribution must be made to the author(s) of the materials. **Please note:** if any or all of the figures and/or Tables are of another source, permission should be granted from that outside source or include the reference of the original source. ASME does not grant permission for outside source material that may be referenced in the ASME works.

As is customary, we request that you ensure full acknowledgment of this material, the author(s), source and ASME as original publisher. Acknowledgment must be retained on all pages where figure is printed and distributed.

Many thanks for your interest in ASME publications.

Sincerely,

Beth Darchi
Publishing Administrator
ASME
2 Park Avenue
New York, NY 10016-5990
darchib@asme.org

Elsevier Copyright
https://www.elsevier.com/about/policies/copyright/personal-use

“

Personal use

Authors can use their articles, in full or in part, for a wide range of scholarly, non-commercial purposes as outlined below:

- Use by an author in the author’s classroom teaching (including distribution of copies, paper or electronic)
- Distribution of copies (including through e-mail) to known research colleagues for their personal use (but not for Commercial Use)
- Inclusion in a thesis or dissertation (provided that this is not to be published commercially)
- Use in a subsequent compilation of the author’s works
- Extending the Article to book-length form
- Preparation of other derivative works (but not for Commercial Use)
- Otherwise using or re-using portions or excerpts in other works

These rights apply for all Elsevier authors who publish their article as either a subscription article or an open access article. In all cases we require that all Elsevier authors always include a full acknowledgement and, if appropriate, a link to the final published version hosted on Science Direct.

”

IEEE Copyright
https://www.ieee.org/content/dam/ieee-org/ieee/web/org/pubs/permissions_faq.pdf

“

Does IEEE require individuals working on a thesis or dissertation to obtain formal permission for reuse?

Textual Material

Using short quotes or referring to the work within these papers) users must give full credit to the original source (author, paper, publication) followed by the IEEE copyright line © 2011 IEEE.

In the case of illustrations or tabular material, we require that the copyright line © [Year of original publication] IEEE appear prominently with each reprinted figure and/or table.

If a substantial portion of the original paper is to be used, and if you are not the senior author, also obtain the senior author’s approval.

Full-Text Article

If you are using the entire IEEE copyright owned article, the following IEEE copyright/ credit notice should be placed prominently in the references: © [year of original publication] IEEE. Reprinted, with permission, from [author names, paper title, IEEE publication title, and month/year of publication]
Only the accepted version of an IEEE copyrighted paper can be used when posting the paper or your thesis on-line.

In placing the thesis on the author's university website, please display the following message in a prominent place on the website: In reference to IEEE copyrighted material which is used with permission in this thesis, the IEEE does not endorse any of [university/educational entity's name goes here]'s products or services. Internal or personal use of this material is permitted. If interested in reprinting/republishing IEEE copyrighted

material for advertising or promotional purposes or for creating new collective works for resale or redistribution, please go to http://www.ieee.org/publications_standards/publications/rights/rights_link.html to learn how to obtain a License from RightsLink.

If applicable, University Microfilms and/or ProQuest Library, or the Archives of Canada may supply single copies of the dissertation.

”